UNIVERSITÀ
DEGLI STUDI
FIRENZE

DOTTORATO DI RICERCA IN
SCIENZE BIOMEDICHE

CICLO XXXVIII

# Lactate as an inducer of wasting in skeletal muscle

Settore Scientifico Disciplinare
BIOS-07A


**Dottoranda**

Dott.ssa Bianca Bartoloni

**Supervisore**

Prof.ssa Tania Fiaschi

**Coordinatore**

Prof. Fabrizio Chiti


Anni 2022-2025

# INDEX

# 1. INTRODUCTION

## 1.1.Skeletal muscle: function, structure and physiology

### 1.1.1. Skeletal muscle function

Skeletal muscle is one of the most dynamic and plastic tissue of the human body. In humans, skeletal muscle represents roughly the 40% of total body weight, being the most abundant tissue and the main protein reservoir. Indeed, it contains 50-75% of all proteins and accounts the 30-50% of whole-body protein turnover [1,2]. Skeletal muscle controls not only locomotion, but it plays a pivotal role in breathing, eating, energy expenditure, and in maintaining the homeostasis of glucose, amino acids, and lipids, thereby contributing to a high quality of life [3]. Therefore, skeletal muscle is essential for movement control, postural support, heat production and metabolic homeostasis [4]. Skeletal muscle is a highly vascularized and innervated tissue, embedded with components of the metabolic and regulatory machinery, thus supporting efficient energy production and cellular homeostasis [5]. From a mechanical perspective, the main function of skeletal muscle is to convert chemical energy into mechanical energy to generate force and power, maintain posture and produce movement. This influences social and personal life, because it allows participation in social and occupational settings, maintains or enhances health and contributes to functional independence. From a metabolic point of view, skeletal muscle is involved in basal energy metabolism. It serves as a storage for important substrates such as amino acids and carbohydrates, it is involved in the production of heat for the maintenance of core temperature, and in the consumption of most of the oxygen and fuel used during physical activity and exercise. Of particular importance is the role of skeletal muscle as a reservoir of amino acids needed by other tissues such as skin, brain and heart for the synthesis of organ-specific proteins. Moreover, amino acids released from muscles contribute to the maintenance of blood glucose levels during conditions of starvation. Of relevance to disease prevention and health maintenance, a reduced muscle mass impairs the body's ability to respond to stress and chronic illness [6].

### 1.1.2. Structure of skeletal muscle

The architecture of skeletal muscle is characterized by a well-defined arrangement of groups of fibers, also referred to as myofibers or muscle cells, organized with their longitudinal axes in parallel and associated with connective tissue. This layer of connective tissue, which surrounds each muscle, is known as epimysium. Within the muscle, groups of fibers are arranged in bundles and surrounded by another layer of connective tissue called the

perimysium. A single skeletal muscle fiber is surrounded by a cell membrane known as the sarcolemma, and contains a cytoplasm called the sarcoplasm [6]. Each myofiber contains long, thin, cylindrical rods called myofibrils, usually 1-2 μm in diameter, which run parallel to the long axis of the muscle fiber, occupying most of the intracellular space. Consequently, cellular organelles such as mitochondria and nuclei are pushed to the periphery of the sarcoplasm [7]. When assembled in a characteristic pattern, the myofilaments form sarcomeres, the basic contractile units of skeletal muscle [5,6]. This dense packaging of contractile proteins and organelles makes the cytosol highly compact, leaving no empty spaces. As a result, this organized structure means that protein and organelle turnover strongly impact on myofiber size and function. During exercise or anabolic hormonal stimulation, new proteins and organelles accumulate within the cytosol, leading to muscle growth due to an increasing cellular volume – a process known as hypertrophy. Conversely, catabolic conditions such as cancer, infections, diabetes, organ failure or inactivity/disuse lead to loss of proteins, organelles and cytoplasm, causing shrinkage of the cellular volume, a condition known as atrophy. Consequently, the size and function of muscle cells depend on a balance between biogenesis/biosynthesis and removal/destruction. This balance is finely regulated by both autologous and non-autologous signals, the latter originating from distal organs or from the interstitial cells surrounding myofibers, including muscle stem cells (SCs) [3]. Muscle SCs represent a heterogeneous population of adult stem cells that differ in lineage potential, gene expression patterns and myogenic differentiation potential, which are all fundamental for skeletal muscle regeneration. The ability of skeletal muscle to regenerate is governed significantly by the interaction between SCs and its microenvironment, called “niche”. From an anatomic point of view, SCs are located between the basal lamina (BL) and the sarcolemma, sequestered within this niche in adult skeletal muscle [5].

Associated with the sarcolemma is a complex of several proteins, which are physically connected to the internal myofilament structure, especially to the actin protein located in the thin filament. The partial or complete absence, or dysfunction of any of these proteins may result in damage to the sarcolemma, muscle weakness and atrophy [6]. Force generation and rapid movement are fundamental features of striated muscle function, driven by sarcomere contraction. The sarcomere is a molecular machinery composed primarily of two alternating sets of protein filaments: thin filaments (α-actin and associated proteins) and thick filaments (myosin and associated proteins) which run parallel to the muscle fiber’s longitudinal axis [5]. The two most abundant contractile proteins are actin and myosin, accounting for approximately 70-80% of the total protein content in a single muscle fiber. Actin forms the core of the thin filament, whereas myosin constitutes the thick filaments. These filaments

are arranged in a parallel and overlapping manner, arrayed into longitudinally repeated banding patterns termed sarcomeres. Sarcomeres aligned in series form myofibrils, and multiple myofibrils are organized in parallel within each muscle fiber. The force-generating capacity of a muscle fiber is largely determined by the number of myofibrils arranged in parallel [8]. The sarcomere and sarcoplasm contain numerous other proteins that contribute to the structure of the cytoskeleton, coupling of the excitation and contraction processes, energy release and the generation of force and power. For instance, there are regulatory proteins such as the calcium-dependent troponin complex (troponins C, I and T) and tropomyosin, which are associated with the actin filament. Other proteins that influence the mechanical and physiological properties of muscle are titin and nebulin [6,9]. Myosin functions both as an enzyme, hydrolysing ATP via its head domain, and as a structural protein through its tail. It is associated with other non-myosin proteins with specialized function, mostly structural, such as myosin-binding proteins (MyBPs) C and H of the M-band. MyBPCs contribute to the precise organization of myosin filaments and regulate force generation by actomyosin complex. In addition, there are more other proteins contributing to the structure of the thick filaments, including titin, a giant elastic protein that extends along its entire length of the thick filament [5]. Actin isoforms polymerize to form thin filaments, an essential component of the contraction machinery. Similarly to thick filaments, thin filaments are associated with proteins that facilitate contraction. The most important ones are troponin (TNN-I, TNN-C and TNN-T), and tropomyosin, which stabilize actin and provide a molecular scaffold for positioning the $Ca^{2+}$-sensitive troponin complex on the filament [5].

Other key cellular components in the sarcoplasm of muscle fibers include a transverse tubular system (T-tubule), the sarcoplasmic reticulum (SR) and a mitochondrial network; the exact amount of these elements may depend on the fiber type. The T-tubule system consists of invaginations of the sarcolemma that conduct nerve action potential into the interior of the cell, while the sarcoplasmic reticulum is responsible for calcium storage, release and reuptake after activation. Lastly, mitochondria form a three-dimensional network throughout the fiber, generating the energy needed for muscle activity when oxygen is available [6].

### 1.1.3. Fiber types

The heterogeneity of human skeletal muscle depends on the significant variability in the biochemical, mechanical and metabolic phenotypes of individual fibers. In the human body, different muscles exhibit diverse relative proportions of fiber types. The most commonly used classification identifies three fiber types: type I (slow, oxidative, fatigue-resistant), IIa

(fast, oxidative, intermediate metabolic properties), and IIb (fast, glycolytic, fatigable) [1,6]. Phenotypically, slow-twitch (Type I) fibers are highly vascularized and rich in mitochondria and myoglobin, displaying high mitochondrial and oxidative enzyme content with low glycolytic activity. These fibers are resistant to fatigue, relying on oxidative metabolism for energy, and contract for prolonged periods while generating relatively low force. In contrast, fast-twitch (Type II) fibers contract more rapidly, sustaining short anaerobic bursts of activity, fatiguing easier than Type I fibers. Type II fibers have a high glycolytic capacity, ensuring adequate ATP production to compensate the accelerated rate of ATP hydrolysis. It is recognized that the pattern of Type II fiber specialization depends on expression pattern of myosin heavy chains isoforms during histogenesis. Type IIa fibers resemble slow-twitch fibers, containing more myoglobin and relying more on oxidative metabolism [5].

From a physiological perspective, the differences between fast- and slow-twitch fibers are based on variations in calcium kinetics, excitation-contraction coupling (ECC) mechanisms, and molecular motor activity, which determine fundamental twitch parameters, such as time to peak tension and half-relaxation time [5].

The main characteristics of each fiber type are summarised in the following table (Tab. 1).

| **Slow oxidative muscle fiber (type I)** | **Fast oxidative muscle fiber (type IIa)** | **Fast glycolytic muscle fiber (type IIb)** |
|---|---|---|
| Low myosin ATPase activity (in comparison to type II fibers) | Higher myosin ATPase activity than type I fibers | Higher myosin ATPase activity than type I fibers |
| High capacity for ATP production through oxidative phosphorylation (aerobic cellular respiration) | High capacity for ATP production through oxidative phosphorylation (aerobic cellular respiration) | Lower capacity for ATP production through oxidative phosphorylation than “red” fibers (anaerobic glycolysis) |
| Very thick capillary network | Thick capillary network | Sparser capillary network |
| High levels of intracellular myoglobin (predominantly red colour) | High levels of intracellular myoglobin (predominantly red colour) | No intracellular myoglobin (predominant colour is white) |
| Ability to maintain function for long periods without exhaustion | Fatigue resistance stronger than type IIb fibers | Fatigue occurs quickly |

**Table 1**. Summary table of muscular fiber types and their main characteristics.

Skeletal muscles are heterogeneous in terms of fiber type and metabolic properties, and therefore may respond differently, often drastically, to the same stimulus. For instance, slow muscles such as the soleus are more resistant to starvation compared to fast muscles. Nevertheless, under conditions of disuse like the one induced by hind limb suspension, the

soleus undergoes atrophy more rapidly than glycolytic (fast) muscles [3,10]. The precise coordination among these components is crucial for maintaining muscle health and proper motor function. Any disruption to this balance can lead to a decline in muscle health and performance, typically characterized by muscle fiber loss, decreased motor output, and in severe cases, mortality [5].

## 1.2. Definition of muscular wasting and skeletal muscle atrophy

Muscle mass is the result of a delicate balance between protein synthesis and degradation. These two processes are sensitive to several factors, such as nutritional status, hormonal balance, physical activity, and injury or disease. Structural, contractile and regulatory protein compartments have been extensively studied due to their crucial roles in mobility, exercise capacity, functioning and health [6]. Indeed, when individuals are involved in adverse pathological and physiological stressors, the fine balance between protein synthesis and degradation in skeletal muscle may be disrupted. This can lead to a decline in muscle mass and strength [11], a condition known as skeletal muscle atrophy. It is characterized by a decrease in muscle fibers cross-sectional area, loss of muscle mass and strength, and disruption of the protein turnover balance [1]. Given its notable health significance, skeletal muscle atrophy was recognized as a distinct disease according to its own International Classification of Diseases, 10$^{th}$ Revision, Clinical Modification (ICD-10-CM) code (M62.84) in 2016 [12]. The prompt loss of muscle mass and strength mainly depends on excessive protein breakdown, and, frequently, reduced protein synthesis [13]. From a histopathological point of view, skeletal muscle atrophy is characterized by muscle alterations, which include myofiber shrinkage, changes in fiber type or myosin isoforms, and net losses of cytoplasm, organelles and total protein, with myofiber diameter reduction being the most notable feature [1].

Skeletal muscle atrophy may develop from inherited disorders (congenital or genetic) or acquired conditions (pathological or physiological), and it is classified as primary skeletal muscle atrophy and secondary muscle atrophy, respectively [1,14,15]. Both types involve muscle fiber type conversion, including shifts from slow muscle fibers to fast muscle fibers, and vice versa. Moreover, muscle loss is considered a negative prognostic factor for the progression of the underlying disease. For example, cancer-associated cachexia, a debilitating condition involving adipose and muscle wasting, leads to a reduction of patients' response to anticancer therapy and therefore reduces the survival of these patients [16]. *Primary muscle atrophy* is a condition that can be caused by a variety of inherited muscle disorders, including congenital and genetic myopathies. Inherited myopathies are often

linked to increasing atrophy, inflammation, metabolic dysfunction, muscle spasm or rigidity. Inherited myopathies can be subclassified as muscular dystrophies, congenital myopathies, mitochondrial myopathies and metabolic myopathies, the latter two being the most common [17]. For instance, congenital myopathies include Nemaline myopathies, whereas muscular dystrophies include Duchenne muscular dystrophy (DMD), Becker muscular dystrophy and myotonic muscular dystrophies (type 1 and type 2) [1].

*Secondary muscle atrophy* occurs hereafter acquired causes, such as systemic disease or physical inactivity. Over time, the absence of muscle contraction and stimulation triggers signalling pathways that promote muscle atrophy, characterized by protein loss and cell apoptosis. As the disease progress, muscle atrophy becomes more pronounced due to protein degradation that exceeds protein synthesis [1]. There are several pathological conditions that can cause muscle atrophy, which include aging-related sarcopenia, cancer cachexia, chronic obstructive pulmonary disease (COPD), diabetes, obesity, chronic kidney disease, heart failure, neurodegenerative disorders, sepsis, burns, and trauma. Other causes include fasting or malnutrition, as well as immobilization due to leg fractures, disuse, or extended bed rest [1].

## 1.3. Clinical relevance of muscular wasting and impact on quality of life

Skeletal muscle atrophy is a very frequent condition among older individuals, but it can also arise hereafter several states, and it is considered a serious comorbidity associated with many disorders. Rapid muscle wasting can also occur in acute illnesses, such as burn trauma and sepsis [18]. In the most severe cases, muscle wasting could progress into critical illness myopathy, with consequent failure of respiratory skeletal muscles and potentially leading to death [16]. Muscle wasting arises also as a physiological response to fasting, malnutrition and aging. The condition where there is a muscle loss associated with age is defined as sarcopenia and affects more than half of individuals over 80 years of age [19]. Moreover, because of defects in myofibril structure, patients with genetic muscular dystrophies also experience muscle wasting. These conditions include DMD, fascioscapulohumeral muscular dystrophy (FSHD) and limb-gridle muscular dystrophy (LGMD) [20]. Muscle atrophy can also be triggered by neurodegenerative diseases, including amyotrophic lateral sclerosis (ALS), which involves denervation of muscles. Furthermore, muscle wasting can be localized to specific muscles in individuals who suffer spinal cord injuries or joint immobilization due to plaster casts [21].

At present, skeletal muscle atrophy represents a critical global clinical challenge, underscoring the urgent need for innovative treatment approaches. This loss of muscle

function can lead to a decrease in quality of life of people affected by this condition, as well as to an augmented morbidity and mortality, and it is currently an incurable debilitating condition [13,14,15,22]. Indeed, even if the prevalence of people suffering from any kind of muscle weakness is elevated, there is no available treatment for muscle wasting, and muscle remains an under-medicated organ [18]. While exercise remains the only accepted strategy to prevent or slow muscle wasting, several promising therapeutic agents are currently under development. A valuable approach may be to further understand the cellular and molecular mechanisms regulating protein balance in muscle, such as identifying diverse cytokines, particularly myostatin, and a common transcriptional program that promotes muscle wasting [13,23].

## 1.4. Molecular mechanisms of muscle wasting

The mechanisms underlying muscle atrophy are highly complex and not fully understood. Continuous muscle protein turnover requires a balance between synthesis and degradation in muscle tissues. Some of the upstream signals of skeletal muscle atrophy caused by diverse diseases include increased oxidative stress, inflammation and decreased mitochondrial function. Moreover, the ubiquitin-proteasome systems, the autophagy-lysosome system, the caspase system, and the calpain system are four primary pathways responsible for protein degradation. The first three systems break down and eliminate substrate proteins, whereas calpains are involved in proteolytic processing rather than degradation, as they cleave protein at specific sites to alter or modulate the structure and function of their substrates [1].

Systemic inflammation and oxidative stress play a pivotal role in disrupting skeletal muscle protein metabolism, leading to skeletal muscle atrophy (Fig. 1). Notably, even if the catabolic conditions are the same, the atrophy program can differ between fast and slow muscles. Each catabolic state not only affects muscle differently in terms of atrophy susceptibility, but also triggers distinct atrophy-related genetic programs, even among different muscles in the same context [10]. Although most pathways that control muscle mass, such as the Insulin/IGF1 or TGFβ/Activin/BMP signalling pathways, affect both protein synthesis and degradation, changes in protein turnover do not always follow the oversimplified view that muscle growth results solely from increased protein synthesis and decreased protein degradation, and that atrophy arises from the opposite condition. As a matter of fact, physical exercise stimulates protein synthesis, but at the same time it also activates autophagy-lysosome and ubiquitin-proteasome-degradative pathways. In contrast, during protein breakdown, amino acids released by the lysosome and proteasome directly stimulate mTOR, potentially enhancing protein synthesis even during muscle atrophy [3].

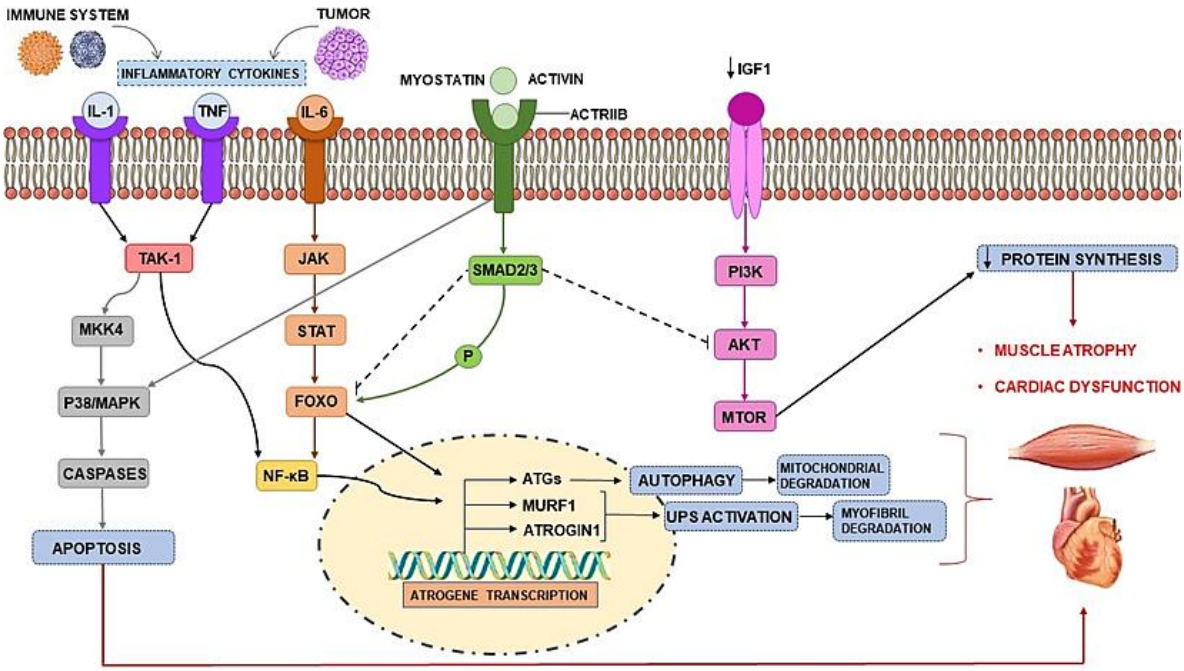


**Figure 1**: Signalling pathways involved in muscle wasting. Activation of inflammatory cytokines (TNF, IL-1, IL-6) leads to the activation of NF-kB and FOXO. The binding of IL-6 to its receptor induces STAT3 expression, which turns into the activation of the NF-κB pathway. Myostatin can also activate protein degradation through FOXOs and decrease protein synthesis, inhibiting AKT through SMAD. The autophagy-lysosome pathway is regulated by the transcription factor FOXO, while activation of p38 and JAK/MAPK signalling trigger caspases-dependent apoptosis. Levels of insulin-like growth factor-1 (IGF-1) are decreased during muscle wasting, thus inhibiting protein synthesis. The ubiquitin-proteasome system (UPS) is initiated by the transcription of the E3 ubiquitin ligases MuRF-1 and MAFbx/atrogin-1 [158].

### 1.4.1. Insulin/IGF-1 – AKT – mTOR signalling pathway and protein synthesis

Insulin and insulin-like growth factor 1 (IGF-1) are two significant anabolic factors that sustain organism and muscle growth. These hormones bind to their specific receptors (the insulin receptor and the IGF-1 receptor respectively), which activate a cascade of phosphorylation events that modulate proteins, enzymes and transcriptional factors in a positive or in a negative way. Insulin is produced by the pancreas, while IGF-1 is predominately synthesized in the liver under the influence of growth hormone and acts as a systemic growth factor. IGF-1 can also be produced by extrahepatic tissues where it plays an autocrine/paracrine role.

The insulin/IGF-1 signalling pathway is implicated in protein synthesis, protein degradation, cellular proliferation and survival, as well as glucose uptake and energy production. Both

insulin and IGF-1 activate the mitogen-activated protein kinase/extracellular signal-regulated kinase (RAS-MAPK-ERK) and the PI3K-AKT-mTOR pathways [3]. Insulin/IGF-1 signalling significantly impacts on a crucial protein implicated in protein synthesis and degradation, the mammalian target of rapamycin (mTOR). mTOR is a serine/threonine kinase capable of integrating various extracellular signals, including nutrients, growth factors, energy status and stress. Its signalling is linked to a variety of physiological processes such as cell survival, energy production and maintenance of cellular metabolic homeostasis [24]. Skeletal muscle maintains a fine balance between protein synthesis and degradation, ensuring the continuous renewal of muscle proteins. In healthy muscle tissue, mTOR signalling pathway plays a central role in regulating protein synthesis and preserving muscle trophism. Specifically, mTOR activity is upregulated during muscle hypertrophy, whereas in conditions of atrophy, markers of mTOR pathway activity are reduced, highlighting the direct involvement of this pathway in maintaining muscle fiber size. Dysregulation of this pathway can lead to pathologic alterations, such as cancer, neurodegeneration, infection, and age-related muscle homeostasis decline [24]. In mammals, mTOR forms two different complexes depending on which proteins it interacts with. One is the rapamycin-sensitive TORC1 complex, which contains Raptor, and the other one is the rapamycin-insensitive TORC2 complex, which comprehends Rictor. mTORC1 regulates several anabolic processes, including protein synthesis, ribosome and mitochondria biogenesis, whereas mTORC2 is related to glucose and lipids homeostasis. Moreover, mTORC2 activates AKT serine/threonine kinase (AKT) protein for protein degradation [24,25]. mTOR is a downstream target of AKT, and in mammalian cells mTOR activity is finely regulated by amino acid availability, which is fundamental for the synthesis of proteins, nucleic acids, glucose and ATP, thus balancing anabolic and catabolic processes [26].

In skeletal muscle the binding of insulin or IGF-1 to IGF-1R on the cell membrane leads to phosphorylation of insulin receptor substrate 1 (IRS-1), an adapter protein that activates phosphatidylinositol 3-kinase (PI3K) [26,27]. Once activated, PI3K generates phosphatidylinositol-3,4,5-triphosphate (PIP3), which recruits 3-phosphoinositide-dependent protein kinase 1 (PDK1) and phosphorylates the protein kinase B or AKT. The tuberous sclerosis complex (TSC1-TSC2) is a target downstream of AKT and inhibits the small G-protein, Ras homolog enriched in brain (Rheb), which is a regulator of mTOR. mTOR combines various stimuli coming both from hormones and from cytokines, nutrients and ATP/AMP ratio. mTORC1 phosphorylates the 70 kDa ribosomal S6 kinase (p70S6K) and eukaryotic initiation factor 4E-binding protein 1 (4EBP1), regulating protein translation.

Once phosphorylated, the p70S6K acts on ribosomal protein S6, eukaryotic translation initiation factor 4B (eIF-4B), and eukaryotic elongation factor-2 kinase (eEF-2K). The phosphorylation of 4E-BP1 regulates eIF-4E availability, dissolving the 4E-BP1/eIF-4E complex [24,25,26,27].

Inhibition of the mTORC1 activates autophagy by phosphorylation of Unc-51 like autophagy activating kinase 1 (Ulk1) in the presence of AMP-activated protein kinase (AMPK). At the same time, activation of mTORC2 via the PI3K/AKT/TSC1-2 pathway leads to the activation of AKT to control protein degradation [19,21]. Once phosphorylated by mTORC2, AKT plays a role as a negative regulator of the transcription factors called forkhead box protein (FOXO), shifting it from the cell nucleus to the cytoplasm. The retention of FOXO in the cytoplasm impedes the regulation of two ubiquitin ligases: Muscle atrophy F-box (MAFbx)/Atrogin-1 and muscle RING finger 1 (MuRF1), both related to ubiquitin-proteasome system signalling, considered the major pathway of proteolytic degradation of eukaryotic cells [24]. Moreover, growth hormone (GH) also induces PI3K-AKT signalling through JAK2-mediated activation of Insulin Receptor Substrate 1 (IRS-1) [18,28].

Besides insulin and GH signalling pathways, mTORC1 can be also activated by amino acids, particularly branched-chain amino acids (BCAAs) such as leucine or its metabolite β-hydroxy-methylbutyrate (HMB) in an AKT-independent manner, as well as other anabolic stimuli including activation of $\beta_2$-adrenoreceptors ($\beta_2$-AR). The stimulation of the guanine nucleotide-binding G protein-coupled receptors (GPCRs) activates the PI3K-AKT signalling pathway via the Gβγ dimer [18]. Another critical downstream target of IGF-1 is the glycogen synthase kinase-3β (GSK3β), which is phosphorylated by AKT. In muscle hypertrophic conditions, GSK3β is phosphorylated, and its activity is inhibited, leading to activation of Eukaryotic Translation Initiation Factor 2B (eIF2B) and transcriptional activator β-catenin [26].

Reduced PI3K–AKT signalling, as occurs during fasting and catabolic diseases, results in decreased protein synthesis, increased FOXO-mediated proteolysis and fibre atrophy. This inhibition of PI3K–AKT signalling results not only from a decrease in insulin and/or IGF1 levels, but also from elevated levels of myostatin, an autocrine inhibitor of normal muscle growth, or its homologue activin A. Indeed, increased levels of both myostatin and activin A occur in pathological states and can cause a rapid loss of muscle mass [13].

Although these pathways are downregulated in various muscle atrophy conditions, the exact relationship and interplay between them in the context of skeletal muscle atrophy and hypertrophy remain unclear [26].

### 1.4.2. TGF-β/Myostatin (GDF-8)/Activin/BMP pathway

The second major signalling pathway that regulates skeletal muscle growth involves myostatin, also known as growth and differentiation factor 8 (GDF8). In contrast to mTOR, myostatin has a potent negative effect on muscle mass, acting as a key inhibitor of protein synthesis [29]. It is a member of the transforming growth factor beta (TGF-β) superfamily, which consists of TGF-βs, activins, bone morphogenetic proteins (BMPs) and growth and differentiation factors (GDFs). BMPs and GDFs mediate downstream intracellular signalling via Suppressor of Mothers against Decapentaplegic 1/5/8 (SMAD1/5/8) proteins, while activins, myostatin, GDF11 and TFG-β via SMAD2/3 proteins [30].

More in detail, the Activin/Myostatin/TGF-β group binds plasma membrane-associated activin type IIB and IIA receptors (ActRIIB/IIA) and TGF-β receptors (TGF-β RIII). Consequently, this binding induces the phosphorylation of SMAD2 and SMAD3 via the recruitment and activation of activin receptor-like kinase (ALK)-4, -7 and -5, to promote the formation of a heterotrimeric complex with SMAD4 [31,32]. Activation of SMAD2/3 and promotes muscle fiber atrophy by suppressing satellite cell proliferation and differentiation. Myostatin accumulation is linked to insulin resistance and protein degradation within muscle fibers. Although the physiological and pathological mechanisms regulating myostatin secretion remain largely unclear, various factors – including glucocorticoids, FOXO1, Nuclear Factor kappa-light-chain-enhancer of activated B cells (NF-κB) and SMAD2/3/4 – can enhance its expression. Once released, myostatin acts both locally in an autocrine way, and systemically through circulation, contributing to catabolic effects [13,31,32].

Another pathway that converges on SMAD4 and controls muscle mass is BMP signalling [33]. BMP/GDF ligands preferentially bind type II receptors, including BMP type II receptor (BMPRII), ActRIIA and ActRIIB [3]. When myostatin binds to its receptor complex, it triggers phosphorylation of the transcription factors SMAD2 and SMAD3, leading to the activation of downstream signalling pathways. One of the key effects of myostatin signalling is the suppression of AKT activity and the activation of FOXO, which together inhibit protein synthesis and promote protein degradation. Moreover, activated SMAD3 is recruited to the SMAD-binding elements in the promoter regions of MuRF1 and MAFbx, where it works synergistically with FOXO to enhance transcription of these ubiquitin ligases.

In addition to myostatin, other members of the TFG-β superfamily, such as Activin A and GDF11, also bind to ActRIIB and activate SMAD2/3 signalling, thereby contributing to the suppression of muscle mass. Like myostatin, these factors inhibit normal muscle growth and can promote muscle wasting, particularly in the context of aging or disease. While myostatin plays a pivotal role in limiting muscle growth in mice, activin A and GDF11 become

increasingly relevant in humans, particularly during aging or disease [13,31,32]. GDF15 has also been shown to promote muscle wasting through the decrease of food intake. Elevated serum levels of GDF15 observed in patients with cancer, chronic kidney disease or COPD could contribute to the development of cachexia by reducing appetite as well as inducing muscle-inherent catabolic pathways [18]. Moreover, high levels of myostatin and activin A can cause a rapid muscle depletion, as observed in cancer and chronic disease. Inhibition of the myostatin/activins axis reduces the level of phosphorylation of SMAD2/3, allowing SMAD4 to interact with phosphorylated SMAD1/5/8, to sustain growth and counteract atrophy [3]. Enhancing follistatin expression, a natural circulating glycoprotein inhibitor of myostatin, results in a significant increase in muscle mass. Transgenic mice overexpressing follistatin exhibited a marked increase in muscle mass. Thus, follistatin administration is another possible approach to impede atrophy. This increase in muscle mass following TFG-β inhibition seems to be partly due to the activation of the PI3K-AKT pathway and mTOR signalling, BMP signalling, AMPK, and Peroxisome proliferator-activated receptor Gamma Coactivator 1-α (PGC1α) and PGC1α4 [13]. Similarly, treatment with ActRIIB antagonists has been shown to prevent muscle wasting and improve muscle function across various cancer models [34]. Collectively, these various studies and recent preclinical findings all strongly suggest that inhibiting the myostatin-activin A pathway could be a potentially useful approach to block various types of atrophy [13].

### 1.4.3. Ubiquitin-proteasome system (UPS)

One of the key signalling pathways involved in muscle protein turnover is the ubiquitin-proteasome system, a crucial protein degradation pathway in eukaryotes. This system can be overactivated in various conditions associated with muscle wasting, such as glucocorticoid treatment, sepsis, fasting, cancer and acidosis. This pathway acts through an enzymatic cascade that begins with the conjugation of target proteins with ubiquitin and ends with their degradation into small peptides and amino acids [35]. Activated ubiquitin is first transferred by E1 to a carrier protein, E2 (ubiquitin-conjugated enzyme). Then, E3 ubiquitin ligases recognize the target proteins and facilitate the covalent attachment of ubiquitin to lysine residues on the substrate protein. This reaction is repeated to form a polyubiquitin chain, and the ubiquitinated proteins are subsequently directed to the 26S proteasome for ATP-dependent degradation. Ubiquitin itself is then released and reused for a new enzymatic reaction [35].

The best-characterized E3 ubiquitin ligases in skeletal muscle are MAFbx/Atrogin-1 and MuRF1 [26]. Atrogin-1 can led to degradation of proteins involved in muscle growth and

differentiation, while MuRF1 and other ligases, such as tripartite motif-containing protein 32 (TRIM32), catalyse the breakdown of myofibrils and cytoskeleton proteins [36]. MuRF1 ubiquitinates several muscle structural proteins, including troponin I, myosin heavy chains (MyHC), myosin light chains 1 and 2. In comparison, Atrogin-1 substrates are mainly involved in growth-related processes or survival pathways [13].

The ubiquitin-proteasome pathway plays a pivotal role in the so-called "atrophy program", which can be over-activated following diverse pathologic conditions associated with muscle atrophy. It is well known that Atrogin-1 and MuRF1 are upregulated in muscle wasting [35]. These conditions include disuse, denervation, inflammation, aging, glucocorticoid increase, high Angiotensin II, and chronic diseases such as cancer, congestive heart failure, chronic kidney disease, COPD and AIDS [26]. Indeed, knockout animals deficient in either Atrogin-1 or MuRF1 are resistant to atrophy, whereas their overexpression causes atrophy, disrupts the integrity of sarcomeric structures, and alters components of thick filaments [35].

MuRF and Atrogin-1 play distinct roles in inducing muscle atrophy. MuRF1 is primarily involved in the proteolysis of sarcomeric proteins and enzymes regulating metabolic processes by ubiquitination of MyHC and enzymes involved in the formation of ATP, respectively. Atrogin-1, instead, downregulates protein synthesis and muscle fiber differentiation by targeting the eukaryotic initiation factor 3 subunit f (eIF3-f) and the myogenic regulatory transcription factor myogenic differentiation 1 (MyoD) [18]. Multiple factors influence muscle homeostasis. Among these, glucocorticoids promote muscle protein breakdown through the activation of the ubiquitin-proteasome system, thus contributing to muscle wasting. Studies have shown that IGF-1 signalling is often altered in many of muscle atrophy-conditions and signalling pathways regulating Atrogin-1 and MuRF1 partially overlap and are regulated by IGF-1 signalling [26]. A decline in anabolic stimuli, such as IGF-1, also triggers the activation of this proteolytic pathway. The reduced activity of the IGF-1/PI3K/AKT signalling cascade has been implicated in initiating the atrophy program. One of the downstream targets of this pathway is the FoxO family transcription factors. Physiologically, AKT phosphorylates FoxO proteins, sequestering them in the cytoplasm and preventing their transcriptional activity. Nevertheless, when anabolic signals like IGF-1 decrease, AKT signalling is inhibited, allowing the translocation of dephosphorylated FoxO into the nucleus. Here, FoxO factors stimulate the transcription of Atrogin-1 and MuRF1 genes.

Although several kinases downstream of AKT, such as GSK3β, MEK and components of the calcineurin signalling pathway, are involved in regulating muscle fiber size, they do not control directly Atrogin-1 expression. Moreover, FoxO3 has been found to regulate the

autophagy pathway, highlighting its role in coordinating the degradation of proteins via the proteasome with the autophagic removal of cellular organelles [35].

Atrogin-1 and MuRF1 are regulated by distinct signalling pathways: Atrogin-1 is predominantly controlled by FoxO, whereas MuRF1 is more influenced by NF-κB. FoxO1 and FoxO3 induce Atrogin-1 expression via promoter activation, while their regulation of MuRF1 appears independent of direct DNA binding. NF-κB signalling, particularly via Inhibitor of κB kinase subunit β (IKKβ) activation, increases MuRF1 expression without affecting Atrogin-1, causing profound muscle wasting. IGF-1/PI3K/AKT signalling inhibits both FoxO and NF-κB pathways, thereby modulating their expression. IGF-1 rapidly and strongly reduces Atrogin-1 expression, and only moderately decreases MuRF1 levels, with protein degradation correlating more strongly with Atrogin-1.

Atrogin-1 and MuRF-1 have numerous muscular targets for protein degradation. Indeed, Atrogin-1 substrates include eIF3-f, desmin and vimentin, while MuRF1 targets myosin heavy chains, MyBP-C, MyLC1/2, stabilizing sarcomeric structures such as titin and regulating muscle metabolism via creatine kinase [26]. Other E3 ligases that are involved in muscle atrophy are MUSA1, SMART, Nedd4, Trim32 and TRAF6, which are regulated by FoxO and IGF-1 [26].

### 1.4.4. Autophagy

Another proteolytic system activated under catabolic conditions is autophagy. Autophagy is a decisive mechanism for all eukaryotic organisms, since it ensures specific rearrangements required for proliferation, cell death and differentiation during embryogenesis and postnatal development. It is activated as an adaptive catabolic process in response to metabolic stresses, including fasting, growth factor depletion, hypoxia and denervation. Basal level of autophagy is fundamental for cellular homeostasis, but its activation under certain conditions can led to cell alteration, resulting in atrophy [35]. Hyperactivation of autophagy contributes to muscle loss in several conditions, such as cancer cachexia, fasting, sepsis, critical illness, cirrhosis, chemotherapy, disuse, denervation and COPD.

Autophagy is continuously active in cells to generate metabolites that sustain cellular core metabolism, to remove damaged components and to promote repair and stress resistance. Therefore, an autophagy impairment induces muscle degeneration and weakness [3]. Autophagy can trigger the selective removal of either specific organelles such as mitochondria or proteins, including protein aggregates. Specificity is achieved through adaptor proteins, such as p62 and Bnip3, which simultaneously interact with

autophagosomes via LC3 and with dysfunctional organelles, damaged proteins and protein aggregates, often labelled by a polyubiquitin chain [3].

FoxO3 is a key regulator of a plethora of autophagy-related genes, including Bnip3, Gabarap, LC3 and Atg12. Bnip3 mediates to FoxO3-induced autophagy by triggering the development of autophagosomes. Moreover, FoxO3 stimulates and controls not only the autophagic lysosomal system, but also the ubiquitin proteasomal system. In addition, the expression of autophagy-related genes under oxidative stress is controlled by the p38/MAPK pathway, although the specific transcription factors downstream of p38MAPK remains unclear [1,35].

FoxO3 can be activated in response to oxidative stress, in association with local alteration in the activity of the antioxidant enzyme Superoxide Dismutase 1 (SOD1). This activation promotes transcription of autophagy-related genes, such as LC3, cathepsin L and Bnip3. Under pathologic conditions, the augmented expression of lysosomal cysteine endopeptidase cathepsin L and LC3 is associated with skeletal muscle wasting. Studies in literature suggest that cathepsin L expression represents an early marker of muscle wasting associated with the activation of proteolytic pathways [35].

FoxO3 is necessary and sufficient for the induction of autophagy in skeletal muscle under different pathologic conditions. A major effector of FoxO3-mediated autophagy in skeletal muscle is Bnip3, as its expression is induced by FoxO3, whereas Bnip3 knockdown blocks FoxO3-induced autophagy [35].

### 1.4.5. The calpain system

Calpains are a family of proteolytic enzymes which have calcium-dependent proteolytic activities, made up of calcium-dependent nonlysosomal cysteine proteases. Calcium ions ($Ca^{2+}$) are required for their activation, binding directly to Protease Core domain 1 and 2 (PC1 and PC2) of conventional calpain. The calpain family includes calpain proteases and calpastatin, an endogenous calpain-specific inhibitor [1].

In skeletal muscle, one of the main triggers of proteolysis is the elevated resting cytoplasmic $Ca^{2+}$, which activates calpains and promotes the degradation of proteins that are subsequently further processed by the ubiquitin-proteasome system, contributing to a dystrophic phenotype. Activation of calpain-mediated proteolysis has been linked to cachexia and age-dependent muscle atrophy.

Calpains have diverse substrates, such as protein kinases, cytokines, transcription factors, lens proteins and calmodulin-binding proteins. Several structural muscle proteins are also substrates of calpains, including desmin, α-actinin and Z-disk anchoring proteins. The main

functions of calpains include cytoplasmic reorganization, regulation of differentiation, and mediation of inactivity-induced mitochondrial dysfunction and oxidative stress in skeletal muscle fibers. There are multiple molecular events leading to an augmented activity of calpains, which cause loss of myofibril integrity and degradation of sarcomeric proteins. Downstream signals involved in calpain-mediated skeletal muscle degradation also include the ubiquitin-proteasome and caspase-3 activation [1].

Sarcopenia, a pathologic consequence of aging, is characterized by loss of muscle mass and function. It is known that sarcopenia is highly reduced by muscle-specific overexpression of calpastatin. Calpains also mediate the degradation of oxidated myofibrillar proteins, suggesting a link between oxidative stress and accelerated myofibrillar proteolysis in disuse-muscle atrophy. Moreover, expression of calpastatin transgene attenuates muscle wasting associated with disuse and prevents the shift from slow to fast of muscle fiber type in muscle unloading. Collectively, these studies demonstrate that calpains play a pivotal role in muscle homeostasis and disease [35].

### 1.4.6. Systemic inflammation and pro-inflammatory cytokines

Aging is usually associated with a moderate increase in inflammation; however, it remains unclear whether this inflammation is a cause or a consequence of the aging process. In contrast, systemic inflammation is a hallmark of cancer, and it is linked to elevated circulating levels of pro-inflammatory cytokines. These cytokines play a central role in muscle wasting and are closely associated with the development of cancer cachexia, a multifactorial wasting syndrome characterized by progressive weight loss and skeletal muscle wasting. The augmented levels of pro-inflammatory cytokines in cancer cachexia are more pronounced than in other forms of muscle atrophy, such as those caused by disuse or aging [37].

The inflammatory response is fundamental and has been extensively studied in the context of skeletal muscle growth and repair, sarcopenia and myopathies [38]. The immune system plays a pivotal role in the protection against pathogens, in tissue and organ repair and remodelling, and in the maintenance of skeletal muscle tissue. Proper regulation of the immune system is therefore necessary to maintain skeletal muscle mass. Increased levels of pro-inflammatory cytokines are associated with decrease in muscle mass, and their excessive production negatively impacts on skeletal muscle [39]. Consequently, inflammation is considered a potent trigger of muscle wasting and cancer cachexia [40].

In the context of elevated systemic inflammation, such as cancer, muscle atrophy is promoted by the canonical and non-canonical NF-κB signalling pathway [18]. The transcription factor

NF-κB is the master regulator of inflammatory responses and apoptosis, and it also plays a crucial role in many types of muscle atrophy. Nevertheless, the specific mechanisms by which NF-κB promotes atrophy remain unclear. Even if the upstream signals that regulate NF-κB function in muscles during different types of wasting are in part unknown, it seems that the activation of the ubiquitin ligase TRAF6 is important. Muscle wasting can be triggered by several pro-inflammatory cytokines, such as Tumor Necrosis Factor α (TNF-α), interleukin-6 (IL-6), interleukin-1 (IL-1) and interferon-γ (IFNγ), which are elevated in sepsis, cancer and other catabolic conditions. Together, they may increase the expression of NF-κB or cause the release of other cytokines [13].

In the inactive state, NF-κB is sequestered in the cytoplasm by inhibitory proteins (IκB). Following certain stimuli, for example the binding of TNF-α or IL-1 to their receptor (TNFR1 and IL-1 respectively), the IκB kinase complex (IKK) phosphorylates IκB, resulting in its ubiquitination and proteasomal degradation. This leads to the nuclear translocation of NF-κB and expression of its target genes [3]. NF-κB target genes encode cytokines, chemokines, cell adhesion molecules, growth factors and diverse enzyme associated with the ubiquitin-proteasome system [38]. Cai *et al.* demonstrated that muscle-specific overexpression of IKKβ in transgenic mice induces severe muscle wasting, mediated at least in part by the ubiquitin ligase MuRF1, but not by Atrogin-1/MAFbx [41]. TNF-α and pro-inflammatory cytokines can also induce insulin resistance and suppress the IGF1-Akt pathway [40].

Tumor necrosis factor-like weak inducer of apoptosis (TWEAK) is a member of the TNF superfamily, which positively modulates NF-κB and the atrophy program. TWEAK can signal through TNF receptor 1 (TNFR1) but has higher affinity for fibroblast growth factor-inducible 14 (Fn14), a small cell surface receptor [39]. Fn14 is upregulated in denervated muscle, allowing NF-κB activation and consequently MuRF1 but not Atrogin-1 expression [3]. Another study shows that the Fn14 receptor is upregulated in aged mice, which also exhibit a reduction in muscle fiber in comparison to young mice [42, 43]. TWEAK/Fn14-induced muscle atrophy is context-dependent, as TWEAK-signalling is augmented in response to denervation but not in response to glucocorticoids. TWEAK additionally regulates muscle mass through AKT inhibition, reducing protein synthesis and indirectly promoting transcription of E3 ligases [42].

The transcription factor Signal Transducer and Activator of Transcription 3 (STAT3) is activated by pro-inflammatory cytokines such as TNF-α, IL-6 and IL-1. IL-6 binds to the IL6R-gp130 complex, which induces the activation of the Janus kinases (JAKs), which in turn phosphorylates and activates STAT3. Activated STAT3 translocates to the nucleus and

induces transcription of target genes such as the suppressor of cytokine signaling 3 (SOCS3). SOCS3 interferes with IGF-1 signalling by inhibiting IRS-1 and impairing protein synthesis [42]. Interestingly, in cancer and sepsis, STAT3 phosphorylation is increased in muscles, and STAT3 inhibition preserves muscle mass in tumor-bearing mice [44]. Moreover, overexpression of STAT3 is sufficient to induce muscle atrophy and to upregulate Atrogin-1 [3].

### 1.4.7. Mitochondria dysfunction

Mitochondria play a fundamental role in maintaining cellular homeostasis and skeletal muscle health, and mitochondrial damage can lead to a series of pathophysiological changes. Indeed, skeletal muscle atrophy can be a consequence of mitochondrial damage, and its molecular mechanisms are very complex [45]. Mitochondria are membrane-bound cell organelles which produce most of the chemical energy required to fuel the metabolic activities of cells. Their primary function is to generate ATP within the electron transport chain (ETC), and ATP represents the primary fuel for cellular metabolic activities. Moreover, mitochondria take part in programmed cell death, apoptosis, calcium regulation, cell metabolism regulation and other biological processes. Skeletal muscle health depends on a proper functioning and integrity of mitochondria, which are interconnected with the sarcoplasmic reticulum and sarcolemma [14,46].

Mitochondria support the basic and contractile energy demands of the skeletal muscle network through ATP generation. However, mitochondrial dysfunction activates catabolic pathways that contribute to muscle atrophy. Indeed, there is forceful evidence supporting the idea that the accumulation of mitochondrial defects contributes to energy deficit and alterations in the balance between protein synthesis and degradation observed in skeletal muscle [14].

Optimal mitochondrial physiology depends on several key processes, including mitochondrial dynamics (mediated by mitochondrial fusion and fission), mitophagy (involving mitochondrial self-clearance and protection), mitochondrial biogenesis, and mitochondrial-derived vesicles formation. In conditions of endogenous and exogenous stresses, reactive oxygen species (ROS) and the mitochondrial membrane potential in skeletal muscle rapidly increase, resulting in mitochondrial functional network disorders, including imbalances in mitochondrial dynamics and mitochondrial autophagy damage. Consequently, skeletal muscle atrophy is often characterized by an accumulation of mitochondrial ROS and a decline in mitochondrial function [14]. Moreover, elevated ROS levels can impede the initial phase of mRNA translation, and oxidative stress can activate

degradation-related signaling pathways, triggering muscle atrophy programs [46]. Mitochondria are highly dynamic organelles that undergo rapid fusion and fission processes to adapt their shape in response to the cellular environment's demands. These processes maintain normal mitochondrial morphology and quantity through continuous fusion and fission, and it helps to isolate damaged mitochondria from a healthy mitochondrial network. Moreover, mitophagy is closely linked to mitochondrial dynamics and removes isolated or damaged mitochondria. Mitochondrial fusion is controlled by Mitofusin 1/2 (Mfn1/2) in the mitochondrial outer membrane and Optic atrophy 1 (OPA1) in the mitochondrial inner membrane. Mitochondrial fission is regulated by Dynamin-related protein 1 (DRP-1), mitochondrial fission factor (Mff) and fission protein 1 (Fis1) [46,47]. Muscle-specific ablation of Mfn1 and Mfn2 causes severe muscular atrophy [3], while OPA1 inhibition leads to mitochondrial defects, ROS production, and release of mitochondrial DNA.

Activation of MuRF1 and Atrogin-1 promotes overexpression of DRP-1 and Fis1, resulting in excessive mitochondrial fission and fragmented mitochondrial network. DRP-1 overexpression induces mitochondrial dysfunction, mitophagy, and energy stress, which ultimately results in an atrophy via the AMPK/FoxO3 pathway [48]. All these events trigger diverse transcription factors, including FoxO3, NF-κB and ATF4, which coordinate the expression of genes related to muscle atrophy [46]. Conversely, the absence of Fis1 leads to mitochondrial swelling and excessive fusion, thereby triggering mitophagy in skeletal muscle.

Mitophagy plays a fundamental role as a cellular autophagic process that specifically targets and removes damaged mitochondria. It is strictly linked to mitochondrial biogenesis, leading to a precise regulation of quantity and quality of mitochondria. This fine regulated process prepares mitochondria for subsequent lysosomal breakdown, ultimately contributing to the restoration of cellular homeostasis. The Parkin E3 ligase and Phosphatase and tensing homolog (PTEN)-induced kinase 1 (PINK1) are the most largely studied pathways involved in mitophagy. When these pathways are activated, the clearance of defective mitochondria increases, preserving a healthy mitochondrial pool. However, it reduces the total mitochondrial density in disuse-induced skeletal muscle atrophy. Sarcopenia can be linked to inadequate Parkin-mediated mitophagy and incremented levels of mitochondrial ROS, causing an acceleration of skeletal muscle atrophy through MuRF-1 activation [46].

Overall, mitochondrial dysfunction, through energy deficits, oxidative stress, impaired dynamics, and defective mitophagy, plays a central role in skeletal muscle atrophy. The close interplay between mitochondria and skeletal muscle is crucial for the maintenance of muscle health and to prevent atrophy [14,46].

## 1.5. Cancer cachexia: a wasting syndrome associated with cancer

### 1.5.1. Definition of cancer cachexia and diagnostic criteria

Cancer cachexia is a multifactorial wasting syndrome characterized by progressive weight loss and skeletal muscle wasting. In 2006, guidelines published in Europe and in the United States defined cachexia as "*a syndrome of complex metabolic disorders associated with underlying disease, characterized by a decrease in muscle mass with or without adipose tissue loss*" [49]. The major symptoms of cancer-related cachexia include rapid loss of body mass, chronic inflammation, anorexia, fatigue, anaemia, and systemic multiple organ failure [50].

Cachexia is strongly associated with different chronic illnesses, such as cancer, chronic heart failure, chronic kidney disease, and chronic obstructive pulmonary disease. Moreover, some acute conditions, including sepsis and burn, often end up with cachexia during the post-acute phase [50,51]. For these reasons, cachexia contributes to the higher rates of morbidity and mortality in the above-mentioned terminal illnesses [52].

Cachexia is now considered to result from metabolic, immunological and neurological abnormalities rather than mere nutritional deficiency [50]. The disorder has distinct tumor-driven components and arises from a variable combination of reduced food intake and metabolic changes, including elevated energy expenditure, excess catabolism, and inflammation. However, cachexia is distinct from starvation and simple malnutrition, which are readily reversible by the provision of adequate nutrients [53].

Pronounced muscle wasting often affects the respiratory muscles, diaphragm and heart leading to respiratory or cardiac failure in severe cases [52]. Patients with cachexia suffer from impaired physical capacity, reduced emotional and social well-boing, poor quality of life and increase mortality [51]. Cancer-associated cachexia also diminishes the therapeutic efficacy of anti-cancer treatments and decrease survival rate, leading to augmented chemotherapy resistance in cachectic individuals. Moreover, excessive loss of skeletal muscle mass and fat can alter the volume of distribution of chemotherapeutic drugs, increasing both drug concentration and susceptibility to treatment-related side effects [49,52].

Weight loss is a hallmark of cancer cachexia and an important prognostic factor for survival in cancer patients. Skeletal muscle mass is maintained through a balance between synthesis and degradation of muscle proteins. An imbalance between these two processes is the major cause of cancer cachexia-related muscle wasting; moreover, resting energy expenditure (REE) is often increased [50]. Weight loss can be induced by diverse catabolic stimuli in the

tumor microenvironment through overactivation of the ubiquitin-proteasome system (UPS) and the autophagy-lysosomal pathway (ALP) [50].

For a long time, cachexia has been considered as an inevitable condition associated with disease progression and was not subject to treatment or research. However, subsequent research has gradually revealed that various molecular mechanisms involving in skeletal muscle, adipose tissue, the digestive system, the central nervous system and the immune system contribute to its development. In particular, substances secreted by the tumor and tumor-induced immune responses and metabolic changes have been suggested to be deeply involved in its pathogenesis [50].

Although the diagnosis of cachexia remains still controversial, specific diagnostic criteria for cancer cachexia were proposed and widely accepted by Fearon *et al*. [54]. There are three criteria included:

1. Weight loss of 5% or more within 6 months (in the absence of simple starvation);
2. Weight loss of 2% or more in patients with a body mass index (BMI) <20 kg/$m^2$ or
3. Weight loss or more in patients with sarcopenia (males <7.26 kg/$m^2$; females >5.45 kg/$m^2$) (Fig. 2).

Cancer cachexia is a continuum that can be divided into three stages: pre-cachexia, cachexia and refractory cachexia, based on the degree of weight loss [50]. Pre-cachexia represents an early stage with mild metabolic disturbance with the absence of obvious cachexia symptoms, while refractory cachexia is due to the severity of this metabolic disorder, and it is a terminal state where there is no mor room for improvement in nutritional status [49]. However, weight loss alone does not reveal the full effect of cachexia on physical function and is not a prognostic variable. The search for specific biomarkers, such as inflammatory factors, may be a helpful direction for the early diagnosis and intervention of cachexia in the future [50].

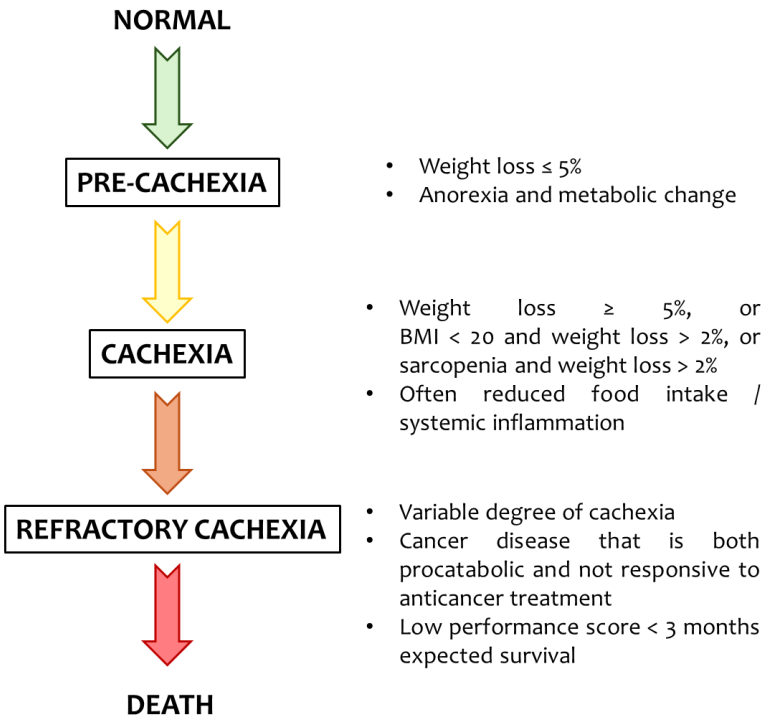


**Figure 2**. Diagnostic criteria for cancer cachexia [49].

### 1.5.2. Epidemiology in cancer patients

Half of cancer deaths worldwide (~8,2 million people per year) are attributed to cancers most frequently associated with cachexia, namely pancreatic (0,33 million deaths), oesophageal (0,40 million), gastric (0,72 million), pulmonary (1,59 million), hepatic (0,75 million) and colorectal (0,69 million) cancers [53]. Cancer-associated cachexia is mainly linked with incurable disease, and it is highly prevalent at the end of life. It is observed in approximately half of elderly cancer patients, with its incidence varying according to cancer type. Cancer cachexia is found in approximately 80% of patients with advanced cancer and accounts for approximately 30% of cancer-associated deaths [49]. Around 20,4% of patients with lung cancer, 60% of pancreatic cancer and even up to 85% of patients with gastrointestinal cancer experience cancer cachexia. Despite its clinical significance, cancer cachexia remains under-diagnosed and undertreated [49]. Between 50 and 80% of cancer patients suffer from cachexia, and complications arising from the condition are responsible for nearly 20% of deaths directly related to it [52]. Additional factors that contribute to the variable prevalence of cachexia include more-advanced cancer stage, sex, advanced age, genetic risk factors, comorbidities and treatment-related catabolic effects [53]. In the United States, the annual prevalence of cachexia in chronic illnesses in estimated to be over 160000 hospital-admitted cases.

While the impact of cachexia on cancer mortality has received increasing attention in recent years, sex-based differences in this syndrome remain poorly understood. Although male patients are generally more severely affect by cancer cachexia, the underlying biological mechanisms between sex-based differences remain poorly understood [51].

### 1.5.3. Pathogenetic mechanisms of muscular wasting in cancer

Cancer cachexia is a multi-organ syndrome which involves interaction of major organs and diverse signalling pathways, thereby causing involuntary muscle and adipose tissue loss, muscular atrophy and inflammation (Fig. 3). Progressive loss of muscle mass is a central element of cancer cachexia and a key predictor of survival.

Muscle atrophy is characterized by loss of myofibrillar proteins, which is associated with functional impairments such as muscle weakness and fatigue - typical features of cancer cachexia. Multiple mechanisms contribute to muscle wasting, primarily through disrupted metabolic homeostasis and proteostasis. These mechanisms include the increase in catabolic processes which accelerate protein breakdown and a decrease in anabolic processes that are essential for protein synthesis [55].

The loss of skeletal muscle mass is the result of an imbalance between protein synthesis and degradation, which is regulated not only by the UPS and ALP, but also by the apoptosis pathway. In the UPS, the ubiquitin E3 ligases MuRF-1 and Atrogin-1/MAFbx act as the two main regulators of muscle protein breakdown [50]. Moreover, metabolic dysfunction is considered a hallmark of both cancer and cachexia and has been shown to impair cancer prognosis. Cancer cachexia involves the action of diverse mediators derived from cancer cells and cells within the tumor microenvironment. However, to date, the molecular mechanisms underlying impaired metabolic regulation are still not fully understood, and the precise mechanisms remains unclear [50].

Clinical data are limited because cachexia occurs at a stage in which patient vulnerability limits the use of invasive metabolic tests and biopsies and disease progression limits the number of patients available for follow-up [53].

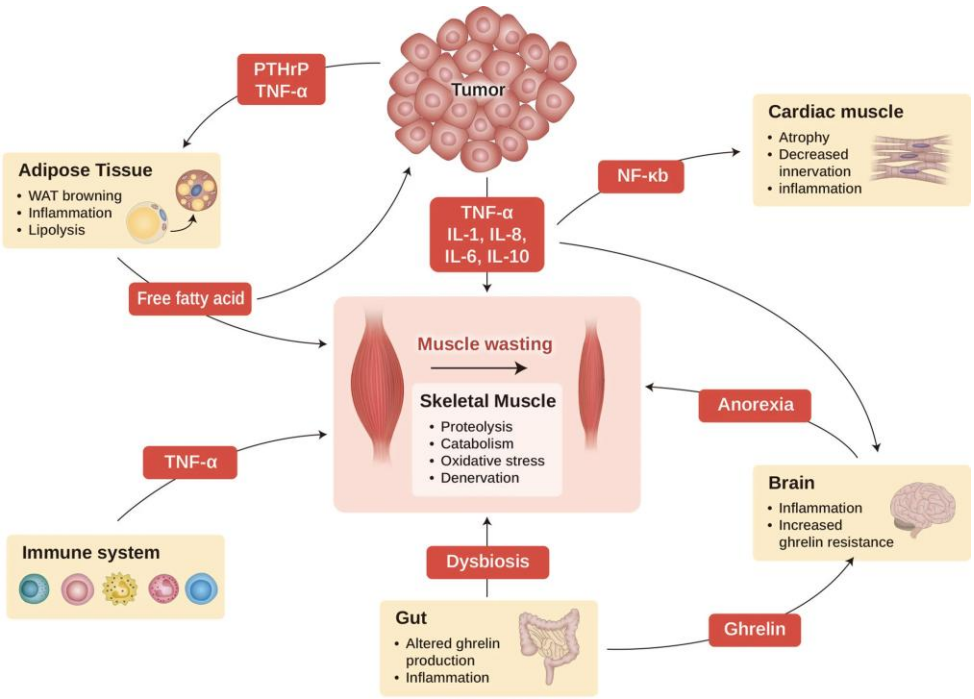


**Figure 3**. Cancer cachexia as a multi-organ syndrome. The scheme illustrates molecular and systemic mechanisms associated with cancer cachexia, highlighting the major organs commonly affected by this syndrome. One of the primary organs involved in skeletal muscle, which is interconnected with alterations in other organs, such as adipose tissue, brain, gut, cardiac muscle and immune system. Tumor cells secrete many factors like cytokines, PTHrP and other mediators, which can induce muscle wasting directly, as well as affecting the other organs, worsening the cachectic condition [56].

- ***Altered energy balance***

Cancer is a condition that profoundly alters the normal homeostatic control of energy balance, and cancer cachexia represents a metabolic disease in which energy intake does not match energy output, causing progressive loss of body mass/wasting and underweight [55]. Energy intake is typically lower than resting energy expenditure in the same patients, indeed wasting in cachexia is impacted by reduced food intake, as less energy is provided to fuel basic metabolic processes [55]. An elevated resting energy expenditure further promotes a negative energy balance and is related in part to tumor metabolism. Tumors compete with other organs and tissues for energy substrates and biosynthetic precursors and possess an intrinsically high metabolic rate [53]. Additional contributions to elevated energy expenditure include inflammation and metabolic cycling, characterized by increased substrate turnover and ATP hydrolysis.

Inflammation is one of the major hallmarks of cachexia and directly stimulates metabolic rate. For instance, the increased glucose flux observed in weight-losing cancer patients may

contribute to energy loss in cachexia [55]. Moreover, energy-wasting cycles between and within organs – so-called futile cycles – have been identified as key contributors to this process. These inter-tissue and intra-tissue cycles involve substrate turnover that consume energy without serving any apparent anabolic or catabolic functions. For example, increased rates of whole-body glycolysis and gluconeogenesis from lactate (the Cori cycle) can increase by more than 300% in cachectic patients [57]. Additionally, futile cycling in brown adipose tissue – where oxidative phosphorylation becomes uncoupled from ATP synthesis, producing heat instead – further enhances inefficiency energy expenditure and contributes to cachexia. Moreover, mitochondrial dysfunction in skeletal muscle might also exacerbate energy inefficiency [54,55].

- ***Pro-cachexia cytokines and signalling pathways involved in cancer cachexia***

A significant factor associated with cancer cachexia is a complex tumor secretome. Tumors secrete a wide range of molecules that stimulate catabolism in target tissues, including numerous pro-inflammatory cytokines, eicosanoids, and other factors with tissue-specific effects, such as heat shock protein 70 (HSP70), HSP90 and members of the TGF-β superfamily. In addition to promoting inflammation, tumors also take part in the generation of catabolic pro-inflammatory factors. These factors lead to humoral, neural, and behavioural outputs which directly activate proteolysis and lipolysis in target organs, mainly skeletal muscle, adipose tissue and cardiac muscle [53] (Fig. 4).

Pro-inflammatory factors with catabolic effects have attracted considerable attention as key mediators of cachexia. Peptide inflammatory mediators involved in this process include interleukin-6 (IL-6), a key regulator of skeletal muscle, as well as interleukin-1 (IL-1), Tumor necrosis factor-α (TNF-α), interferon-γ (IFN-γ), leukaemia inhibitory factor (LIF), growth differentiation factor 15 (GDF15) and TNF-like weak inducer of apoptosis (TWEAK). These signalling molecules are produced by tumor and immune cells, and signal through their respective cell-surface receptors, activating selective transcription factors. Consequently, there is the promotion of the transcription of ubiquitin-proteasome and autophagy components, and their activity is sufficient to promote catabolism in target organs such as skeletal muscle [53].

Beyond inflammatory cytokines, several other circulating factors have been described to exhibit pro-cachectic activity towards skeletal muscle. One such factor is Activin A, a member of the TGF-β superfamily produced by both tumor and immune cells. In cultured myotubes, activin A promotes atrophy, and its overexpression in mice leads to skeletal muscle and body weight loss [58]. Another important pro-cachexia cytokine is TWEAK,

which belongs to the TNF family. It signals through TNF receptor superfamily member 12A (TNFRSF12A). Overexpression of TWEAK in tumors correlates with cachexia. In rodent models of cancer cachexia, there is a strong up-regulation of two of the main components of the ATP-dependent ubiquitin-proteasome pathway: MuRF1 and Atrogin-1/MAFbx. The expression of these E3 ubiquitin ligases is under the control of the transcription factors FoxO1 and FoxO3.

The PI3K/AKT/mTOR pathway is a major regulator of protein synthesis and skeletal muscle homeostasis [50]. Through activation of mTOR complex 1 (mTORC1), AKT promotes anabolic processes in muscle tissues. mTORC1 is a central cellular kinase that integrates multiple signalling pathways, allowing the regulation of anabolic and catabolic processes, including autophagy and lysosomal biogenesis [53]. In cancer cachexia, due to inflammatory factors and cytokines or decreased IGF-1 levels, AKT activity is reduced. This reduction causes FOXO dephosphorylation and nuclear translocation, leading to transcriptional activation of genes involved in degradation of myofibrillar proteins, triggering muscle atrophy program and inducing muscle-protein catabolism [53]. In addition to proteolysis, FOXO transcription factors play a pivotal role in regulating genes involved in the autophagy system. In cachexia, their upregulation leads to excessive activation of autophagy pathways, contributing to enhanced skeletal muscle breakdown. Indeed, patients with cancer-associated cachexia show elevated levels of autophagy markers, such as Beclin-1 [59]. FOXO proteins are also modulated by other signalling pathways. For instance, PGC-1α contributes to the maintenance of the oxidative phenotype of skeletal muscle and protects against oxidative stress. PGC-1α overexpression enhances AKT activity, thereby increasing FOXO phosphorylation and suppressing its catabolic function [50,60].

The E3 ubiquitin ligases and autophagy-related genes are also regulated by other transcription factors, such as NF-κB and STAT3, which plays a central role in promoting both cancer growth and muscle wasting. STAT3 is the main effector of the IL-6/JAK2 signalling pathway, which controls muscle mass, growth, repair and regeneration. Eskiler *et al.* [61] showed that activation of the JAK/STAT pathway induces atrophy in myocytes. Specifically, IL-6 binds to the gp130 and IL-6Rα receptor complex, activating the JAK2 and STAT3. This pathway increases the expression of suppressor of cytokine signalling 3 (SOCS3), a negative regulator of cytokine signalling that inhibits the insulin/insulin-receptor/AKT growth-promoting pathway. In mouse models bearing CT26 tumors, serum IL-6 levels were significantly higher compared with controls, resulting in STAT3 activation and upregulation of Atrogin-1, MuRF-1 and MST, ultimately driving muscle degradation [62]. Similarly, Pettersen *et al.* [63] reported that IL-6 trans-signalling strongly enhances

STAT3 phosphorylation, accelerates autophagy and correlates with a decrease in the survival of patients with cachexia.

Another critical regulator of muscle protein degradation is the NF-κB family, composed of five subunits that interact with each other to form homodimers or heterodimers. NF-κB signalling is activated by various immune receptors, including Toll-like receptors and TNF receptors. Once activated, NF-κB induces the expression of MuRF-1 and Atrogin-1. Beyond protein breakdown, NF-κB can also mediate lipolysis associated with malignant cachexia. This pathway is often controlled by various protein and nucleic acid regulators [50].

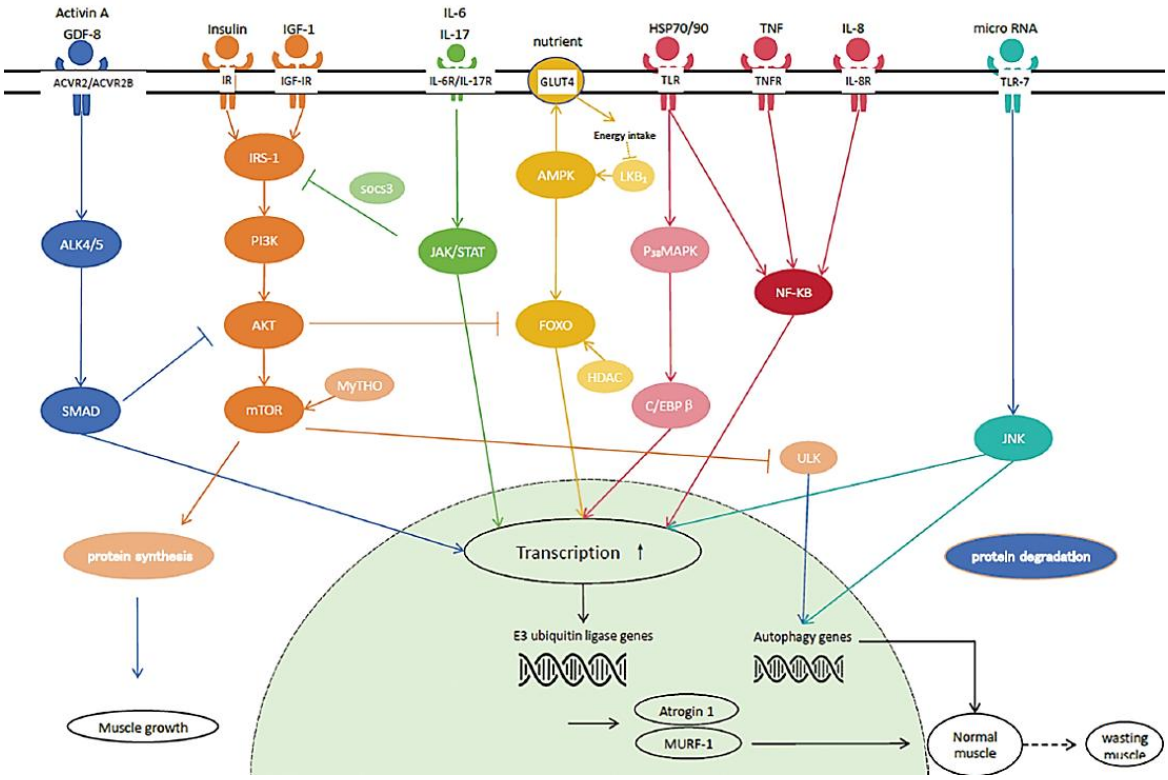


**Figure 4**. Signalling pathways regulating muscle growth and atrophy. Multiple intracellular pathways contribute to muscle wasting by activating E3 ubiquitin ligases and autophagy genes. These catabolic effects in muscle are mediated by key transcription factors, such as p38 MAPK, FOXO proteins, NF-κB and SMAD. The activation of these transcription factors is further enhanced by JAK-STAT and JNK signalling. Moreover, inhibition of the PI3K-AKT-mTOR pathway suppresses protein synthesis, thereby promoting muscle wasting [50].

### 1.5.4. Therapeutic implications

The complexity of the pathogenesis of cancer cachexia-associated muscle atrophy is not completely understood, and refractory cachexia is very difficult to treat [64]. Currently, no effective pharmacological therapies are available to prevent or to treat cancer cachexia. However, several treatments that stimulates appetite and promote weight gain can improve quality of life of affected patients. Despite these interventions, cachexia is considered an irreversible condition, and supplementation with conventional nutritional support alone is insufficient to halt its progression. This limitation represents a significant obstacle to effective palliative care, patient management and overall quality of life [52].

Treatment strategies for cancer cachexia of ESMO guidelines in 2021 and are reported in the following table (Tab. 2).

| | |
|---|---|
| **Nutritional intervention** | Improve food intake, tube feeding, EN/EP, probiotic supplementation |
| **Muscle strenght and endurance training** | Physical exercise and resistance exercise |
| **Psychosocial interventions** | Family care; psychosocial care |
| **Pharmacological interventions** | Corticosteroids, progestins, cannabinoids, androgens, Olanzapine, NSAIDS, Prokinetics, Ghrelin receptor-agonists |
| **Anti-tumor treatments** | Surgery, radiotherapy, chemotherapy, targeted therapy, immunotherapy |

**Table 2**. Treatment strategies for cancer cachexia of ESMO guidelines in 2021. Cancer cachexia treatment includes nutritional intervention, muscle strength and endurance training, pharmacological and psychosocial interventions. Moreover, anti-tumor treatments may be necessary and important in the strategy to treat cancer-induced cachexia [50].

## 1.6. The multiple roles of lactate in skeletal muscle wasting

For a long time, molecules generated during physiological cellular metabolism were considered merely as metabolic waste [65]. Over the past few years, their role has been reconsidered, since these molecules can coordinate a lot of biological processes through their binding to receptors or specific transporters. Lactate is one of these multifunctional metabolites, acting as an intracellular signalling mediator and as an extracellular ligand [66,67]. Lactate plays diverse roles within human body, functioning not only as a a metabolic intermediate but also as a signalling molecule, together with a recently discovered role as an epigenetic regulator. In mammas, lactate is considered both the end product of glycolysis and a substrate for mitochondrial respiration, making it a critical link between glycolytic and oxidative pathways. Moreover, increasing evidence indicates that lactate is essential for energy and redox homeostasis [68]. Lactate is the principal messenger in a complex feedback loop system. According to the Lactate Shuttle Hypothesis, communication between cells that produce lactate and those that utilize or respond to it can transcend compartment barriers occurring within and among cells, tissues and organs [69]

Lactate can induce autocrine, paracrine and endocrine-like effects and it is involved in various pathways in different cell types and tissues, mediating regulatory effects. These include modulation of immune system and inflammatory responses, promotion of wound healing through enhanced angiogenesis, inhibition of lipolysis in adipocytes and neuroprotective actions [68]. Moreover, lactate signalling contributes to epigenetic regulation through lactylation of lysine residues of histones, which stimulates gene transcription from chromatin and may represent a potential mechanism for the maintenance of homeostasis [68].

As a signalling molecule, lactate acts through the binding to the G-protein coupled receptor GPR81, known also as HCAR1 (Hydroxycarboxylic Acid Receptor 1), which triggers the typical signalling cascade of the G-protein coupled receptors. More recently, lactate has been shown to influence chromatin state and gene transcription directly through the binding to histones.

However, lactate accumulation and shuttling may be pathological, since it provides energetic and anabolic support to cancer cells. In this context, lactate can function as an oncometabolite in several types of cancer, through the modulation of lactate-sensing proteins, such as monocarboxylate transporters (MCTs) or GPR81 itself [66,70]. This leads to tumor proliferation and dissemination, escape from the immune system and therapy resistance [66]. The aggressiveness of certain types of cancer is associated with augmented lactate production, accumulation and increased glucose uptake, even under aerobic

conditions – a phenomenon known as the "Warburg Effect". This effect describes the presence of cancer cells for glucose fermentation over oxidative phosphorylation, even in the presence of oxygen [18]. This intensified lactate production, known as lactagenesis, appears to be closely associated with carcinogenesis [66,68,69].

### 1.6.1. Lactate as a cellular metabolite

Skeletal muscle is a highly dynamic tissue that plays a fundamental role in locomotion, posture maintenance, and energy metabolism [71]. It has a significant contribution in energy expenditure, metabolic regulation, homeostasis, glucose metabolism, and lactate production [72]. Nearly 99% of lactic acid is dissociated into lactate anions ($La^-$) and protons ($H^+$) at a physiological pH range [68].

In humans, lactate is mainly composed of L (+) enantiomer (L-form), which is the only form detected in the serum of healthy individuals. Serum D-lactate concentrations typically range from 0,013 to 0,2 mM, whereas L-lactate levels may range from slightly above 1,14 mM at rest, 15 mM after an intense exercise, and 30 mM in certain cancer tissues. For an adult weighting about 70 kg, approximately 1,400 mmol of lactate are produced daily, mainly by the muscle (25%), skin (25%), brain (20%) and intestines (10%). To maintain the serum concentrations between 1 and 2 mM, about 60-120 mmol of lactate needs to be removed from the blood every hour. Lactate is usually removed immediately from various tissues such as skeletal muscle, or it may be released and taken up by exercising muscle [68]. The majority of the lactate (approximately 75-80%) is either oxidized locally or taken up by active skeletal muscle [73], heart [74], brain [75], or liver, where it serves as a substrate for gluconeogenesis [76].

Therefore, lactate plays two key metabolic roles: (1) it acts as an energy source, and (2) it is the main gluconeogenic precursor. Beyond its role as an oxidative fuel, lactate provides carbon skeletons for glucose synthesis. In this context, skeletal muscle and liver are metabolically connected through the Cori cycle, an organ-organ lactate shuttle. In this cycle, lactate is transported from muscle to liver, where it is converted into pyruvate by hepatic lactate dehydrogenase (LDH) and subsequently utilized for gluconeogenesis [68].

As both the end product of glycolysis and the substrate for oxidative phosphorylation (OXPHOS) or gluconeogenesis, lactate can represent the link between different metabolic pathways. In 1985, George Brooks proposed the “Lactate Shuttle Hypothesis”, which points out that lactate can be up taken by intracellular organelles, such as mitochondria and peroxisomes, or secreted into the bloodstream to be used as a fuel by other tissues and organs [77,78]. This theory includes *intracellular* lactate shuttles, such as cytosol-mitochondrial

and cytosol-peroxisome exchanges, and *cell-to-cell* lactate shuttle, which facilitate lactate transfer between different cell types [79]. For example, in contracting skeletal muscle, lactate production and utilization can occur simultaneously. It has been proposed that myocytes have two metabolic compartments: one for glycolysis (cytoplasm) and the other one for oxidative metabolism (mitochondria). According to this model, cytosolic lactate enters mitochondria via lactate transporters (the intracellular lactate shuttle), and it is oxidized to pyruvate through the mitochondrial lactate oxidation complex (mLOC) located at the inner mitochondrial membrane [68].

Lactate production in skeletal muscle results from lactic fermentation, a process activated during intense anaerobic exercise [80]. Under these conditions, glucose is metabolized through glycolysis to produce pyruvate, which, under hypoxic conditions or high energy demands, is converted into lactate by LDH. This reaction provides a rapid mechanism for oxidized NAD regeneration, thereby sustaining glycolysis and ATP production [77] (Fig. 5).

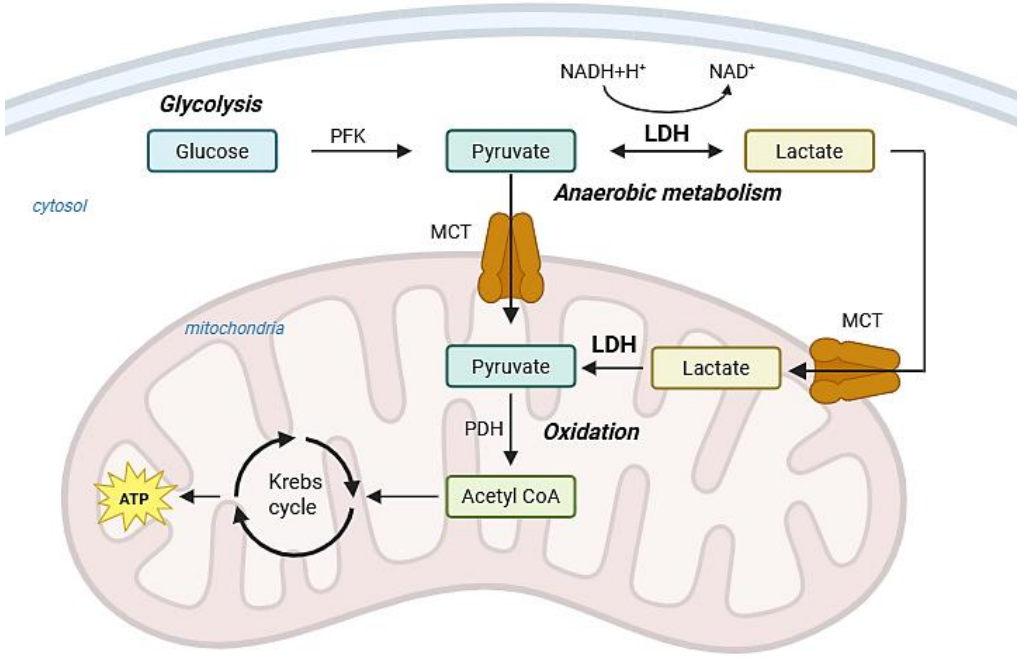


**Figure 5**: Glucose metabolism leading to pyruvate and lactate production. Glucose is converted into pyruvate in the cytosol through glycolysis. Under aerobic conditions, pyruvate is transported into mitochondria via monocarboxylate transporters (MCTs), where is converted into acetyl-CoA by the pyruvate dehydrogenase complex (PDC), which requires thiamine diphosphate (TPP) as a cofactor. Acetyl-CoA then enters the tricarboxylic acid (TCA) cycle (also known as the Krebs cycle), leading to ATP production through oxidative phosphorylation. Under anaerobic conditions, mitochondrial oxidation is reduced, and lactate dehydrogenase (LDH) catalyses the conversion of pyruvate into

lactate in the cytosol. Excess lactate can subsequently be transported back into mitochondria via MCTs and re-oxidized to pyruvate, fuelling the TCA cycle. The figure was created with biorender.com.

LDH is a tetrameric enzyme which belongs to the 2-hydroxy acid oxidoreductase family. As previously mentioned, it plays a pivotal role in the metabolic switch of oxidative phosphorylation to glycolysis, and it contributes to the balance between carbohydrate catabolism and anabolism. During the conversion of pyruvate to lactate, the regeneration of $NAD^+$ from NADH is fundamental for ongoing glycolysis. Moreover, LDH is also involved in gluconeogenesis, where lactate is metabolized to glucose through a reverse LDH reaction. In addition, lactate oxidation provides substrates for the tricarboxylic acid (TCA) cycle, thereby linking anaerobic and aerobic metabolism. However, high levels of LDH in the blood may be linked to various pathological conditions, such as traumatic injury, liver diseases, some types of anaemia, heart attack, viral infection and cancer.

From a structural point of view, LDH is a tetrameric enzyme composed of two distinct subunits: M (muscle type) and H (heart type), which are differentially expressed in diverse tissues. In skeletal muscle, there is a prevalence of the M subunit, and it facilitates the conversion of pyruvate into lactate under anaerobic conditions. In contrast, cardiac tissue mainly expresses the H subunit, which catalyses the oxidation of lactate to pyruvate, supporting continuous aerobic metabolism [81]. The myocardium requires a constant energy supply, which is supported by the conversion of lactate into pyruvate. The H subunit of LDH has its maximal activity at low pyruvate concentrations, but it is inhibited when pyruvate levels are elevated, whereas the M subunit remains active in the presence of high concentrations of pyruvate. The M subunit is also known as LDHA, while the H subunit as LDHB. Combinations of these two subunits generate five LDH isozymes (LDH1-LDH5), which differ in their kinetic properties and tissue distribution [82].

Lactate is transported across cytoplasmic and intracellular compartments by MCTs, which function as proton-lactate symporters [68]. In skeletal muscle, lactate is extruded from muscle cells along with hydrogen ions in a 1:1 ratio through facilitated diffusion via the monocarboxylate transporter 4 (MCT4). Once in the interstitial space or bloodstream, lactate can be co-transported with a hydrogen ion by monocarboxylate transporter 1 (MCT1), also known as SLC16A1, where it is converted back into pyruvate and oxidised [83]. The involvement of lactate transport in metabolic regulation has been widely investigated [79]. Recent scientific evidence indicates that aerobic glycolysis, and thus lactate production, can also occur under non-cancerous stress conditions, including high-altitude exposure, trauma,

sepsis, pancreatitis, and heart failure [78]. As a result, lactate is now widely considered as a valuable and functional metabolite, replacing the traditional perspective that elevated lactate levels are indicative of cellular anaerobic metabolism [84].

In skeletal muscle, lactate can be directly oxidised within mitochondria (Fig. 6). The mitochondrial oxidation of lactate has been demonstrated through several approaches, including magnetic resonance spectroscopy, confocal microscopy, and immunohistochemistry [85,86]. Extensive studies in healthy human subjects have identified that the main lactate oxidation site is the mLOC. Within this complex, lactate is converted by mitochondrial LDH into pyruvate, which enters the Krebs cycle. This mechanism is important in skeletal muscle, as it provides an effective mechanism for ATP regeneration when energy demand is high, for example during high intensity exercise. The mLOC consists of mitochondrial LDH, which is anchored to the outer side of the inner mitochondrial membrane and associated with cytochrome oxidase (COX) and mitochondrial MCT1. The exergonic redox reactions of the mitochondrial electron transport are coupled with lactate oxidation. Ultimately, MCT1 facilitates the transport of pyruvate across the inner mitochondrial membrane [86].

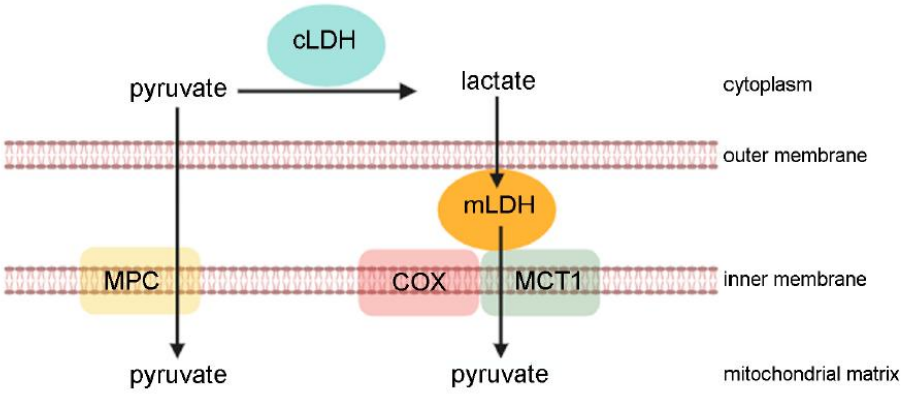


**Figure 6**: Lactate oxidation within mitochondria. Lactate produced in the cytoplasm by cytoplasmatic LDH (cLDH) can enter the mitochondrial intermembrane space, freely crossing the outer mitochondrial membrane. Within this space, the mitochondrial LDH (mLDH) converts lactate into pyruvate, which then enters the mitochondrial matrix through the MCT1 transporter. MCT1, located in the inner mitochondrial membrane, together with cytochrome oxidase (COX) and mLDH, forms the so-called “lactate mitochondrial oxidation complex”. Cytoplasmic pyruvate can directly enter the mitochondrial matrix via the mitochondrial pyruvate carrier (MPC), also situated in the inner mitochondrial membrane. Once in the matrix, pyruvate becomes the substrate for the pyruvate dehydrogenase complex, which catalyses its conversion into acetyl-CoA [87].

During muscle contraction, the metabolic rate of skeletal muscle increases in an exponential way, and the high ATP consumption is buffered by modulating the rates of glycolysis and glycogenolysis [88]. In conditions of resting in healthy individuals, lactate concentrations in the muscles and arterial blood are typically around 1,0 mM [88]. However, lactate levels can highly fluctuate, leading to significant changes in the lactate/pyruvate ratio, which dynamically affect the $NAD^+$/NADH redox balance. Consequently, lactate production plays a pivotal role in metabolic regulation and cellular redox homeostasis. In this context, lactate can influence the generation of reactive oxygen species (ROS) by an enzymatic and a non-enzymatic mechanism, mainly involving ROS production through mitochondria respiration [89]. In particular, mitochondrial lactate metabolism contributes to ROS production, specifically hydrogen peroxide ($H_2O_2$), through a flavin-dependent lactate oxidase (LOX) pathway.

### 1.6.2. Lactate as a signalling molecule

The signalling functions of lactate at the extracellular level are mediated by its interaction with GPR81, a G protein-coupled receptor (GPCR). GPR81 is primarily located on the plasma membrane, but it has also been found also in other intracellular organelles, such as mitochondria, thus implying a role for GPR81 in lactate trafficking between the plasma membrane and intracellular compartments [90]. Although GPR81 is mainly expressed in the adipose tissue, it is also present in skeletal muscle, liver, spleen, kidney and brain [68,91]. Activation of GPR81 occurs at lactate concentrations between 0,2 and 1,0 mM, leading to cyclic AMP (cAMP) downregulation and inhibition of protein kinase A (PKA)-mediated signalling [92]. Recent studies have also identified a non-canonical pathway for GPR81, resulting in the inhibition of Toll-loke receptor 4 (TLR-4) and NOD-like receptor pyrin-domain-containing protein 3 (NLRP3) inflammasome, both of which mediate the production of pro-inflammatory mediators such as IL-1β and IL-18 [93,94].

GPR81 is a $G_i$-type G protein-coupled receptor that activates the $G_i$ signalling pathway. This receptor is involved in metabolic regulation of multiple tissues and cell types, influencing the $G_i$ signalling pathway and its associated molecular mediators. Upon agonist binding, a GDP-GTP exchange in the GPCR α subunit. The resulting downstream signalling is driven by secondary messengers such as cAMP and $Ca^{2+}$, depending on the specific α subunit type involved, although Gα -independent signalling also exists [67].

- *cAMP-PKA signalling pathway*

Cyclic adenosine monophosphate (cAMP) is a second messenger that mediates various biological responses to extracellular signals, such as cell migration, differentiation, proliferation and apoptosis. G proteins activate the cytomembrane adenylyl cyclase (AC) which catalyses the conversion of ATP into cAMP, leading to the activation of the downstream protein kinase A (PKA). In contrast, the activated $G_i$ signal decreases AC activity and the production of cAMP.

In adipose tissue, GPR81 exerts an anti-lipolytic effect through activation of the intracellular $G_i$ signal. The inhibition of cAMP levels and PKA activity will decrease the activity of hormone sensitive lipase (HSL) and adipose triglyceride lipase (ATGL), that leads to lipolysis inhibition. In cultured skeletal muscle cells, GPR81 increases the levels of triglyceride (TG) and the expression of Malonyl-CoA-acyl carrier protein trans acylase (MCAT) through inhibiting the cAMP response element (CRE)-binding protein (CREB), a transcriptional cofactor protein modulating cellular metabolism and immune response [95].

- *ERK1/2 signalling pathway*

GPR81 plays an important role in cellular metabolism by influencing the phosphorylation of extracellular regulated protein kinases (ERK1/2). This receptor has been shown to modulate metabolic activity in diverse tissues and cells, such as brain, skeletal muscle, and osteoblasts. Since ERK1/2 is crucial for many metabolic signalling pathways, including proliferation, differentiation, apoptosis and survival, GPR81 could have a significant role in maintaining metabolic balance. GPR81 activates ERK1/2 signalling primarily through the $G_i$ signalling pathway, following dissociation of the $G_{i\alpha}$ and $G_{i\beta\gamma}$ subunits. The $G_{i\alpha}$ subunit enhances ERK1/2 activation indirectly by inhibiting AC, thereby lowering cAMP levels and PKA activity. This process activates Ras, the upstream molecule of C-Raf. As a result, the inhibitory effect on C-Raf is diminished, boosting ERK1/2 activity. On the other hand, the $G_{i\beta\gamma}$ subunit promotes ERK1/2 activation through pathways involving phospholipase C (PLC), protein kinase C (PKC) and protein kinase B (PKB). [95]

#### 1.6.2.1. Multiple effects of lactate-GPR81 signalling in different cell types

GPR81 is predominantly expressed in adipose tissue in mice, rats and humans, where lactate signalling via GPR81 inhibits lipolysis, promoting lipid accumulation (Fig. 8). These effects have also been observed in skeletal muscle. GPR81 primarily signals via $G_{i\alpha}$, suppressing the PKA pathway, thereby contributing to insulin-mediated inhibition of lipolysis by reducing cAMP production [67]. Ahmed *et al.* demonstrated that GPR81 might also be linked to obesity. Indeed, mice lacking GPR81 (*Gpr81*-null) do not show any difference in body weight when fed a normal diet; however, when fed a high-fat diet, *Gpr81*-null mice show a significant reduction in weight gain compared to wild type controls [96].

Beyond adipose tissue, lactate plays also an important metabolic role in the brain, specifically during exercise and in the shuttling of lactate between astrocytes and neurons. The recent discovery of GPR81 expression throughout the brain and in the retina has shed a light on unknown mechanisms through which lactate acts as a signalling molecule in neuroprotection, angiogenesis and neuronal activity regulation. GPR81 is expressed in neurons, astrocytes and endothelial cells within the cortex, hippocampus, blood-brain barrier and retinal. Physical exercise promotes angiogenesis in the brain, and this effect is due to exercise-induced increases in circulating lactate, which activates GPR81 in endothelial cells [91]. GPR81 knockout mice show increased neuronal activity suppression via both $G_{i\alpha}$ and $G_{i\beta\gamma}$ subunits. In rodents, lactate affects learning and memory, and it is associated with neuroplasticity, neurogenesis and neuroprotection [67].

The signalling effects mediated by lactate are influenced by factors such as lactate concentration, extracellular pH and nutrient availability within the cellular microenvironment [97]. Recent studies have demonstrated that lactate produced through aerobic glycolysis exerts immunosuppressive effects under conditions like sepsis, cancer, chronic inflammation and autoimmune diseases [98,99].

GPR81 has an important role in tumor growth, as cancer cells generate large amounts of lactate, exporting it into the extracellular milieu. This role could be autocrine where extracellular lactate acts on GPR81 expressed on tumor cells themselves. On the other hand, this role could be paracrine where extracellular lactate produced by cancer cells act on GPR81 expressed on non-cancer cells in the tumor microenvironment, such as immune cells, endothelial cells, adipocytes and fibroblasts. Both mechanisms could influence the growth and proliferation of tumor cells as there is a functional crosstalk between tumor cells and stromal cells. Elevated extracellular lactate levels in tumors are linked to poor prognosis, supporting a tumor-promoting role for GPR81 signalling [68,91].

GPR81 is expressed in various tumors from patients and cancer cell lines. *In vivo*, GPR81 levels correlate with tumor growth and metastasis in pancreatic patients, and both dramatically decrease upon GPR81 silencing. Lactate signalling via GPR81 promotes angiogenesis, impairs antitumor immunity and increase DNA repair. Angiogenesis is promoted through PI3K/AKT-cAMP-CREB signalling, leading to pro-angiogenic amphiregulin (AREG) production, as observed in breast cancer. Moreover, lactate impairs antitumor immunity, through GPR81 signalling in tumor-infiltrating dendritic cells, downregulating MHC-II expression and reducing type I interferon (IFN) production through $G_{i\beta\gamma}$-$Ca^{2+}$-calcineurin signalling. GPR81 signalling also induces programmed death-ligand 1 (PD-L1) expression in lung cancer via TAZ/TEAD activation, impairing T cell cytotoxicity. Lastly GPR81 is involved in upregulating DNA repair proteins and the drug-exporting transporter ABCB1 via the $G_{i\alpha}$-PKC-ERK pathway [67]. Interestingly, lactate can also inhibit proinflammatory responses in macrophages through both cAMP-independent and GPR81-indepenent manner [100]. It also augments the production of anti-inflammatory cytokine, such as IL-10 in dendritic cells and reduce the production of pro-inflammatory IL-12 in response to Toll-like receptor (TLR) stimulators [101]. Additionally, lactate downregulates TNF-α, NF-kB and PTX-3, and upregulates IL-23 in monocytes and transiently suppressing chemokine expression [102]. In human cytotoxic T cells, lactate inhibits proliferation and cytokine production, thereby reducing their cytotoxic activity [103,104].

Lactate also contributes to reparative angiogenesis by recruiting endothelial progenitor cells, stimulating endothelial cell migration, activating procollagen factors and enhancing collagen deposition within the extracellular matrix [105,106]. Furthermore, it has been reported that oral administration of the GPR81 agonist 3-Chloro-5-hydroxybenzoic acid (CHBA) in mice significantly increases the weight of plantaris and soleus muscles, an effect associated with increased phosphorylation of ERK1/2 proteins [107].

In human skeletal muscle**,** GPR81 is predominantly expressed in type II glycolytic fibers, compared with type I oxidative fibers. These type II fibers are known to generate the highest levels of lactate, suggesting a potential autocrine signalling role for lactate [108]. One of the main downstream targets of PKA is the CREB protein. Thus, activation of GPR81 by lactate, leads to a lower PKA activity, which leads to reduced CREB phosphorylation. Although exercise increases lactate levels, its impact on CREB phosphorylation in skeletal muscle remains unclear so far [108]. Beyond its role in lipolysis regulation, lactate has also been shown to induce the expression of genes involved in lactate and energy metabolism in

skeletal muscle, as demonstrated by Hashimoto *et al.* [86]. However, it is still uncertain whether this gene regulatory effect is mediated through GPR81 signalling.

Finally, the lactate signalling through GPR81 is also implicated in several additional physiological and pathological processes, including retinal function, osteoblast differentiation via GPR81-$G_{i\beta\gamma}$-PLC-PKC-AKT signalling, regulation of inflammation during labour, suppression of innate immunity, and homeostatic control in intestinal, renal, cardiovascular and atherosclerotic tissues [67].

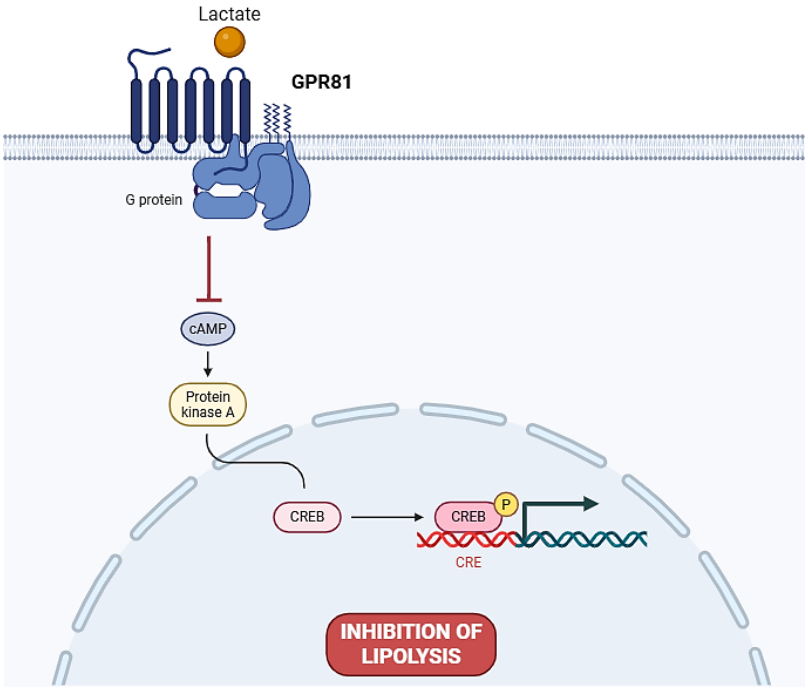


**Figure 7**: Lactate signalling through GPR81. Ligand binding leads to the activation of inhibitory G proteins and the decreased production of cyclic AMP (cAMP). In turn, Protein Kinase A (PKA) activity and phosphorylation of CREB transcription factor are reduced, thus leading to decreased lipolysis. The figure was created with biorender.com.

### 1.6.3. Lactate in skeletal muscle diseases

Lactate has been linked to various diseases, including obesity and insulin resistance, the latter being one of the major challenges leading to the development of type 2 diabetes [109]. The involvement of lactate in the onset of insulin resistance has been reported in skeletal muscles of rats, where augmented amounts of plasma lactate suppressed insulin-stimulated glycolysis. This results in reduced glucose uptake and disruption of the insulin signalling cascade [110].

In cancer cachexia, a severe metabolic condition associated with oncologic disease that causes significant weight loss and worsens clinical outcomes, lactate production is markedly

increased. Skeletal muscles from cachectic mice showed higher MCT1 expression and a significantly elevated lactate/pyruvate ratio, indicating the increased production and release of lactate by the tissue [111]. Similarly, in myotubes, cachectic conditions are associated with increased lactate levels and reduced oxygen consumption [112,113]. The cachectic phenotype is associated with a metabolic shift towards lactic fermentation. Inhibition of LDH with sodium oxamate prevents the development of cachectic condition, thus demonstrating the role of this metabolic conversion in the onset of the cachectic condition [112]. Furthermore, the lactate/pyruvate ratio appears decreased in muscles of cachectic mice, due to increased lactate production. Treatment with 2-deoxyglucose, which blocks glycolysis and pyruvate formation, prevents the development of cachectic features in mice, further confirming lactate's pivotal role in the onset of cancer cachexia [114]. Importantly, GPR81 ablation is sufficient to prevent the onset of cancer cachexia in both adipose tissue and skeletal muscle [115], highlighting lactate's significance in the onset and progression of this pathology.

Mutations in the gene-encoding lactate transporter MCT1, or altered expression of the protein, are observed in muscular diseases. In McArdle disease (Glycogen Storage Disease Type V, MD), a metabolic myopathy characterized by impaired glycogenolysis due to a deficiency in muscle glycogen phosphorylase, patients exhibit elevated MCT1 levels [116]. This increase may represent a compensatory mechanism to sustain energy production in the absence of glycogenolysis [117]. MCT1 is encoded by the SLC16A1 gene, which consists of five exons interspersed by four introns [118]. Mutations in this gene are linked to clinical conditions, such as recurrent severe ketoacidosis, a pathology that occurs when ketone formation exceeds ketone utilization. It is caused by homozygous or heterozygous mutations in the SLC16A1 gene. Furthermore, a missense mutation in the MCT1 gene can impair lactate transport and muscle injury in humans [119].

Novel evidence indicates that single-nucleotide polymorphism (SNP) can be useful biomarker for assessing genetic background to predict therapeutic responses and prognosis in cancer patients [120]. In this context, SNP in the MCT1 gene could be used as a prognostic indicator in colorectal cancer patients and as a predictive marker in adjuvant chemotherapy [121].

## 2. MATERIALS AND METHODS

### 2.1. Materials

C2C12 murine myoblasts were from ECACC (European Collection of Authenticated Cell Cultures, Salisbury, UK). The murine 3T3L1 preadipocytes and CT26 colon carcinoma cell lines were obtained from ATCC (American Type Culture Collection, Manassas, VA, USA).

Muscles biopsies from patients were obtained through a collaboration with the AOUC-Careggi University Hospital in Florence, Italy. All procedures were conducted in accordance with ethical standards and approved by the relevant Ethics Committee, ensuring compliance with institutional and national regulations for research involving human subjects.

Male C57BL/6J mice were purchased from The Jackson Laboratory (Bar Harbor, ME, USA). They were fed with a standard diet (Carfil quality, Oud-Turnhout, Belgium); the solidified water was from Solid Drink, Triple A Trading, Tiel, The Netherlands) and AdipoRon was from Bio-Techne (Minneapolis, MN, USA).

Unless differently specified, all reagents were obtained from Sigma-Aldrich, Inc (St. Louis, MO, USA); SDS-PAGE materials and ECL detection reagents were from Bior-Rad Laboratories, (Hercules, CA, USA). Anti-STAT3 and Anti-αSMA primary antibodies were from Abcam (Cambridge, UK). Anti-vimentin, anti-MHC, anti-LDH-A, anti-acrp30, anti-citrate synthase primary antibodies and the STAT3 Inhibitor III WP10676 were from Santa Cruz Biotechnology (Dallas, TX, USA). Anti-pSTAT3 primary antibody was from Cell Signalling (Danvers, MA, USA). Anti-GPR81 primary antibody was from Protein Tech. Anti-MHC primary antibody for confocal analysis was from Abcam (Cambridge, UK). Anti-Atrogin-1 primary antibody was from Invitrogen (Thermo Fisher Scientific, Waltham, MA, USA). Diff-Quick staining kit was from Medion Diagnostic (Düdingen, Switzerland). Palmitic acid was from Fluorochem (Hadfield, UK).

Sodium oxamate, DAPI (4'-6-Diamidino-2-phenylindole), sodium L-lactate, 3,5-dihydrobenzoid acid, α-Cyano-4-hydroxycinnamic acid (CHC) were from Sigma-Aldrich, Inc (St. Louis, MO, USA); the inhibitor of STAT3 WP1066 was from Santa Cruz; Auranofin was from Merck.

High-Capacity cDNA Reverse Transcription Kit and PowerTrack™ SYBR Green Master Mix for qPCR were from Applied Biosystems™; GPR81 and LDH-A RT-PCR primers, RNase-free water were from Invitrogen.

K-LATE kit for lactate assay was from Megazyme (Bray, Ireland); MCT4 (SLC16A3) ELISA Kit was from Abbexa (Cambridge, UK); QuantiChrom$^{TM}$ Lactate Dehydrogenase Kit (D2DH-100) was from BioAssay Systems (Hayward, Ca, USA); Thioredoxin Reductase

Assay Kit was from Sigma-Aldrich, Inc (St. Louis, MO, USA). 2'-7'-dichlorofluorescein-diacetate (DCF-DA) was from Sigma-Aldrich, Inc (St. Louis, MO, USA).

## 2.2. Methods

### 2.2.1. Cell culture

Murine C2C12 myoblasts, murine CT26 colon carcinoma cells and murine 3T3L1 preadipocytes were grown in a medium consisting of Dulbecco's Eagle's modified (DMEM, Euroclone, Milan, Italy) supplemented with 10% Fetal Bovine Serum (FBS), L-glutamine 100X (200 mM), Penicillin-Streptomycin 100X in a 5% $CO_2$ humidified atmosphere.

For differentiation into myotubes, sub-confluent C2C12 were shifted into growth medium consisting of DMEM containing 2% Horse Serum (HOS). C2C12 were maintained for four days in differentiating medium until well-differentiated myotubes were obtained from myoblasts fusion.

For the differentiation of 3T3L1 into adipocytes, 3 x $10^3$ cells per $cm^2$ were seeded and grown until reaching about 70% confluence. Cells were maintained for three days in MDI induction medium composed of 0.5 mM of 3-isobutyl-1-methylxanthine, 1 µM of dexamethasone, and 10 µg/mL of insulin. After three days, MDI induction medium was replaced with DMEM containing 10% FBS and 10 µg/mL of insulin. After an additional three days, insulin-containing medium was replaced with DMEM containing 10% FBS that had been replaced every two days until fully differentiated adipocyte-like cells were obtained.

Human primary adipose stem cells (ASCs) were isolated from the stromal vascular fraction derived from visceral adipose tissue biopsies conducted after receiving written informed consent (Local Ethical Committee's approval Ref. Protocol 58-11 03/06/2011), as described elsewhere [122]. ASCs were cultured in DMEM supplemented with 20% FBS, 2 mM of L-glutamine, 100 U/mL of penicillin, 100 µg/mL of streptomycin, and 1 µg/mL of Amphotericin-B. Cells were incubated at 37 °C in a humidified 5% CO2 atmosphere. For the experiments, ASCs between passages 2 and 7 were used. For adipose differentiation, 5 x $10^4$ ASCs were plated in 6-well plates and induced to differentiate into mature adipocytes using a differentiation medium (DMEM containing 10% FBS, 0.5 mM 3-isobutyl-1-methylxanthine, 1 µM dexamethasone, 10 µM insulin and 1 µM rosiglitazone) for 15 days. ASCs cultured for the same period in DMEM containing 10% FBS were used as a control.

### 2.2.2. C2C12 spheroid formation

Spheroids are three-dimensional (3D) cellular models that form from the spontaneous aggregation of cells in culture in complete DMEM medium supplemented with 2% HOS. Once C2C12 cells reach 70-80% sub-confluence, cells are detached using Trypsin-EDTA 1X (in PBS, without Phenol Red, without calcium, without magnesium, sterile filtered), counted and seeded to form spheroids. Each spheroid consists of 30000 cells, and approximately 8-10 spheroids were seeded per condition. To promote spontaneous cell aggregation, a 96-well concave-bottom multiwell plate is used. After 72 hours, spheroid formation is observed, after which the spheroids are treated with 30% CM CT26, 20 mM lactate and 10 mM DHBA for 48 hours.

### 2.2.3. Conditioned Media preparation

CT26 colon carcinoma cell line and fibroblasts isolated from abdominal muscles of cancer patients were cultured in growing medium until sub-confluence. Cells were then washed twice with PBS, and then serum-free medium was added for 48 hours. The Conditioned Medium (CM) was then centrifuged at 1500 rpm for 10 minutes to remove debris and immediately used for myotube treatment or stocked at -80 °C. For the treatment of myotubes, CM CT26 was diluted at 30% final concentration (and in the case of CM obtained from fibroblasts, CM was diluted at 50% final concentration) in differentiating medium (HOS 2%). Myotubes were treated for 24 hours.

### 2.2.4. Measurements of width of myotubes, diameter of spheroids and width ad area of lipid droplets

Measurements of the width of myotubes, the diameter of spheroids and the width and area of lipid droplets were obtained using ImageJ software version 1.8. For myotubes, at least five randomly chosen fiends of each sample were used, and, for each field, a minimum of five myotubes were measured. For spheroids, at least 8-10 spheroids for each condition were measured, and for each, the diameter was measured twice. For adipocytes, at least ten randomly chosen fields for each sample were used, and, for each adipocyte, a minimum of 20 lipid droplets were measured. The mean value is reported in the bar graph.

### 2.2.5. Abdominal muscle biopsies and fibroblasts isolation

Muscle biopsies are taken from the abdominal muscle from patients with gastrointestinal tract tumors, specifically: colorectal adenocarcinoma, pancreatic head adenocarcinoma, hepatocellular carcinoma, gallbladder adenocarcinoma, intrahepatic cholangiocarcinoma, liver metastases from colorectal cancer, and metastases from duodenal adenocarcinoma. Muscle biopsies were washed in Phosphate-buffered saline (PBS), and any adipose tissue was carefully removed using sterile forceps and scalpels. Muscles that were not immediately used for experiments were stored at -80 °C.

Fibroblast primary cultures were obtained from fresh biopsies, which were washed in PBS and carefully fragmented with sterile scissors and scalpels, and subsequently transferred into a Petri dish. Each Petri dish will contain at least 10 small pieces of muscles and to promote the spontaneous migration of fibroblasts from tissue fragments to growing medium, a sterile microscope slide was placed on top of them. Cells were maintained in DMEM medium supplemented with 20% FBS, L-glutamine 100X, Penicillin-Streptomycin 50X and Amphotericin B 50X during the initial phase, and later with 10% FBS L-glutamine 100X, Penicillin-Streptomycin 50X and Amphotericin B 50X in a 5% $CO_2$ humidified atmosphere. Once fibroblasts outgrowth was established, the microscope slide was removed and maintained in growth medium.

### 2.2.6. Evaluation of Oxygen Consumption Rate (OCR)

After myotubes and adipocytes treatment, cells were detached, washed with PBS, and suspended in 1 mL of growing medium. Cell suspension was transferred to an airtight chamber maintained at 37 °C. A Clark-type $O_2$ electrode (Oxygraph Hansatech, Norfolk, England), and it was used to assay myotube and adipocyte oxygen consumption over 10 minutes. Oxygen consumption rate (OCR), measured as nmol/mL/min, was obtained, and the OCR was normalized with respect to the total protein content of each sample and is reported in the bar graph as nmol $O_2$ /min/mg.

### 2.2.7. Lactate assay

Lactate assay was performed in culture medium using the K-LATE kit (Megazyme, (Bray, Ireland)) according to the manufacturer's instructions. Prior to the treatment of myotubes and adipocytes, lactate amount was measured in CM CT26. To obtain the amount of lactate exclusively produced by myotubes and adipocytes, lactate quantity in CM CT26 was subtracted from lactate in the medium obtained from treated myotubes and adipocytes. Data were normalized using total protein content in each sample, thus obtaining mg/mL of lactate.

In muscles, the amount of lactate (mg/ml) was normalized on the weight in mg of muscular biopsies.

### 2.2.8. Immunoblot assay

Cells were lysed for 20 minutes on ice in 100 µL of complete radioimmunoprecipitation assay (RIPA) buffer (150 mM NaCl, 100 mM NaF, 2 mM EGTA, 50 mM Tris HCl pH 7,5, 1 mM orthovanadate, 2% triton, 0,1% SDS, and 0,1% protease inhibitor cocktail). Muscles biopsies were first mechanically lysed using a mortar and pestle, using liquid nitrogen. Subsequently, 500 µL of complete RIPA buffer was added to each sample. Lysates were then centrifugated at 14000 rpm at 4 °C for 10 minutes, and the supernatant was recovered. Total protein content of each sample was obtained using the Bradford assay (Bio-Rad Laboratories, Hercules, USA). The same quantities of proteins for each sample were separated using SDS-PAGE and transferred onto PVDF membranes. PVDF membranes were incubated with a specific primary antibody in 2% non-fat dry milk solution (PBS, 0,05% tween) at 4 °C for 24 hours and with horseradish-conjugated secondary antibody for 1 hour at room temperature. Specific protein bands were detected using chemiluminescence reactions induced by probing PVDF membranes with ECL (Bio-Rad Laboratories, Hercules, CA, USA) and quantified using ImageJ software (version 1.8). Coomassie-stained PVDF membranes or Red Ponceau-stained PVDF membranes were used for normalization, and the mean values are reported in the bar graph as arbitrary units.

### 2.2.9. Cellular fractionation

Myotubes treated for 48 hours with CM CT26, 20 mM lactate and 10 mM DHBA were detached and washed with PBS. Then, cells were transferred into 500 µL of fractionation buffer (20 mM HEPES pH 7,4, 10 mM KCl, 2 mM $MgCl_2$, 292,24 mM EDTA, 380,35 mM EGTA, 1 mM DTT, 0,1% protease inhibitor cocktail), and myotubes were incubated 15 minutes on ice. Using 1 mL syringe, cell suspension was passed through a 27-gauge needle 10 times and was left on ice for 20 minutes. Cell suspension was then centrifuged at 3000 rpm for 5 minutes: the pellet contains nuclei and the supernatant contains cytoplasm, membrane and mitochondria. The pellet of nuclei was sonicated and resuspended in 100 µL of complete RIPA buffer. The supernatant was transferred into a fresh tube and centrifuged at 8000 rpm for 5 minutes. The pellet contains mitochondria, while the supernatant was transferred to a fresh tube and kept on ice and this contains the cytoplasm and membrane fraction. Pellet containing mitochondria was resuspended in 100 µL of complete RIPA buffer. Cellular fractions were then centrifugated at 14000 rpm at 4 °C for 10 minutes, and

the supernatant was recovered. Total protein content of each sample was obtained using the Bradford assay (Bio-Rad Laboratories, Hercules, USA).

### 2.2.10. RNA extraction

LDH-A and GPR81 expression in abdominal muscle biopsies were assessed by RT-qPCR. Total RNA was extracted from 50-100 mg of muscles through homogenization in 1 ml of TRI Reagent (Sigma-Aldrich, St Louis, MO, USA) in a Dounce homogenizer (Sigma-Aldrich). Samples were allowed to stand for 5 minutes at room temperature. Then it was added 0,2 ml of chloroform per ml of TRI Reagent used. Samples were shaken vigorously for 15 seconds and let stand for 2-15 minutes at room temperature. The resulting mixtures were centrifuged at 12000 xg for 15 minutes at 2-8 °C. Centrifugation separates the mixture into 3 phases: a red organic phase (containing protein), an interphase (containing DNA) and a colourless upper aqueous phase (containing RNA). The aqueous phase was transferred to a fresh tube and 0,5 ml of 2-propanol was added. Samples were let stand for 5-10 minutes at room temperature and then centrifuged at 12000 xg for 10 minutes at 2-8 °C. The RNA precipitate and forms a pellet. The supernatant was removed, and the RNA pellet was washed in 1 ml of 75% ethanol, then samples were centrifuged at 7500 xg for 5 minutes at 2-8 °C. The RNA pellet was air-dried for 5-10 minutes and then resuspended in an appropriate volume of RNase-free water (Invitrogen).

### 2.2.11. Reverse transcription and Real-Time Quantitative PCR (RT-qPCR)

Abdominal muscles RNA was converted to cDNA using a high-capacity cDNA reverse transcription kit (Applied Biosystems), according to the manufacturer's instructions and it was used a T100$^{TM}$Thermal Cycles (Bio-Rad Laboratories). For the experiments, 2 µg of total RNA was used per 20 µL reaction. It was prepared a RT master mix composed of: 10X RT Buffer, 25X dNTP mix (100 mM), 10X RT Random Primers, MultiScribe$^{TM}$ Reverse Transcriptase, RNase Inhibitor and Nuclease-free water. Temperature and cycling parameters were: 25 °C for 10 minutes, 37 °C for 120 minutes, 85 °C for 5 seconds and then 4 °C at indetermined time. cDNA concentrations were measured using a Nanodrop. To assess LDHA and GPR81 expression, RT-qPCR primers were used (Invitrogen):

- LDHA Forward: AGATTCCAGTGTGCCTGTATG
- LDHA Reverse: ACCTCTTTCCACTGTTCCTTATC
- GPR81 Reverse: GTAGGTGAAGCTGAGGGTTATG
- GPR81 Forward: GCGTGTCTGCTAGACTCTATTT

GAPDH was used as ana expression control (Forward: GGCAAATTCAACGGCACAGTC Reverse: TCGCTCCTGGAAGATGGTG). RT-qPCR was performed using SYBR Power Green PCR master mix with a CFX96$^{TM}$ Real-Time System (Bio-Rad), according to the manufacturer's instructions. It was used the same amount of cDNA for each sample. PCR conditions were 95 °C for 2 minutes (1 cycle) for the enzyme activation, followed by 40 cycles of 15 seconds denaturation at 95 °C and 60 seconds annealing at 60 °C. Relative expression of LDHA and GPR81 was determined using the delta delta Ct method.

### 2.2.12. Diff-Quick Stain

The Diff-Quick Stain is a rapid Romanowsky-type staining method, characterized by its metachromatic properties. It consists of an alcoholic fixative and two dyes. The first dye contains an acidic eosin dye, which has an affinity for basic cellular components that appear pink to purple, the second dye is a basic methylene blue dye, which binds to nucleic acids that appear blue. Myotubes, after removal of the culture medium, were washed with PBS. The fixative solution was then added for 30 seconds and subsequently aspirated. Solution 1 (eosin) was applied for 30 seconds and then removed. Finally, Solution 2 (methylene blue) was added for 30 seconds and then aspirated. After removal of the final solution, the multiwell containing myotubes was washed with PBS and then images were acquired using an optical microscope.

### 2.2.13. TrxR activity assay

Muscle biopsies were lysed in complete RIPA buffer containing a human protease inhibitor cocktail (Sigma-Aldrich), and the same quantities of proteins were used for the enzymatic assay. TrxR activity was measured by using a commercial colorimetric assay kit (Sigma Aldrich, CS0170) based on the reduction of 5,5'-dithiobis(2-nitrobenzoic acid) (DTNB) with NADPH to 5-thio-2-nitrobenzoic acid (TNB) at 412 nm, according to the manufacturer's instructions. This kit also contains an inhibitor solution of mammalian thioredoxin reductase, that is necessary to determine the reduction of DTNB due only to the TrxR activity, since even other enzymes present in biological samples could reduce this substrate. Results were normalized to the cellular protein content and reported as U/mg.

### 2.2.14. Red Oil staining

After the treatment, adipocytes were washed with PBS and then fixed with 4% paraformaldehyde for 30 minutes at 4 °C. Cells were treated with 60% isopropanol for 5 minutes and then with Oil Red working solution (#01391, Sigma-Aldrich, St Louis, MO, USA) (3-part Oil Red: 2-part water) for 15 minutes at room temperature. After three washes with water, cells were photographed under the optical microscope.

### 2.2.15. Animals

Male C57BL/6J mice aged 19,5 months were obtained from The Jackson Laboratory (Bar Harbor, ME, USA). Animals were acclimatized and monitored for two weeks. At 20 months of age, mice were matched for body weight and food intake, then randomly assigned to two experimental groups and studied until 23 months of age: untreated old mice (O) and old mice treated with AdipoRon (O-AR) for 3 months. A standard diet (Carfil Quality, Oud-Turnhout, Belgium) was provided throughout the study. Drinking water was replaced by solidified water (Solid Drink, Triple A Trading, Tiel, The Netherlands), which was renewed daily. In the treated group (O-AR), AdipoRon (Bio-Techne, Minneapolis, MN, USA) was incorporated into the solid drink at a dose of 50 mg/kg/day for the entire 3-month period. For comparison, a cohort of 3-month-old mice (Y) was included. These young mice are equivalent to 20-year-old humans and are commonly used as controls for studies of sarcopenia. Mice were housed under standardized conditions, including constant temperature (22 °C), controlled humidity (40-60%), and a 12-hour light/dark cycle (lights on from 7 a.m. to 7 p.m.), in environmentally enriched cages with social housing. Caged were cleaned weekly. Body weight and food intake were measured weekly throughput the protocol.

At sacrifice, Y-mice were euthanized at 3 months of age and O/O-AR mice at 23 months of age. Skeletal muscle from both upper and lower limbs, as well as the liver, heart, subcutaneous adipose tissue, epididymal adipose tissue, brown adipose tissue, and tibia were collected and weighed. Tibial length was measured with a calliper. Depending on the experiment, tissues were either processed immediately or stored at -80 °C for subsequent analyses [123].

### 2.2.16. LDH activity assay

The LDH activity assay was conducted on lysates of triceps of young, old and old Adiporon-treated mice using the QuantiChrom$^{TM}$ Lactate Dehydrogenase Kit (D2DH-100) (BioAssay Systems, Hayward, Ca, USA), according to the manufacturer's instructions. Data were normalized using total muscular protein content in each sample, thus obtaining U/L of LDH activity.

### 2.2.17. MCT4 ELISA assay

An ELISA Assay was performed on muscular lysates of triceps of young, old and old Adiporon-treated mice in order to evaluate MCT4 levels. It was used the Mouse Monocarboxylate Transporter 4 / MCT4 (SLC16A3) ELISA Kit (Abbexa, Cambridge, UK), according to the manufacturer's instructions. The Optical Density (OD) is measured spectrophotometrically at 450 nm in a microplate reader, from which the concentration of SLC16A3 can be calculated.

### 2.2.18. Statistical analysis

Data are presented as means ± from at least three independent experiments. Statistical analysis of the data was performed using Student's *t* test or via one-way ANOVA conducted using GraphPad Prism (GraphPad Holdings, LLC, San Diego, CA, USA) version 8.0. A *p*-value < 0,05 was considered statistically significant.

## 3. AIM OF THE THESIS

Lactate, once considered a mere by-product of anaerobic glycolysis, is now recognized as a multifunctional molecule with metabolic, signalling and epigenetic roles. In particular, lactate participates in mitochondrial metabolism, regulates gene transcription and signal through the GPR81 receptor. Thus, lactate is essential in physiological contexts. However, its accumulation can contribute to pathological conditions, supporting tumor metabolism and promoting muscle degeneration.

Given these premises, the aim of this thesis was to investigate the role of lactate both as a metabolic substrate and as a signalling molecule in skeletal muscle and adipose tissue. Specifically, the research focused on two distinct contexts. The first is tumor-associated muscular wasting, a condition observed in cancer cachexia. In this contest, monolayer and three-dimensional cell cultures were used, as well as muscle biopsies obtained from patients with gastrointestinal tumors. The second context is aging-associated wasting, known as sarcopenia, which was studied both *in vitro* in myotubes and *in vivo* in murine models. Moreover, since wasting is a condition that not only involves muscular tissue, it was also analysed in adipose tissue through experiments conducted on adipocytes.

Studying the role of lactate in these multiple contexts may provide the foundation of new approaches to therapeutic interventions targeting muscle wasting, both in cancer-associated cachexia and in age-related sarcopenia.

# 4. RESULTS

## 4.1. Treatment with sodium lactate and the GPR81 agonist, 3,5-DHBA, induces phenotypic and metabolic changes in myotubes

Although the molecular mechanisms underlying muscle wasting in aging or cancer cachexia are widely studied, the possible role of phenotypic and metabolic changes in the onset of these conditions are unexplored so far. To evaluate whether lactate may play a role in inducing muscle wasting, both as a metabolite and as a signalling molecule, experiments were conducted using sodium lactate and a lactate receptor GPR81 agonist, 3,5-Dihydroxybenzoic acid (3,5-DHBA). For this aim, myotubes originated by differentiation of C2C12 murine myoblasts were treated with conditioned medium (CM) obtained cultivating murine colon carcinoma CT26 cell line for 24 hours. Moreover, differentiated myotubes were also treated with lactate at 20 mM concentration and with 3,5-DHBA at 10 mM concentration for 24 hours. CM CT26 treatment induces a cachectic phenotype in myotubes, both leading to phenotypic and metabolic alterations [112]. These experiments were carried out to understand if lactate could trigger and promote muscle wasting in myotubes with similar effects provoked by CM CT26 treatment. Figure 8A shows that CM CT26 treatment (used at 30%) leads to a reduction in myotube width, a hallmark of muscle wasting. The same results were obtained treating myotubes with lactate and DHBA. Indeed, in all the treatments, there is a statistically significative reduction in myotube thickness, as reported in the bar graph in figure 8B. Moreover, to evaluate if lactate is involved in metabolic changes in myotubes, oxygen consumption, expressed as Oxygen Consumption Rate (OCR), and the levels of extracellular lactate have been assayed. Myotubes treated with lactate and DHBA show lower levels of OCR compared to control myotubes (Figure 8C), and higher amounts of extracellular lactate (Figure 8D). The same results were obtained from CM CT26 treatment. These results demonstrate that lactate and its signalling cascade may be involved in metabolic changes in myotubes similarly to CM CT26 treatment, leading to muscle wasting.

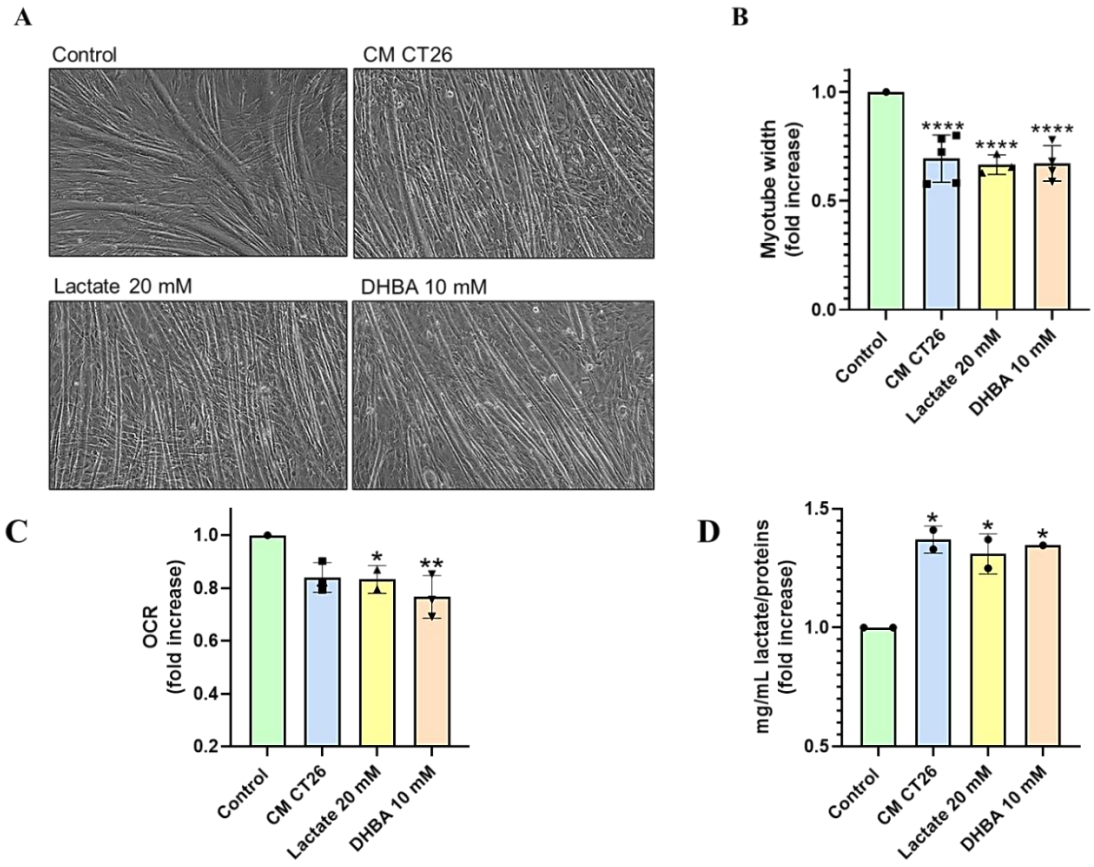


**Figure 8**. Lactate and 3,5-DHBA induce phenotypic and metabolic alterations in myotubes. Four days-differentiated myotubes were treated with CM CT26 (30%, final percentage), 20 mM lactate and 10 mM DHBA for 24 hours. (**A**) Representative optical microscope images of control myotubes and treated myotubes with CM CT26, 20 mM lactate and 10 mM DHBA. Magnification: 10X. (**B**) Measures of myotube width, obtained with ImageJ by randomly chosen at least five fields. (**C**) Analysis of oxygen consumption rate (OCR). (**D**) Assay of lactate amount in myotubes. All the values in the bar graphs are reported as fold increase, considering control myotubes as 1. CM CT26: conditioned media from colon cancer cell CT26. *$p$<0,05; ** $p$<0,001; **** $p$<0,0001. N=3.

## 4.2. Three-dimensional C2C12 spheroids treated with CM CT26, sodium lactate and 3,5-DHBA exhibit decreased diameter and lower levels of MHC

Three-dimensional cultures reproduce more accurately tissue structure rather than monolayer cultures, thus offering numerous advantages. To confirm the results obtained in monolayer myotubes, spheroids were produced using C2C12 murine myoblast cell line that are cultured directly in differentiation medium. C2C12 spontaneously aggregates after three days forming differentiated spheroids. As described for myotubes, the obtained spheroids were treated with CM CT26, 20 mM lactate and 10 mM DHBA for 48 hours. Figure 9A shows representative images of spheroids after 48 hours treatment. The bar graph in figure 4B shows the diameter of spheroids, pointing out that diameter of treated spheroids with CM CT26, lactate and DHBA is reduced compared to control ones. This effect is probably caused by the decrease of myotube width, that leads to the formation of smaller spheroids. Moreover, it was also assessed the expression level of MHC, a muscular differentiation marker. Figure 9C and B show the Western Blot analysis of MHC, in which treated C2C12 spheroids (with CM CT26, lactate and DHBA) express lower levels of MHC compared to control spheroids. These data suggest that treatment with CM CT26, lactate and DHBA induces phenotypic changes, and presumably metabolic ones as well, not only in two-dimensional cultures, but also in three-dimensional myotube cultures.

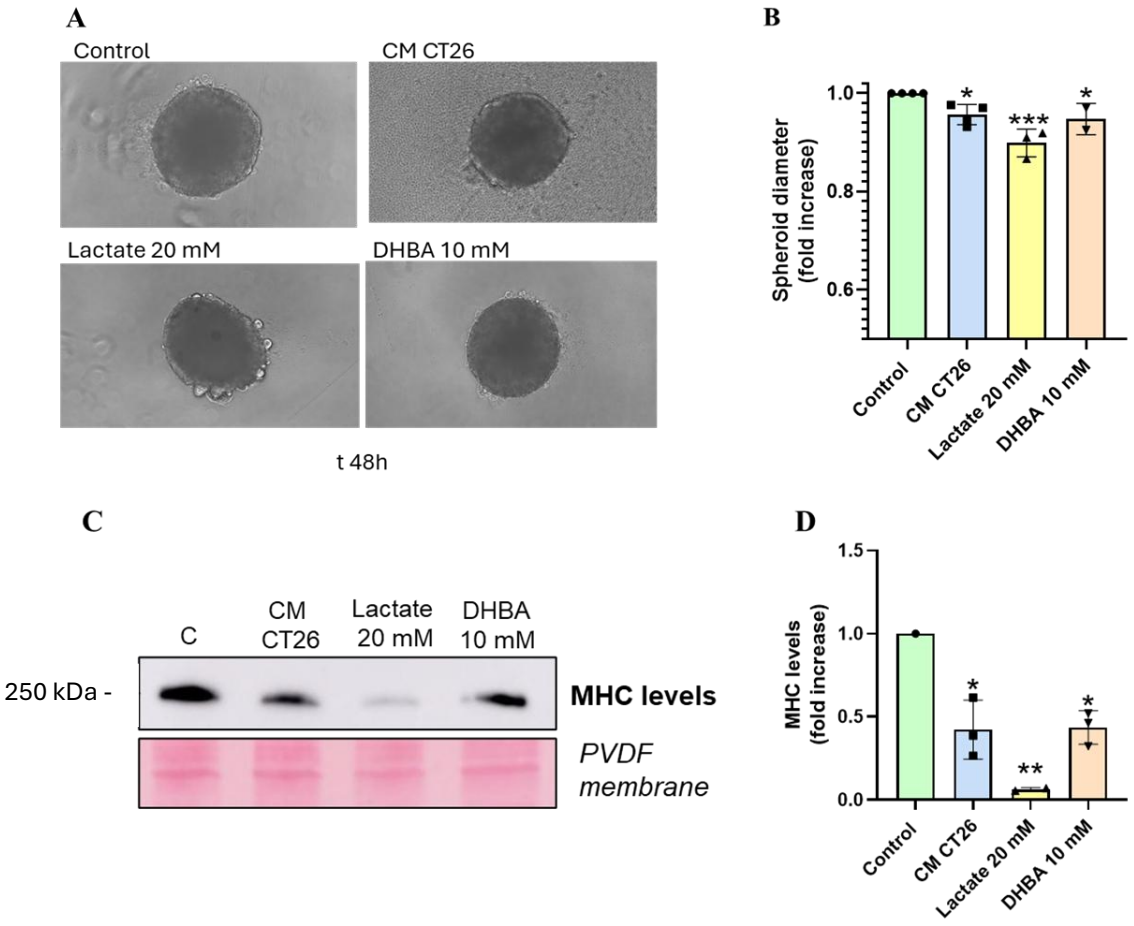


**Figure 9**. C2C12 spheroids treated with CM CT26, 20 mM lactate and 10 mM DHBA. Spheroids obtained from C2C12 myoblasts were treated for 48 hours. (**A**) Representative optical microscope images of control C2C12 spheroids and treated with CM CT26, 20 mM lactate and 10 mM DHBA. Magnification: 4X. (**B**) Analysis of diameter of spheroids. The measures showed are obtained measuring diameter with ImageJ in at least eight spheroids per condition, with two measures per spheroid. (**C**) MHC immunoblot. Red Ponceau-stained PVDF membrane was used for normalization, and the mean values are reported in the bar graph (**D**). All the values in the bar graphs are reported as fold increase, considering control spheroids as 1. CM CT26: conditioned media from colon cancer cell CT26. *$p$<0,05; ** $p$<0,001, *** $p$<0,001. N=3.

## 4.3. Lactate and 3,5-DHBA are involved in STAT3 signalling pathway activation

Signal transducer and activator of transcription 3 (STAT3) signalling pathway plays a critical role in regulating skeletal muscle mass, repair and disease. It is known that prolonged STAT3 activation in muscles is responsible for muscle wasting leading to the activation of protein degradation pathways [124]. Moreover, the STAT3 signalling pathway plays a prominent role also in the induction of cancer cachexia [113]. Given these data, it was analysed whether lactate and GPR81 agonist could induce STAT3 activation. Hence, myotubes were treated with CM CT26 (30%) and 10 mM DHBA for 5 and 10 minutes. As reported in figure 10A and B, CM CT26 induces high STAT3 phosphorylation (Tyr705) five minutes and fifteen minutes after the stimulation, compared to control myotubes. Similarly, myotubes treated with DHBA show incremented levels of STAT3 phosphorylation after stimulation (Figure 10C, D). Myotubes were also treated with 20 mM lactate for 5, 10, 20, 30 and 60 minutes. As reported in Figure 2E and 2F, STAT3 phosphorylation levels increase with increasing stimulation time. This results in activation of the STAT3 pathway, which decreases after 60 minutes. These data suggest that CM CT26 induces STAT3 signalling activation, as well as DHBA and lactate treatment. This indicates that lactate alone and its signalling via GPR81 can activate STAT3 signalling pathway.

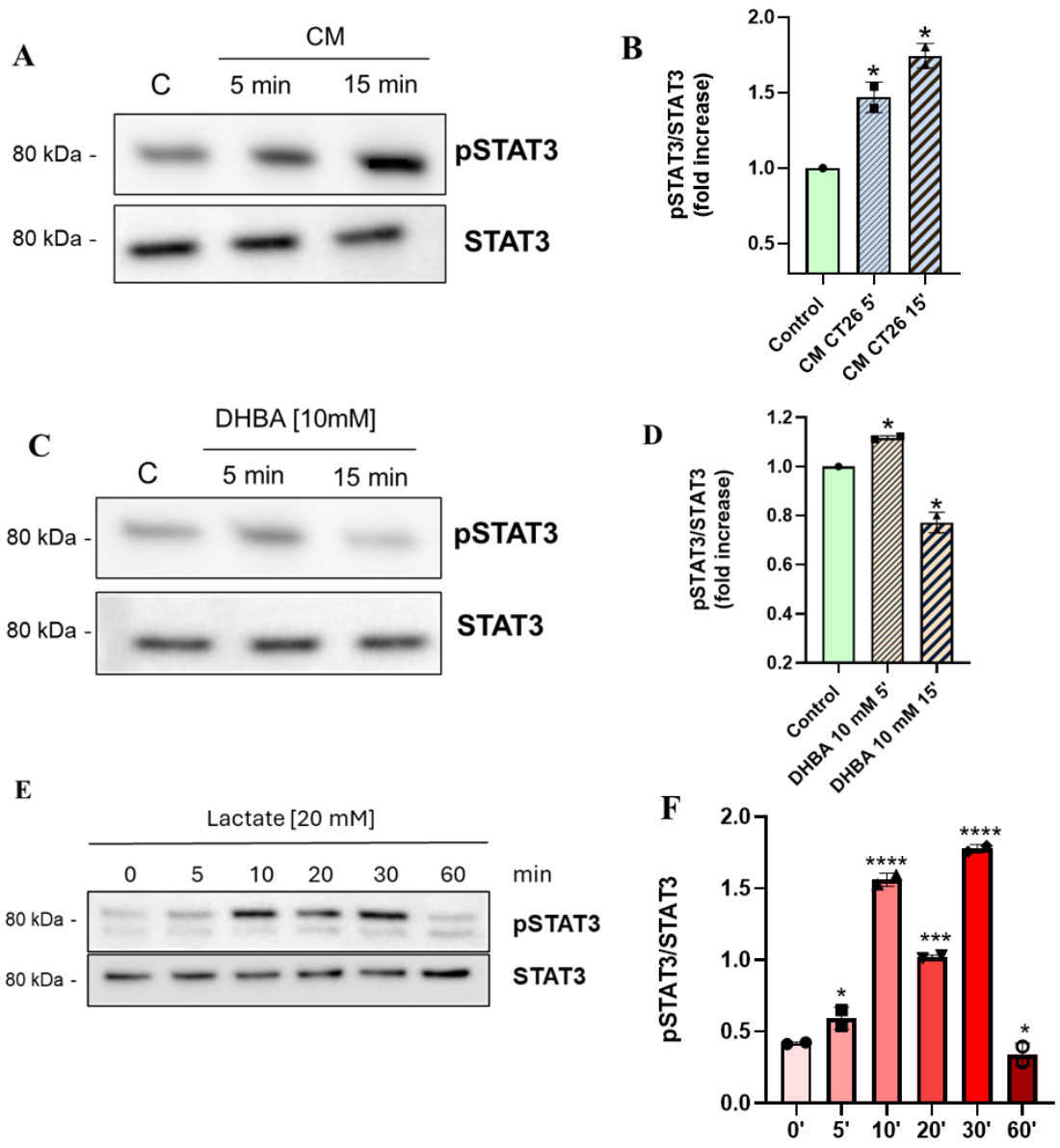


**Figure 10**. CM CT26, lactate and 3,5-DHBA treatments activate STAT3 signalling pathway on myotubes. Myotubes were stimulated with CM CT26 (30%), 10 mM DHBA and 20 mM lactate for the indicated period (Figure 2 A-F). STAT3 phosphorylation (Tyr705) has been analysed by immunoblot. (**A**; **C**; **E**) pSTAT3 and STAT3 immunoblot. pSTAT3 levels were normalized on STAT3 levels, and the bar graphs (**B**; **D; F**) report the mean values. CM CT26: conditioned media from colon cancer cell CT26. * $p$<0,05, *** $p$<0,001, **** $p$<0,0001. N=2.

## 4.4. Mitochondria isolated from myotubes treated with CM CT26 show augmented levels of LDH-A and incremented amount of lactate

Since the presence of Mitochondrial Lactate Complex (mLOC) in mitochondria has been largely reported [125], it was investigated whether CM CT26 could change lactate amount in these organelles. These experiments were conducted on myotubes treated with CM CT26 for 48 hours. To verify the efficiency of the fractionation procedure, a Western Blot was performed against citrate synthase, an enzyme localized in the mitochondrial matrix. As shown in figure 11A and 11B, citrate synthase was detected exclusively in the mitochondrial fraction of both control and treated myotubes. The analysis of LDH-A expression points out that LDH-A levels are reduced in the cytoplasmatic fraction of myotubes treated with CM CT26, whereas an increase in LDH-A level was observed in the mitochondrial fraction under the same conditions (Figure 11C and 11D). To further evaluate lactate amount in the different fractions, a lactate assay was performed. Figure 11E indicates that lactate levels decrease in the cytoplasm of treated myotubes compared to controls, whereas an increase of the metabolite was observed in mitochondria. Collectively, these results suggest that mitochondrial lactate could play a role in the induction of myotubes degradation.

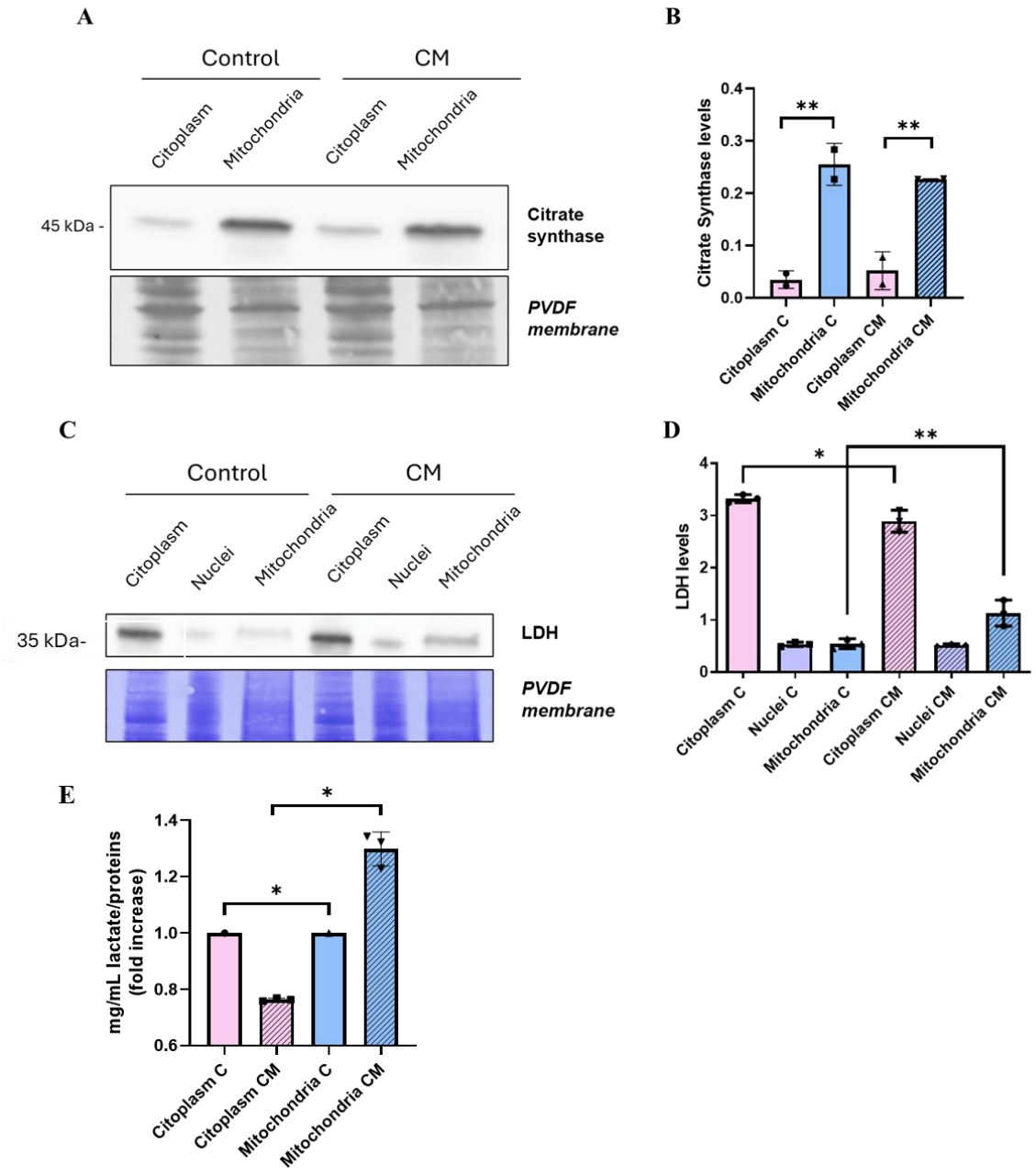


**Figure 11**. Cellular fractionation of myotubes treated with CM CT26 for 48 hours. (**A**) Immunoblot for citrate synthase. Blue Coomassie PVDF membrane was used for normalization, and the mean values are reported in the bar graph in figure (**B**). (**C**) Immunoblot for LDH-A. Blue Coomassie PVDF membrane was used for normalization, and the mean values are reported in the bar graph in figure (**D**). (**E**) Lactate assay. The values in the bar graphs of lactate assay are reported as fold increase, considering control myotubes as 1. C: control myotubes. CM: conditioned media from colon cancer cell CT26 (CM CT26). The values in the bar graph in figure (**E**) are reported as fold increase, considering cytoplasm and mitochondria of control myotubes as 1. **p*<0,05; ***p*<0,001. N=3.

## 4.5. Treatment with α-Cyano-4-hydroxycinnamic acid (CHC), an inhibitor of MCT1, prevents wasting features in myotubes

Monocarboxylate Transporter 1 (MCT1) is a proton-linked membrane transporter that mediates the uptake of lactate and other monocarboxylates, playing a key role in cellular energy metabolism and the lactate shuttle between tissues. To investigate the possible role of extracellular lactate in the induction of muscle wasting, differentiated myotubes were treated with CM CT26 contained α-Cyano-4-hydroxycinnamic acid (CHC), an inhibitor of MCT1, for 48 hours. Figure 12A shows control and treated myotubes stained with haematoxylin-eosin. The bar graph in figure 12B shows that CM CT26 induces a decrease in myotube width, whereas co-treatment with CHC restores myotube width comparable to the control ones. Additionally, the expression levels of MHC and atrogin-1 were evaluated. Treatment with CM CT26 led to a reduction in MHC and an increase in atrogin-1 expression, whereas co-treatment with CHC restored the levels comparable to control myotubes. Finally, lactate levels were measured, and the graph in Figure 12D shows that myotubes treated with CM CT26 exhibit higher lactate levels, which are reduced upon co-treatment with CHC. Together, these results indicate that MCT1 transporter is involved in the promotion of wasting phenotype in myotubes.

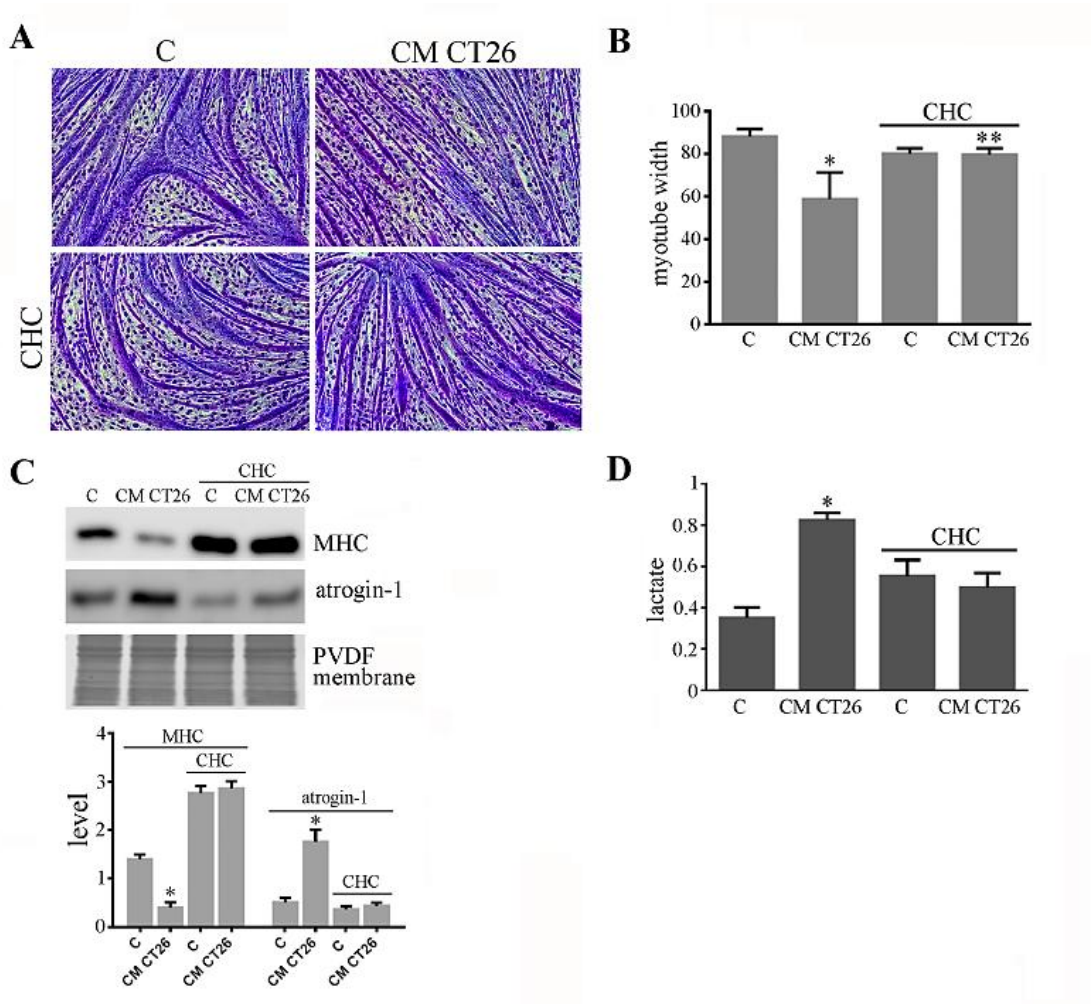


**Figure 12.** CHC prevents wasting phenotype in myotubes. (**A**) Representative optical microscope images of treated myotubes with CM CT26 and 1 µg/mL CHC, stained with haematoxylin-eosin. Magnification: 10X. (**B**) Measures of myotube width, obtained with ImageJ using at least five fields randomly chosen. (**C**) MHC and atrogin-1 immunoblot. Red Ponceau-stained PVDF membrane was used for normalization, and the mean values are reported in the bar graph (**D**). * $p$<0,05; ** $p$<0,001. N=3.

## 4.6. Abdominal muscles of cachectic patients show increased levels of intramuscular lactate

Previous experiments performed on myotubes showed that wasting myotubes produced higher levels of lactate compared to controls. Based on these findings, lactate production was subsequently analyzed in abdominal muscle biopsies from donor patients. Biopsies were obtained from individuals with gastrointestinal cancer undergone surgical resection. Samples were classified as either cachectic or non-cachectic according to established diagnostic criteria for cachexia. Specifically, patients who had experienced a body weight loss of 5% or more in the last six months were classified as cachectic while the other are included in the non-cachectic group. As illustrated in the bar graph in figure 13, abdominal muscle samples from cachectic patients exhibited significantly higher lactate production compared to those from non-cachectic patients. These findings point out that elevated lactate levels are not restricted to myotubes *in vitro* but are also evident in human muscle tissue under conditions of muscular wasting. However, additional human samples would be needed in order to obtain even more concrete data.

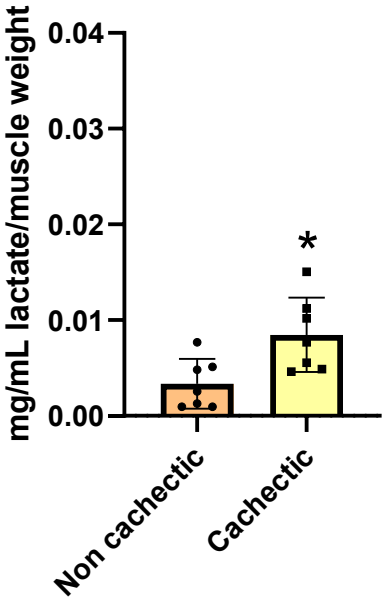


**Figure 13**. Lactate assay shows incremented levels of lactate in muscular biopsies of cachectic patients. The amount of lactate was reported in mg/ml normalized on the weight of muscular biopsies. * $p$<0,05. Muscle samples used=10.

### 4.7. Relative expression of *Ldha* and *Gpr81* are augmented in abdominal muscles of cachectic patients

LDH-A is the enzyme which catalyses the conversion of pyruvate into lactate. Since abdominal muscle biopsies of cachectic patients produce augmented levels of lactate, Real-Time Quantitative PCR (RT-qPCR) was performed to quantify the expression levels of Lactate Dehydrogenase A gene (*Ldha*). The graph in Figure 14A shows an augmented relative expression of *Ldha* in cachectic muscles versus non-cachectic muscles. This result suggests that an increase in *Ldha* expression in cachectic muscles is associated with an increase in extracellular lactate, compared to the non-cachectic counterpart.

Since it was previously demonstrated that abdominal muscles of cachectic patients produce higher levels of lactate, it was investigated whether lactate could increment its signalling pathway through the binding to GPR81. This has been assayed by RT-qPCR to quantify expression levels of *Gpr81* gene. Figure 14B points out incremented relative expression of *Gpr81* in abdominal muscles of cachectic patients, compared to the non-cachectic counterpart. This could indicate that augmented levels of lactate could induce an increase in expression levels of GPR81 receptor, leading to a potential increase in this signalling pathway.

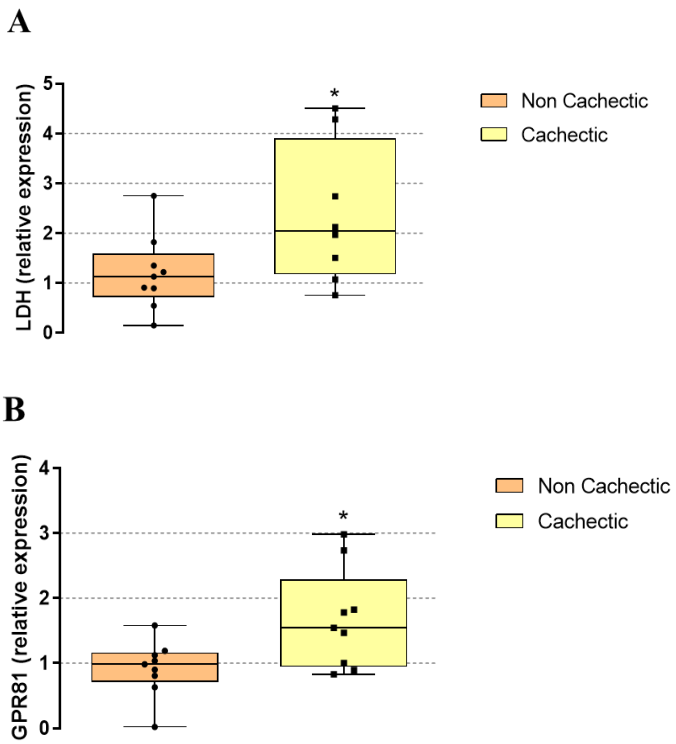


**Figure 14**. (**A**) Relative expression levels of *Ldha* in abdominal muscles of cachectic and non-cachectic patients. (**B**) Relative expression levels of *Gpr81* in abdominal muscles of cachectic and non-cachectic patients. In both panels expression levels were obtained performing a qRT-PCR.

* $p$<0,05. Muscle samples used=10.

## 4.8. Human fibroblasts isolated from abdominal muscles of cancer patients express vimentin and show incremented levels of α-Smooth Muscle Actin (α-SMA)

Fibroblasts are typical cells of connective tissue of mesenchymal origin, which play key roles in disease, tissue homeostasis, cancer progression, inflammatory and fibrotic conditions, and wound healing processes. One of the major components of the tumoral stroma are the cancer-associated fibroblasts (CAFs), which secrete growth factors, inflammatory ligands and extracellular matrix proteins that promote tumor proliferation, therapy resistance and immune exclusion. For these reasons, CAFs have been historically considered tumor-promoting components [126]. Given the relevance of fibroblasts in tumor progression and their abundance in the stroma, fibroblasts were isolated from abdominal muscle biopsies obtained from subjects with gastrointestinal cancer and from healthy subjects. To confirm successful isolation, Western Blot analyses were performed for vimentin and α-Smooth Muscle Actin (α-SMA). Vimentin, a cytoskeletal structural protein, is considered a marker for mesenchymal cells such as fibroblasts, whereas α-SMA is a contractile protein typical of activated fibroblasts. Figure 15 illustrates the Western Blot results for vimentin and α-SMA, and the relative PVDF membrane for the quantification. The bar graph in Figure 15B shows band quantification, showing that vimentin expression is detectable in healthy fibroblasts and in fibroblasts derived from tumor patients. Notably, vimentin levels are reduced in fibroblasts derived from patients. Conversely, the bar graph in figure 15C shows increased α-SMA expression in fibroblasts derived from patients, suggesting that these cells are in an activated state compared with healthy fibroblasts.

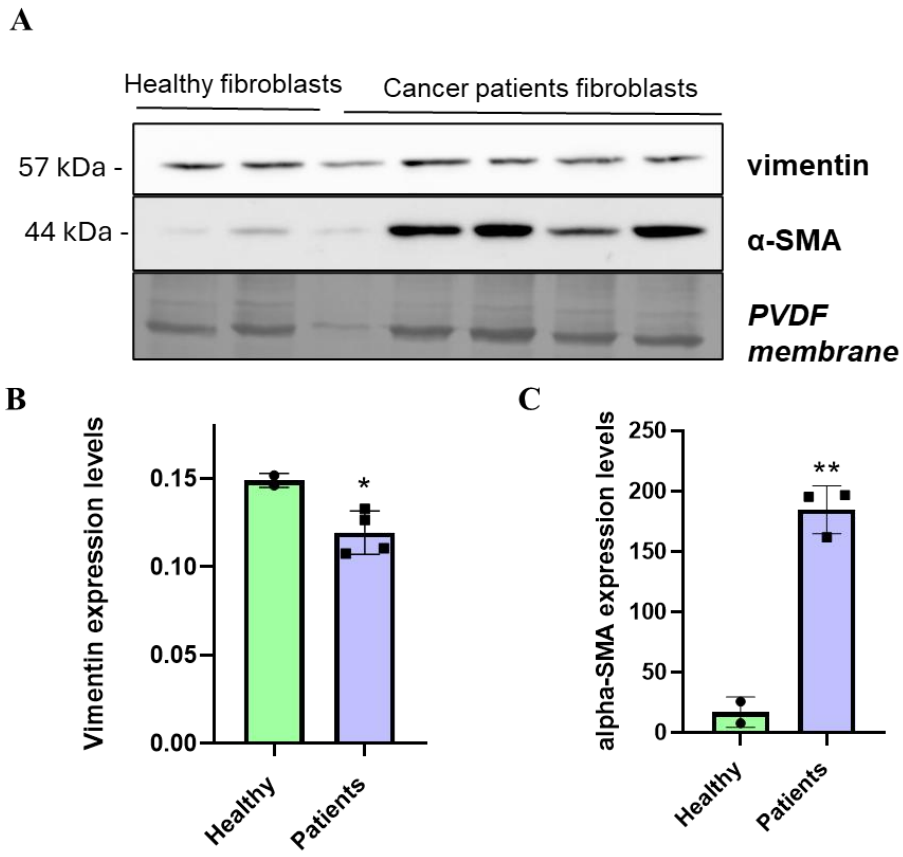


**Figure 15**. Fibroblasts isolated from muscle biopsies of cancer patients show vimentin expression and incremented levels of α-SMA expression levels. (**A**) Vimentin and α-SMA immunoblot. Red Ponceau-stained PVDF membrane was used for normalization, and the mean values are reported in the bar graphs (**B**; **C**). Healthy: fibroblasts derived from healthy individuals; Patients: fibroblasts derived from gastrointestinal cancer patients. * $p$<0,05; ** $p$<0,01. Healthy fibroblasts used=2; cancer patients fibroblasts used=5.

## 4.9. Lactate production is augmented in human fibroblasts derived from abdominal muscles of cancer patients

Levels of intracellular lactate produced by fibroblasts derived from healthy abdominal muscles and from patients were evaluated by lactate assay. As reported in figure 16, fibroblasts derived from abdominal muscles of cancer patients exhibit augmented levels of lactate compared to those derived from healthy subjects.

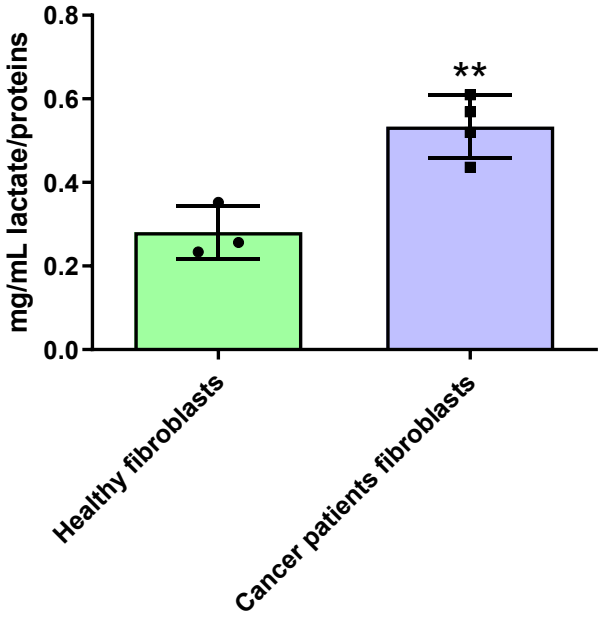


**Figure 16**. The lactate assay shows incremented levels of lactate in fibroblasts derived from abdominal muscles biopsies of cachectic patients. The amount of lactate was reported in mg/ml normalized on total protein content. Healthy fibroblasts: fibroblasts derived from healthy individuals; cancer patient's fibroblasts: fibroblasts derived from gastrointestinal cancer patients. ** $p$<0,005. Healthy fibroblasts used=3; cancer patients fibroblasts used=5.

## 4.10. LDH-A and GPR81 levels are increased in human fibroblasts isolated from cancer patients

Since fibroblasts derived from cancer patients produce higher amounts of lactate compared to the one derived from healthy subjects, the expression levels of GPR81 and LDH-A were evaluated by immunoblot. Fibroblasts of healthy patients were also treated with CM CT26 (50% final percentage) for 48 hours. The graph in figure 17A illustrates the immunoblot against GPR81 and LDH-A and the relative PVDF membrane used for normalization. The bar graphs in Figure 17B and 17C show band quantification, and a statistically significative increase in the expression of GPR81 and LDH-A can be observed. This could suggest that the lactate produced by fibroblasts derived from patients could trigger an autocrine loop, whereby lactate produced could enter fibroblasts via MCT1 or bind to GPR81 and activate the signalling cascade.

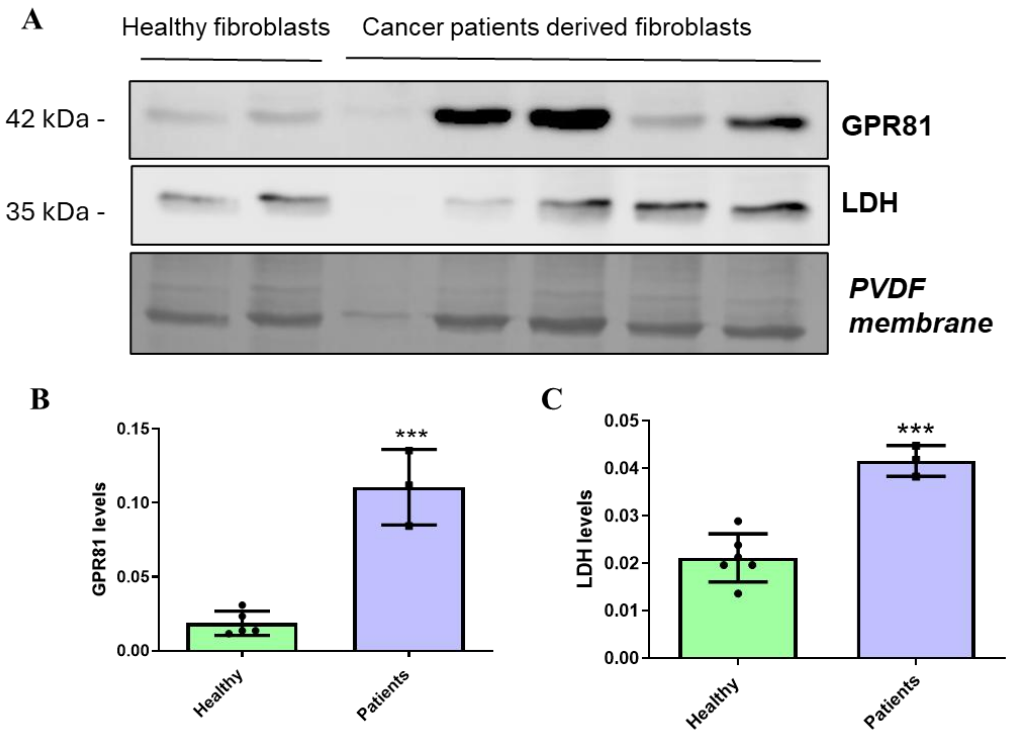


**Figure 17**. Fibroblasts isolated from muscle biopsies of cancer patients show augmented expression levels of GPR81 and LDH. (**A**) GPR81 and LDH immunoblot. Red Ponceau-stained PVDF membrane was used for normalization, and the mean values are reported in the bar graphs (**B**; **C**). Healthy fibroblasts: fibroblasts derived from healthy individuals; cancer patient's fibroblasts: fibroblasts derived from gastrointestinal cancer patients. *** $p$<0,001. Healthy fibroblasts used=2; cancer patients fibroblasts used=5.

## 4.11. C2C12 myotubes treated with conditioned medium (CM) obtained from fibroblasts derived from cachectic patients show muscle wasting phenotype

The potential crosstalk between muscle-derived fibroblasts and muscle fibers was investigated using C2C12 myotubes. For this aim, conditioned medium (CM) from fibroblasts of cachectic and non-cachectic patients were prepared. Myotubes were treated with 50% CM for 48 hours. Figure 18A and the bar graph in figure 18B show that treatment with CM from fibroblasts of cachectic patients leads to a reduction in myotube thickness, a hallmark of muscle wasting. This CM induces a statistically significant reduction in myotube width compared to untreated myotubes and to those treated with CM from non-cachectic patients. These results suggest that fibroblasts can produce and secrete factors capable of inducing phenotypic, and potentially metabolic changes in muscle fibers.

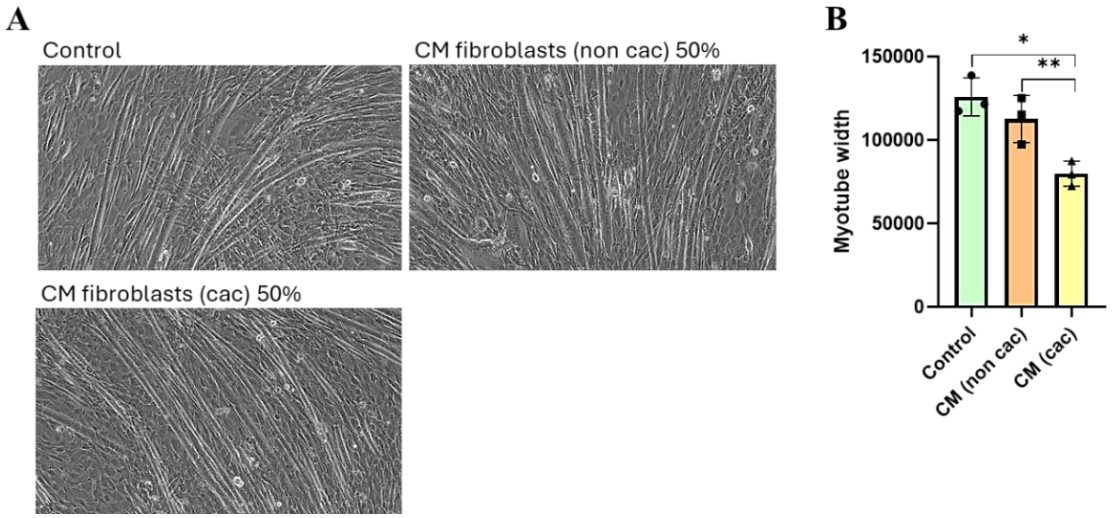


**Figure 18**. Myotubes treatment with CM obtained from fibroblasts derived from cachectic patients shows muscle wasting phenotype. Four-days differentiated myotubes were treated with CM from fibroblasts derived from patients (non-cachectic and cachectic) or differentiating medium (C, control) for 48 hours. (**A**) Representative optical microscope images of treated myotubes with or without fibroblast CM. Magnification: 10X. (**B**) Analysis of CM effects in myotube width. The measures showed are obtained measuring myotube width with ImageJ in at least five randomly chosen fields. Non cac: non cachectic; cac: cachectic. * $p$<0,05; ** $p$<0,01. N=3.

## 4.12. Abdominal muscles of cachectic patients show incremented levels of Thioredoxin Reductase (TrxR), a key enzyme for redox homeostasis

The intracellular redox homeostasis is a dynamic balance between levels of free radical species, antioxidant enzymes and small molecules at the core of cellular defence mechanisms. The thioredoxin (Trx) system is an important detoxification system regulating redox milieu and it is one of the key regulators of cells' proliferative potential. Augmented oxidative stress is a hallmark of highly proliferative, metabolically hyperactive cancer cells, which are forced to metabolize antioxidant enzyme to balance the increase in free radical concentration and prevent irreversible damage and cell death. It is well-known that antioxidant detoxifying systems are fundamental for cancer cell survival upon exposure to anti-cancer drugs [127]. Thioredoxin Reductase (TrxR) plays a fundamental role in defending cells against ROS and in maintaining a reduced intracellular environment. It has been found that TrxR is significantly elevated in human cancer, evidenced by its association with the promotion of tumor cell proliferation, inhibiting tumor cell apoptosis and enhancing tumor drug resistance [128]. Since an increase in ROS amount has observed in wasted myotubes, a TrxR assay was performed on muscle lysates of cachectic and non-cachectic patients. The graph in figure 19 shows that TrxR activity is higher in muscles of cachectic patients compared to the non-cachectic ones. This finding may support the hypothesis that elevated TrxR activity plays a key role in tumor progression, since cachexia is a condition that typically develops during advanced stages of cancer. Indeed, TrxR activity in muscles of subjects affected by cancer-related cachexia could represent a critical factor in the development of this condition, as activity is lower in non-cachectic patients.

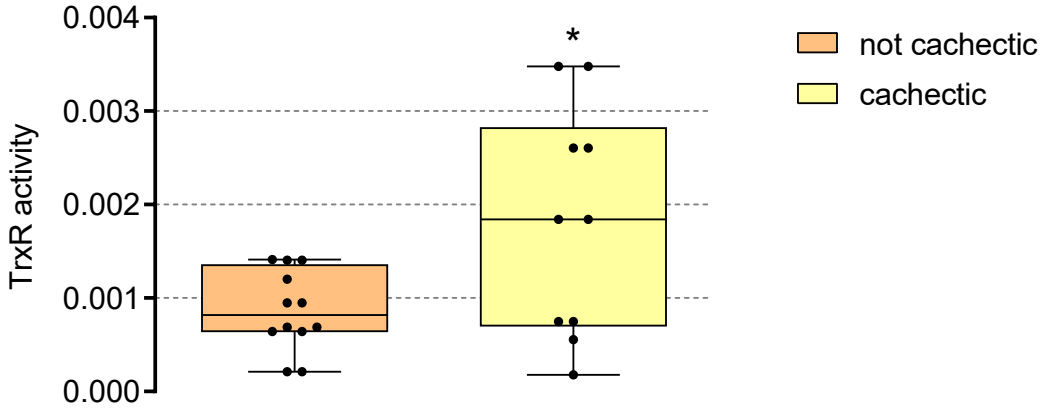


**Figure 19**. TrxR activity assay performed on muscles of non-cachectic and cachectic patients. Enzyme activity levels of TrxR are reported in U/µL (units per µL), with the data normalized on

muscle weight in milligrams (mg). One enzymatic unit (U) is defined as the amount of enzyme that catalyses the conversion of 1 micromole of substrate per minute under the specific assay conditions. * $p$<0,05. Muscle samples used=10.

## 4.13. Auranofin, a Thioredoxin Reductase (TrxR) inhibitor, reduces wasting in myotubes

Since TrxR increased activity was measured in cachectic patients in comparison to the non-cachectic counterpart, TrxR activity has measured in myotubes treated with CM CT26 for 48 hours. Figure 20 A shows that treated myotubes exhibited enhanced TrxR activity compared to the control ones. However, this increased activity is not associated with enhanced TrxR levels, as shown by immunoblot (Fig. 20B).

Auranofin is a gold-compound which inhibits thioredoxin reductase (TrxR), a key enzyme in the Trx system that regulates cellular redox balance. As TrxR overexpression is linked to aggressive tumors and poor patient survival, targeting the TrxR system with Auranofin may offer a promising strategy [129]. To study the possible role of TrxR in the CM CT26-induced wasting, differentiated myotubes were treated with CM CT26 containing 25 nM Auranofin for 48 hours. Figure 20A shows that myotubes treated with CM CT26 alone has augmented TrxR activity compared to control myotubes. However, immunoblot reported in figure 20B shows no difference in TrxR1 levels in control myotubes and treated ones with CM CT26.

As shown in figure 20C and in the corresponding quantification in the bar graph in figure 20D, CM CT26 treatment leads to a reduction in myotube width, whereas co-treatment with Auranofin restores myotubes width to levels comparable to those observed in control myotubes. In addition, an immunoblot analysis was performed to assess the expression of Atrogin-1, an E3 ubiquitin ligase which plays a key role in muscle protein degradation (Figure 20E). As illustrated in Figure 20F, Auranofin treatment resulted in a reduction of Atrogin-1 expression levels, compared to CM CT26 treatment alone. Collectively, these findings suggest that Auranofin may counteract cancer-associated muscle wasting by modulating pathways involved in muscle protein degradation, acting probably on TrxR.

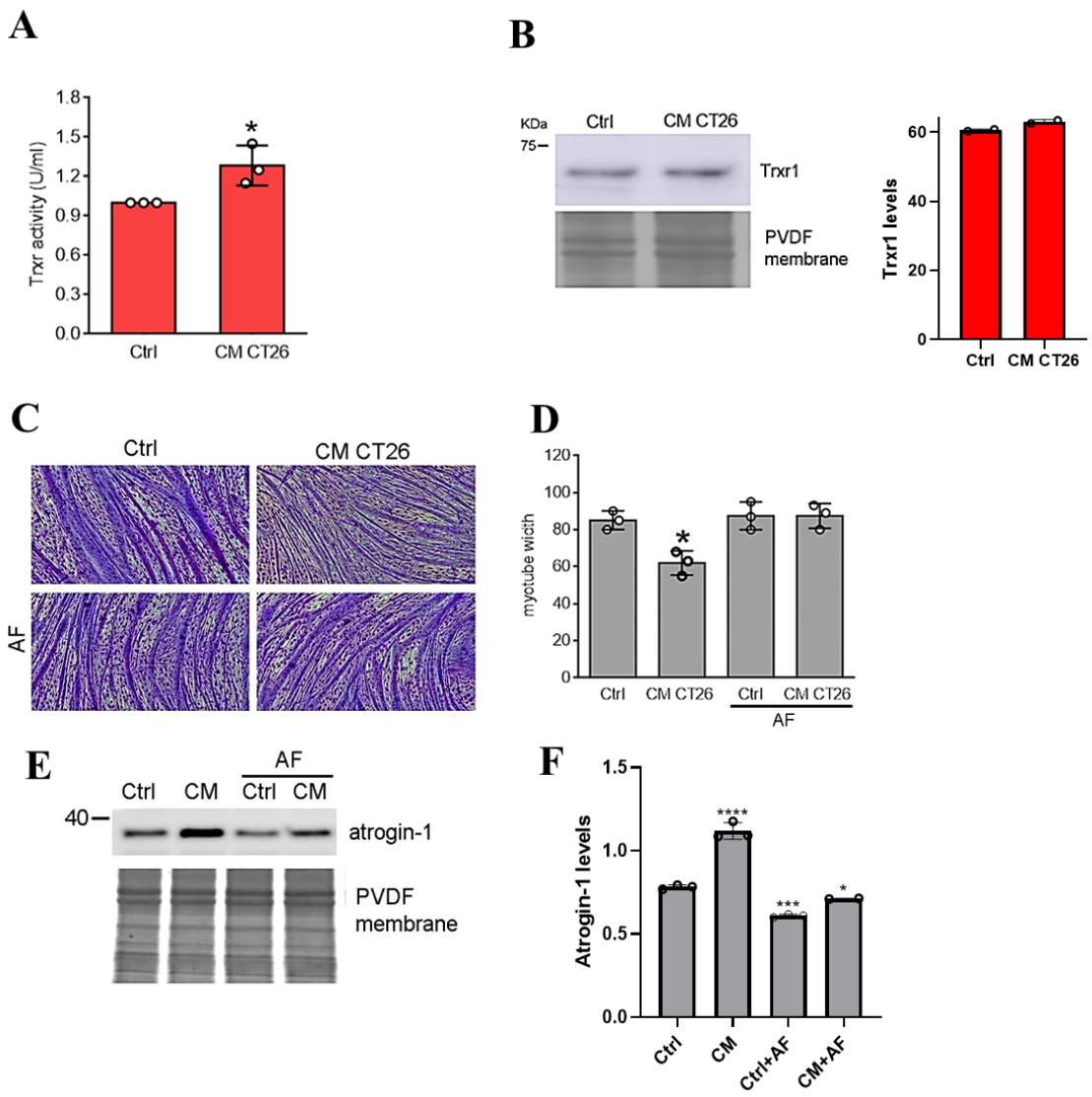


**Figure 20**. Auranofin counteracts wasting in myotubes treated with CM CT26. (**A**) Enzyme activity levels of TrxR are reported in U/µL (units per µL). (**B**)TrxR1 immunoblot. Red Ponceau-stained PVDF membrane was used for normalization, and the mean values are reported in the bar graph. (**C**) Representative optical microscope images of treated myotubes with CM CT26 and CM CT26 with 25 nM Auranofin, stained with haematoxylin-eosin. Magnification: 10X. (**C**) Measures of myotube width, obtained with ImageJ by randomly chosen at least five fields. (**E**) Atrogin-1 immunoblot. Red Ponceau-stained PVDF membrane was used for normalization, and the mean values are reported in the bar graph (**F**). * $p$<0,05. ***$p$<0,001 **** $p$<0,0001. N=3.

## 4.14. Palmitic acid induces muscle wasting in myotubes, that is released by oxamate co-treatment

Palmitic acid (PA) is a long-chain saturated fatty acid, known to induce lipotoxicity in skeletal muscle cells. PA leads to mitochondrial dysfunction, oxidative stress and atrophy, resembling a condition of cellular aging [130]. In order to analyse PA effects on myotubes, C2C12 were first terminally differentiated and then treated with 1 mM PA for 48 hours. Figure 21A shows representative images of myotubes, showing that the treatment with PA induces a significative reduction in myotubes width, as reported in the bar graph in figure 21B. Moreover, this phenotypic alteration is associated with an augmented extracellular lactate level, as shown in figure 21C. These findings indicate that palmitic acid treatment exerts a detrimental effect on myotubes, promoting muscle wasting, as evidenced by a reduction in myotube width and MHC decrease (Fig. 21D) associated with an increase in lactate production.

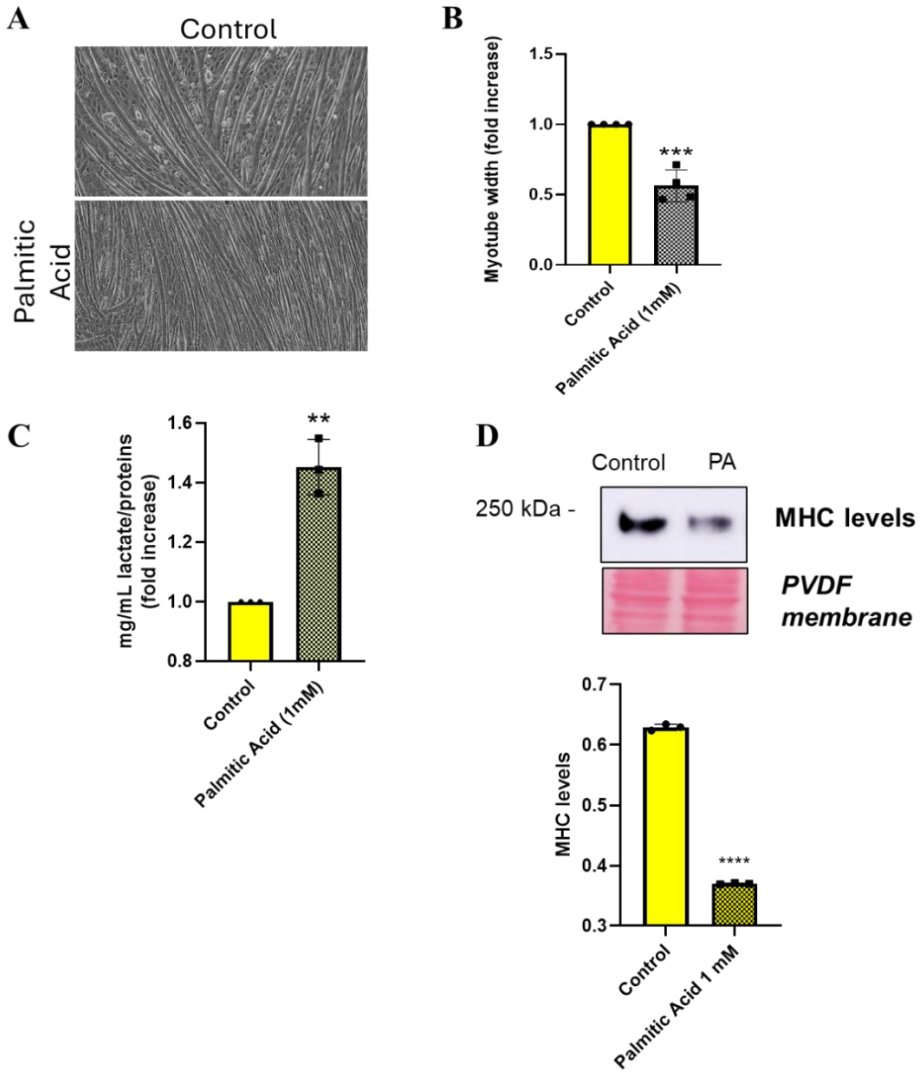


**Figure 21**. Palmitic acid treatment induces a muscle wasting phenotype in myotubes. (**A**) Representative optical microscope images of control myotubes and treated myotubes with 1 mM

Palmitic Acid (PA). Magnification: 10X. (**B**) Measures of myotube width, obtained with ImageJ by randomly chosen at least five fields. (**C**) Assay of lactate amount in myotubes. (**D**) MHC immunoblot. Red Ponceau-stained PVDF membrane was used for normalization, and the mean values are reported in the bar graph. All the values in the bar graphs are reported as fold increase, considering control myotubes as 1. ** $p$<0,005; *** $p$<0,001, **** p<0,0001. N=4.

To analyse whether lactate is involved in this phenomenon, myotubes were co-treated with PA and oxamate, a competitive inhibitor of lactate dehydrogenase (LDH). Differentiated myotubes were co-treated with 1 mM PA and with different concentrations of sodium oxamate (10, 25 and 50 mM) for 48 hours. Co-treatment of myotubes with oxamate and PA did not result in a reduction of myotube width, in contrast to treatment with PA alone. Representative optical microscopy images are shown in Figure 22D, and the corresponding myotube width measurements are shown in the bar graph in figure 22E. The graph clearly indicates a statistically significant increase in the width of co-treated myotubes compared to those exposed to palmitic acid alone.

In conclusion, these data suggest that palmitic acid exposure led to muscle cell atrophy and lactate increase. Interestingly, simultaneous treatment with sodium oxamate blocks these effects, preserving myotube integrity.

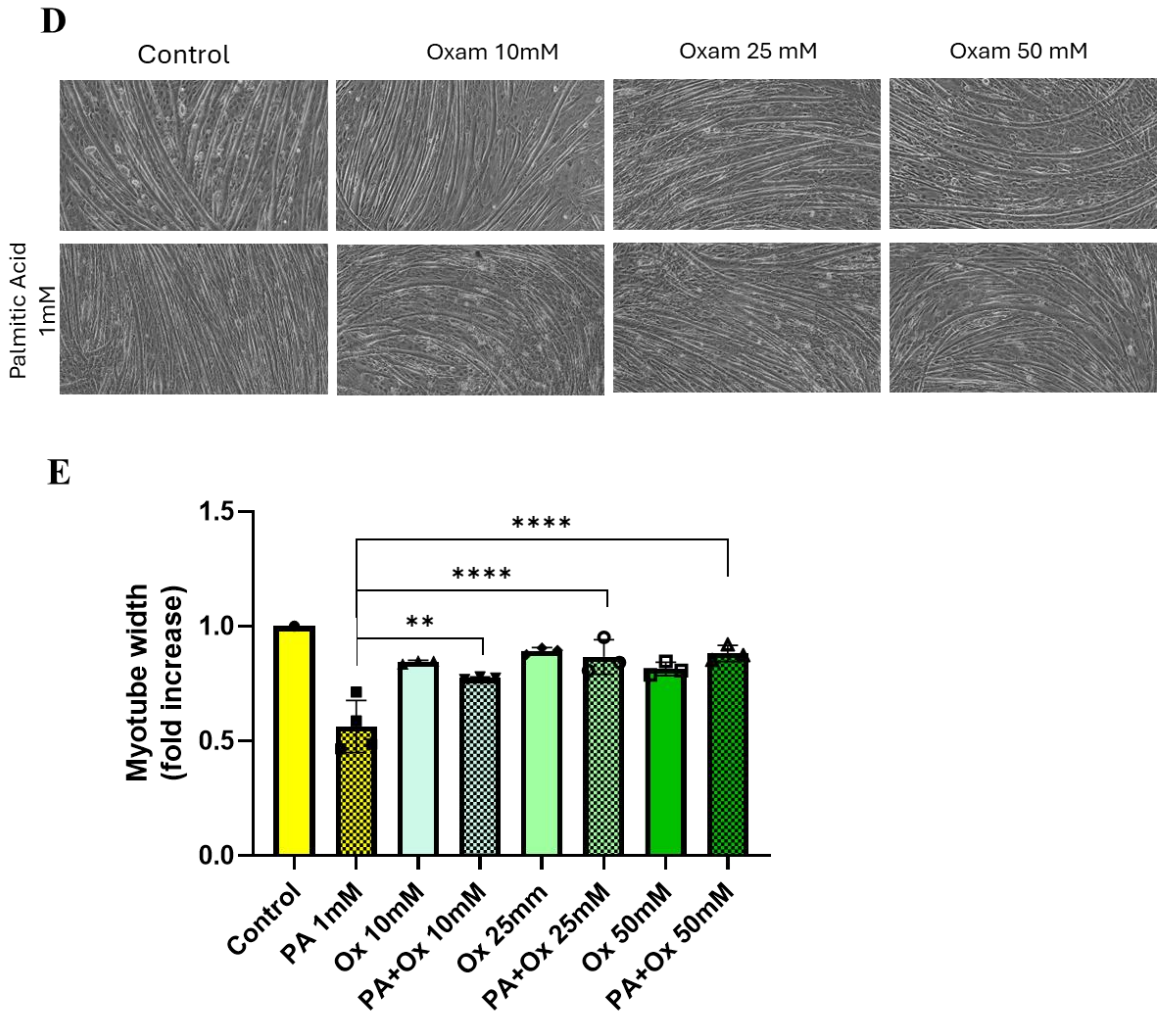


**Figure 22**. Oxamate mitigates palmitic acid-induced muscle wasting. (**D**) Representative optical microscope images of control myotubes and treated myotubes with 1 mM Palmitic Acid (PA). Magnification: 10X. (**E**) Analysis of measures of myotube width. The measures showed are obtained measuring myotube width with ImageJ in at least five randomly chosen fields. All the values in the bar graph are reported as fold increase, considering control myotubes as 1. Ox: sodium oxamate. ** $p$<0,005; *** $p$<0,001; **** $p$<0,0001. N=3.

## 4.15. In the triceps of aged mice was observed an increase in lactate production

To confirm the results obtained in myotubes, some experiments have been performed in mice. I carried out these experiments during my PhD abroad at the Université Catholique de Louvain, in Brussels, Belgium. I was in the Department of Endocrinology, Diabetes and Nutrition (EDIN unit), where I spent three months under the supervision of Professor Abou-Samra. A lactate assay was performed on triceps muscles of young mice (3 months old) and aged mice (23 months old). As shown in figure 23, intramuscular lactate levels in the triceps of aged mice are higher compared to those in young mice, suggesting that lactate could be involved in the process of muscle degeneration during aging.

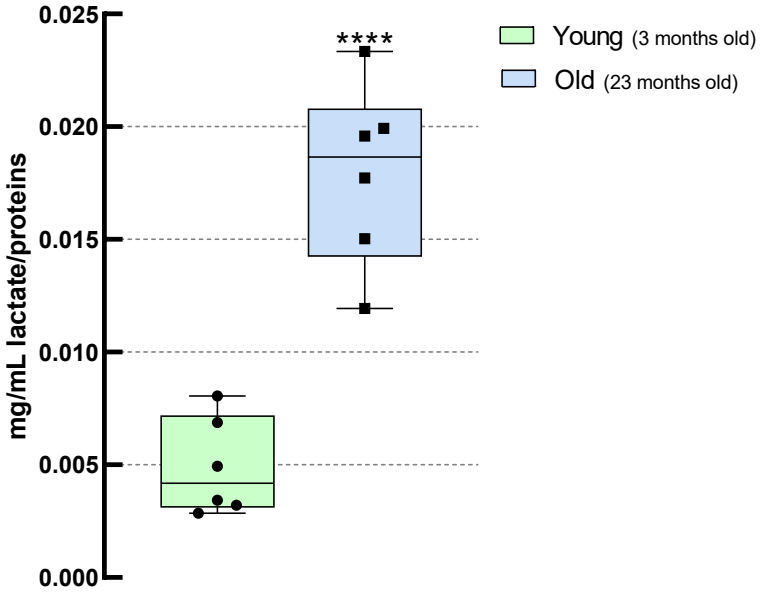


**Figure 23.** Lactate assay shows augmented levels of intramuscular lactate in the triceps of aged mice, compared to lactate levels measured in young mice. Mg/ml lactate are normalized on total muscular protein content. **** $p$<0,0001. Mice used for each condition = 6.

### 4.16. Triceps of aged mice show an augmented activity and expression of LDH-A

The activity of lactate dehydrogenase A (LDH-A) was assessed through a quantitative colorimetric kinetic assay. As shown in Figure 24A, triceps of old mice have elevated levels of LDH-A activity, compared to triceps of young mice. Moreover, the expression level of LDH-A through western blot analysis has been analysed. Figure 24B shows that triceps of aged mice have incremented expression levels of LDH-A, compared to the younger counterpart. LDH-A quantification of both groups of mice was shown in figure 24C. These results point out a significant difference in LDH-A expression patterns and activity between muscles of young and aged mice.

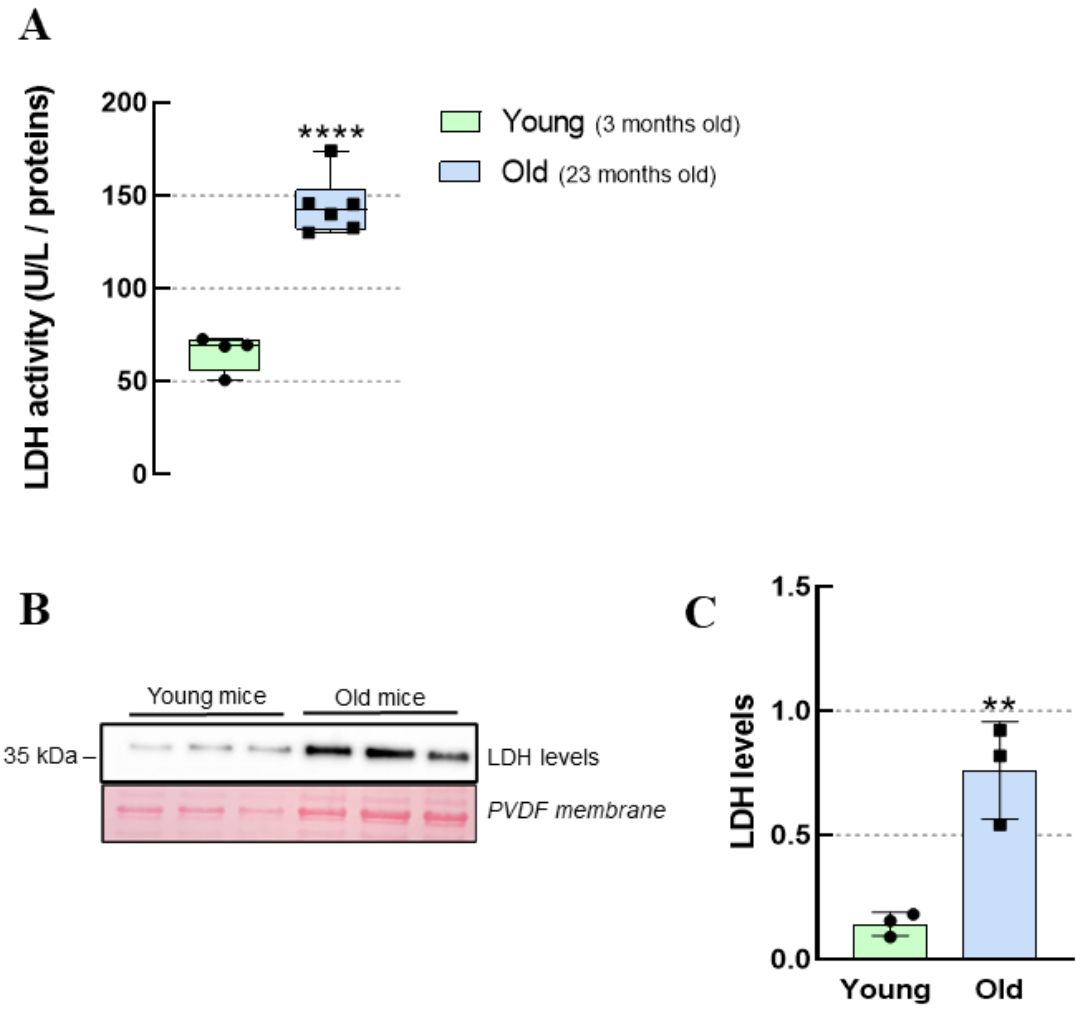


**Figure 24**. Different LDH-A activity and expression levels between triceps of young and old mice. (**A**) LDH-A activity assay. U/L are normalized on total muscular protein content. **** $p$<0,0001. (**B**) LDH-A immunoblot. PVDF membrane was used for normalization, and the mean values are reported in the bar graph (**C**). ** $p$<0,01. Mice used for each condition = 6.

### 4.17. In the triceps of aged mice there is an increase in levels of Monocarboxylate Transporter 4 (MCT4)

Since an increased level of lactate associated with raised LDH-A level and activity have been observed in triceps of aged mice in comparison with younger animals, an ELISA assay was performed to assess the expression levels of Monocarboxylate Transporter 4 (MCT4). As reported in figure 25, there is an evident and significant increase of MCT4 expression levels in old mice compared to the young ones. This increase in lactate may be related to the upregulation of MCT4, the transporter responsible for exporting lactate out of the cell. The augmented expression of MCT4 could therefore play a role in the accumulation of lactate within the muscle.

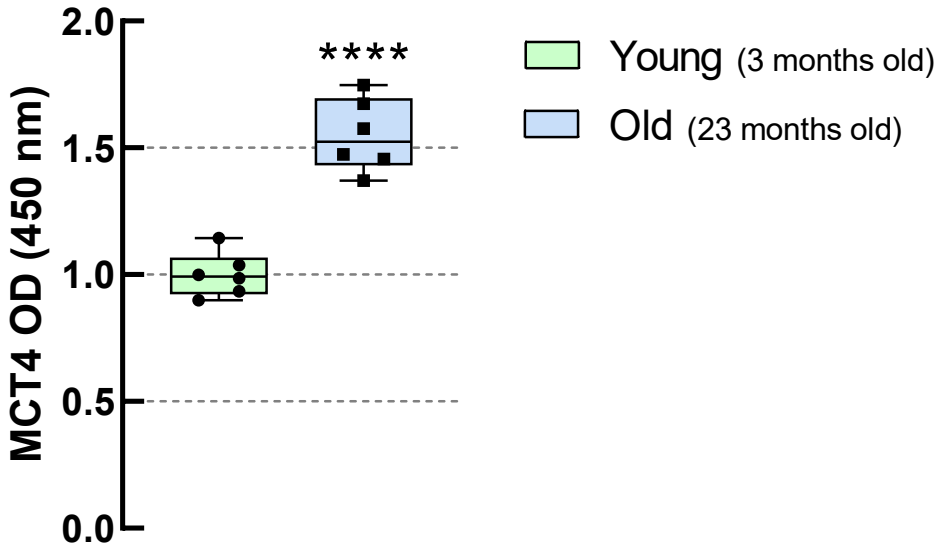


**Figure 25**. An ELISA Assay was performed in both triceps of young and old mice to evaluate potential differences. The Optical Density (OD) is measured spectrophotometrically at 450 nm in a microplate reader. **** $p$<0,0001. Mice used for each condition = 6.

## 4.18. Triceps of aged mice show increased levels of GPR81 expression

To understand if lactate signalling could be involved in muscular wasting in sarcopenia, lactate receptor GPR81 expression was evaluated through an immunoblot analysis. Figure 26A shows that triceps of old mice have a statistically significant raise of GPR81 expression levels, compared to the triceps of young mice. The graph in figure 26B represents the bar graph of GPR81 quantification of both groups.

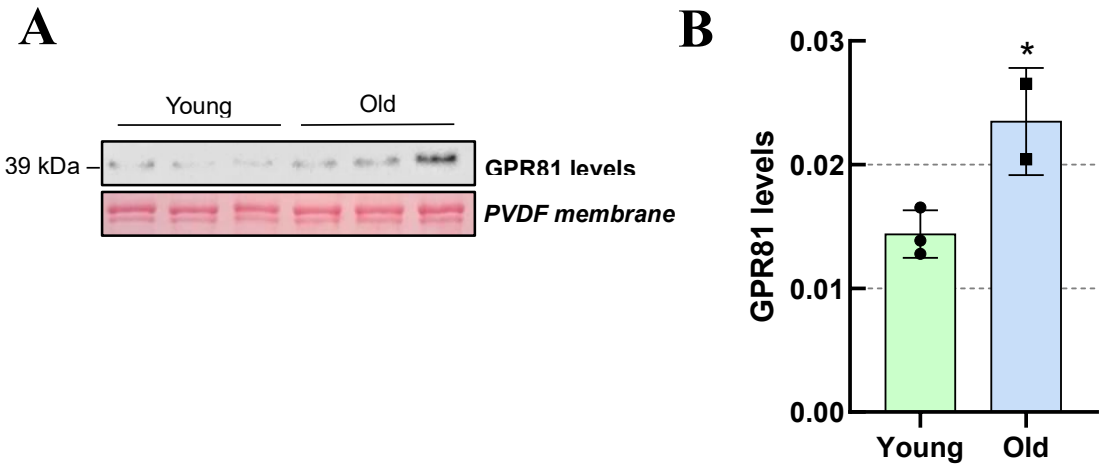


**Figure 26**. Different GPR81 expression levels between triceps of young and old mice. (**A**) GPR81 immunoblot. PVDF membrane was used for normalization, and the mean values are reported in the bar graph (**B**). * $p$<0,05. Mice used for each condition = 6.

## 4.19. The treatment of aged mice with the adiponectin agonist *AdipoRon* alleviates sarcopenia, restoring a condition similar of young mice

AdipoRon, a synthetic agonist of AdipoRon, has shown various beneficial effects on muscle metabolism [131;132]. To investigate the potential effect of this compound on muscular wasting, we performed experiments to evaluate if AdipoRon treatment in aged mice could restore a condition similar to younger animals. Firstly, a lactate assay on triceps of young mice, old mice and old mice treated with AdipoRon (50mg/kg/day) has been carried on. As shown in figure 27A, AdipoRon treatment in aged mice leads to a reduction in intramuscular lactate production compared to untreated aged mice. The graph points out that lactate levels in treated mice are comparable to those observed in young mice, indicating that AdipoRon treatment diminishes the elevated lactate levels in old mice. Concerning LDH-A, the enzyme activity in figure 27B shows increased LDH-A activity, while a statistically significant decrease is observed in treated aged mice compared with non-treated aged mice due to AdipoRon treatment. Moreover, immunoblot analysis was conducted to determine whether treatment of aged mice with AdipoRon could affect the expression levels of LDH-A and GPR81. As shown in figure 27C, AdipoRon treatment led to a reduction in LDH-A expression levels in aged mice, with normalized values reported in the bar graph. Similarly, western blot image in figure 27D demonstrates a decrease in the triceps of AdipoRon treated-aged mice compared to their untreated counterpart. Finally, to investigate whether AdipoRon also affects MCT4 expression, an ELISA Assay was performed. Graph in figure 27E indicates that AdipoRon treatment in aged mice leads to a marked reduction in MCT4 expression levels compared to untreated controls. In conclusion, administering AdipoRon to aged mice reduces the detrimental effects associated with muscle wasting due to sarcopenia. Notably, AdipoRon seems to restore muscle characteristics to a condition comparable to that observed in young mice for what concerning lactate levels, LDH-A activity, LDH-A and GPR81 expression levels and MCT4 expression. Collectively, these findings suggest that AdipoRon treatment may have the potential to reverse sarcopenia-related muscle wasting.

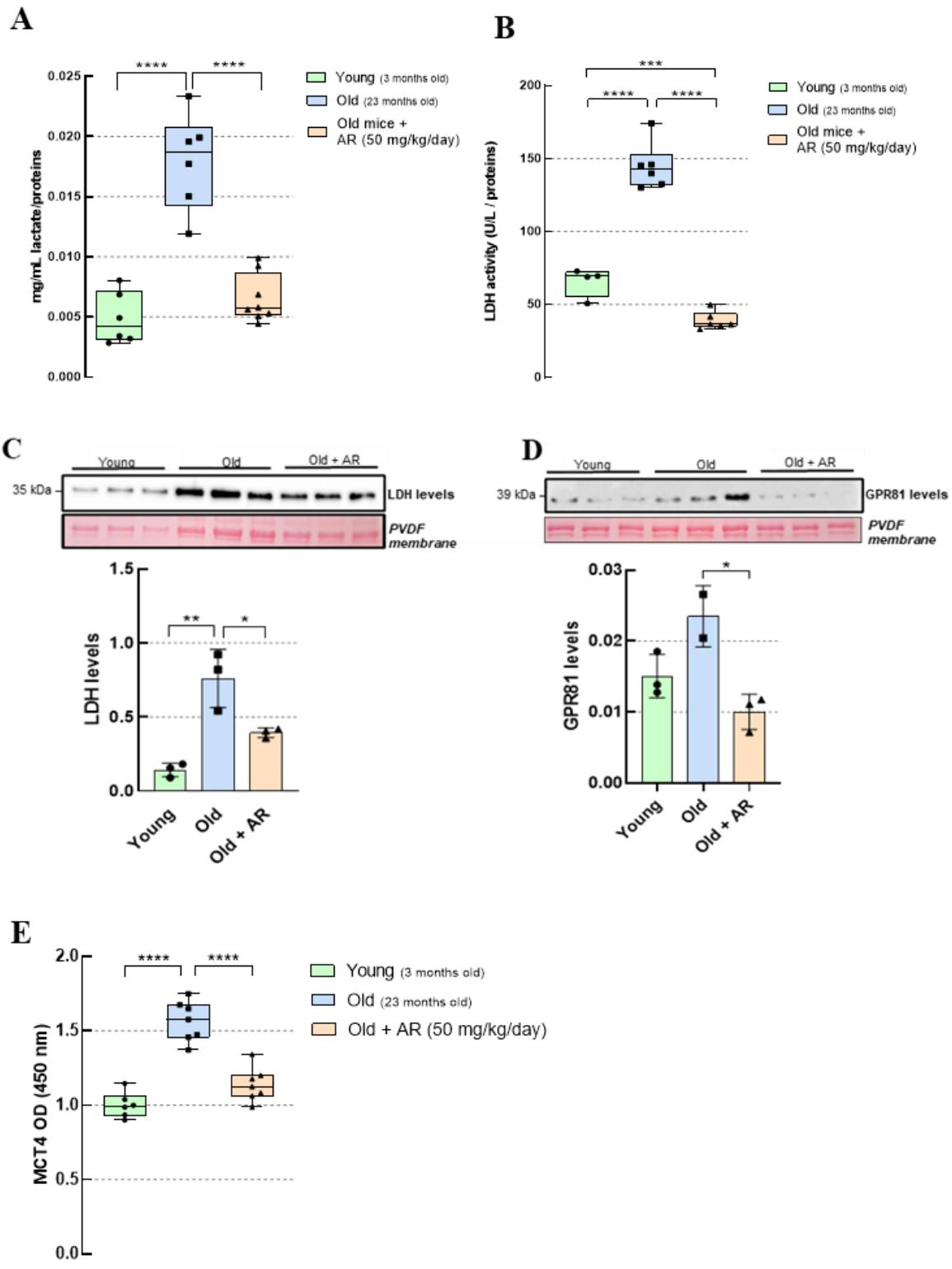


**Figure 27**. AdipoRon treatment alleviates muscular wasting associated with sarcopenia. (**A**) Lactate assay; mg/ml lactate are normalized on total muscular protein content. **** $p$<0,0001. (**B**) LDH activity assay. U/L are normalized on total muscular protein content. ** $p$<0,01; **** $p$<0,0001. (**C**) LDH immunoblot. PVDF membrane was used for normalization, and the mean values are reported in the bar graph. * $p$<0,05; ** $p$<0,01. (**D**) GPR81 immunoblot. PVDF membrane was used for

normalization, and the mean values are reported in the bar graph. * $p$<0,05. (**E**) ELISA Assay. The Optical Density (OD) is measured spectrophotometrically at 450 nm in a microplate reader. **** $p$<0,0001. Mice used for each condition = 6.

## 4.20. CM CT26 treatment induces metabolic alterations and LDH up-regulation in adipocytes

Cachexia is a multi-organ condition that not only affects skeletal muscle tissue, but also involves adipose tissue, leading to a profound wasting. For this reason, the effects of CM CT26 and the involvement of lactate in adipose tissue were analyzed, using mature adipocytes obtained from the differentiation of 3T3 cell line cells.

The treatment of murine adipocytes with CM CT26 induces a cachectic phenotype, characterized by reduced cell area (Figure 28A, B) and decreased amount of adipocyte droplets (Figure 28C, D).

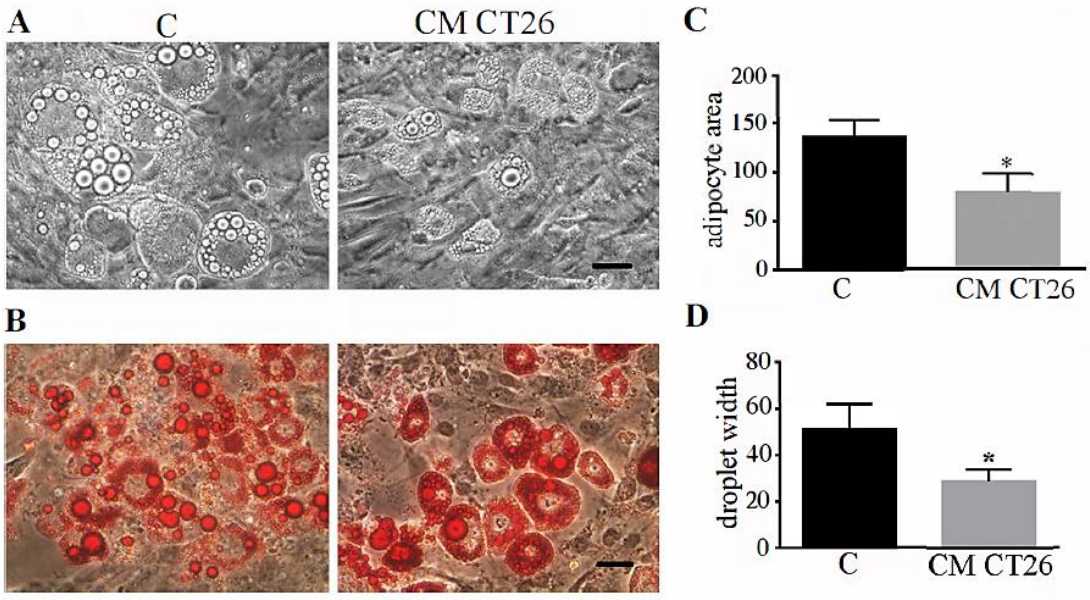


**Figure 28**. The treatment of murine adipocytes with CM CT26 induces cachectic features. Adipocytes were treated with CM CT26 for 48 hours. (**A**) Representative images of control (C) and CM CT26-treated adipocytes. (**B**) Red oil staining. (**C**) Area of adipocytes. (**D**) Width of lipid droplets. The measures showed in (**C**) and (**D**) are obtained measuring adipocyte area and lipid droplets with ImageJ in at least ten randomly chosen fields. C, control adipocytes; *$p$<0,05; n=4; scale: 50 µm.

Furthermore, lactate production and oxygen consumption appear altered in CM CT26-treated adipocytes with lower consumption (Figure 29A) and increased lactate production (Figure 29B). The same metabolic alterations have been observed in human adipocytes treated with CM CT26 (Fig 29D, E). Human adipocytes were differentiated *in vitro* from

human primary adipose stem cells (ASCs) isolated from visceral adipose tissue biopsies. These metabolic alterations are associated with LDH up-regulation in both murine (Figure 29C) and human (Figure 29F) adipocytes after CM CT26 treatment. These findings suggest that CM CT26 promotes cachectic features and metabolic perturbations associated with an augmented LDH content in murine and human adipocytes.

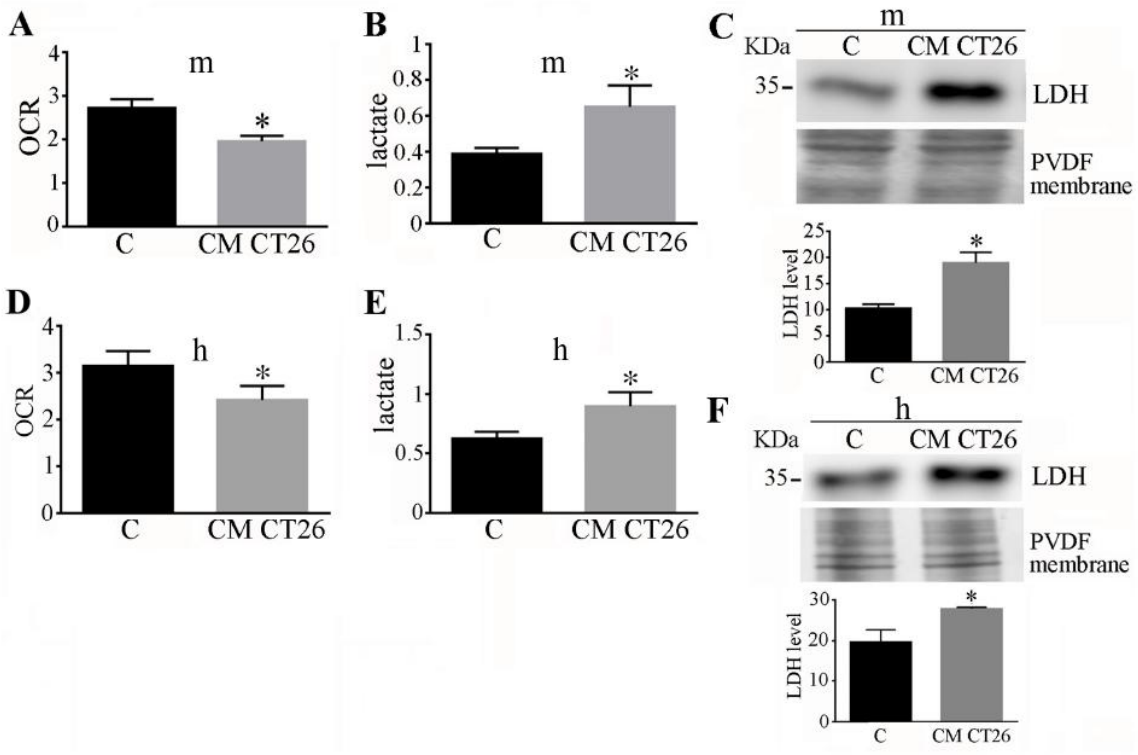


**Figure 29**. The treatment of murine and human adipocytes with CM CT26 induces metabolic alterations and LDH up-regulation. Adipocytes were treated with CM CT26 for 48h. (**A**, **D**) Analysis of oxygen consumption reported as oxygen consumption rate (OCR). (**B**, **E**) Lactate assay. (**C**, **F**) LDH immunoblot. Coomassie-stained PVDF membrane was used for normalization, and the mean values are reported in the bar graph. C, control adipocytes; m, murine adipocytes; h, human adipocytes. CM CT26: conditioned media from colon cancer cells CT26; LDH: lactate dehydrogenase; *$p$<0,05; n=3.

## 4.21. Metabolic alterations are involved in the formation of cachectic features in adipocytes

To dissect the role of metabolic modifications in the onset of cachectic features, the LDH inhibitor oxamate (50 mM) was added to CM CT26. Figure 30 shows that oxamate impedes the acquisition of both phenotypic and metabolic cachectic features in adipocytes. The adipocytes treated with CM CT26 containing oxamate displayed lipid droplet widths and cell area similar to the control cells (Figure 30A-C). Moreover, oxamate hindered the increase in lactate production (Figure 30D), the upregulation of LDH (Figure 30E), and the decrease in oxygen consumption (Figure 30F) induced by CM CT26. These findings suggest that increased lactate production plays a role in the induction of cachexia in adipocytes, as highlighted by the beneficial effects provided by oxamate.

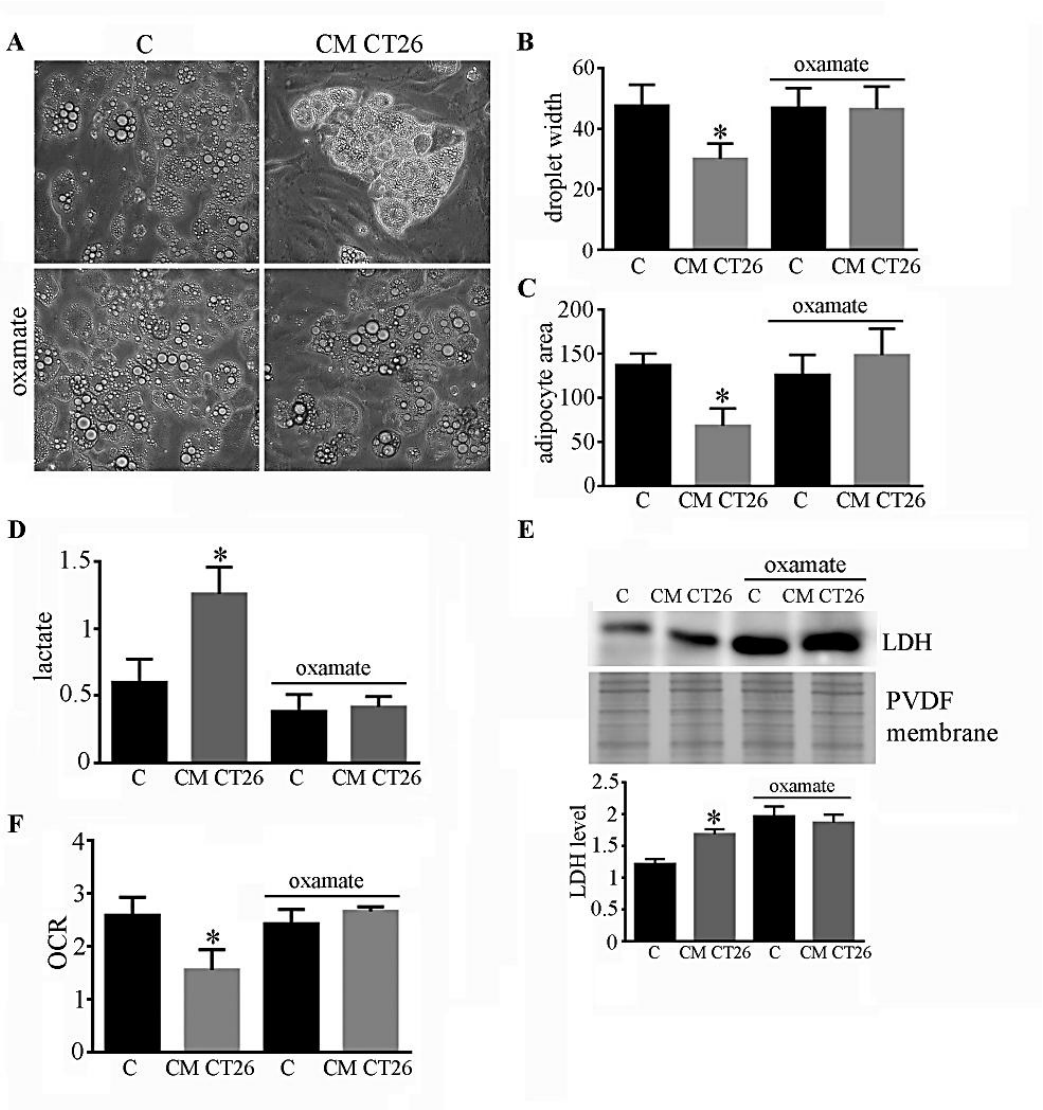


**Figure 30**. Inhibition of LDH by oxamate hinders the effects induced by CM CT26. Murine adipocytes were treated with CM CT26 for 48 h. Where indicated, oxamate (50 mM) was added to CM CT26 and to the control. (**A**) Representative images of adipocytes. (**B**) Measures of droplet width

and (**C**) adipocyte area. The parameters in (**B**, **C**) were obtained using at least ten randomly chosen fields, and the mean values are reported in the bar graphs. (**D**) Lactate assay. (**E**) LDH level obtained using immunoblotting. PVDF membrane was used for normalization, and the mean values are reported in the bar graph. (**F**) Oxygen consumption rate (OCR); CM CT26: conditioned media from colon cancer cell CT26; LDH: lactate dehydrogenase; * $p < 0.05$; n = 3; scale: 50 μm.

## 4.22. CM CT26-treated adipocytes show decreased adiponectin levels

It was assayed the level of adiponectin, one of the main adipokines secreted by adipose tissue. Murine adipocytes treated with CM CT26 displayed a greatly decreased level of adiponectin synthesis (Figure 31A) and secretion (Figure 31B) since a lower amount of adiponectin was observed in the medium in comparison with that secreted by the control adipocytes. The same effect was observed after the treatment of adipocytes with IL-6, a cytokine greatly involved in the onset of cancer cachexia.

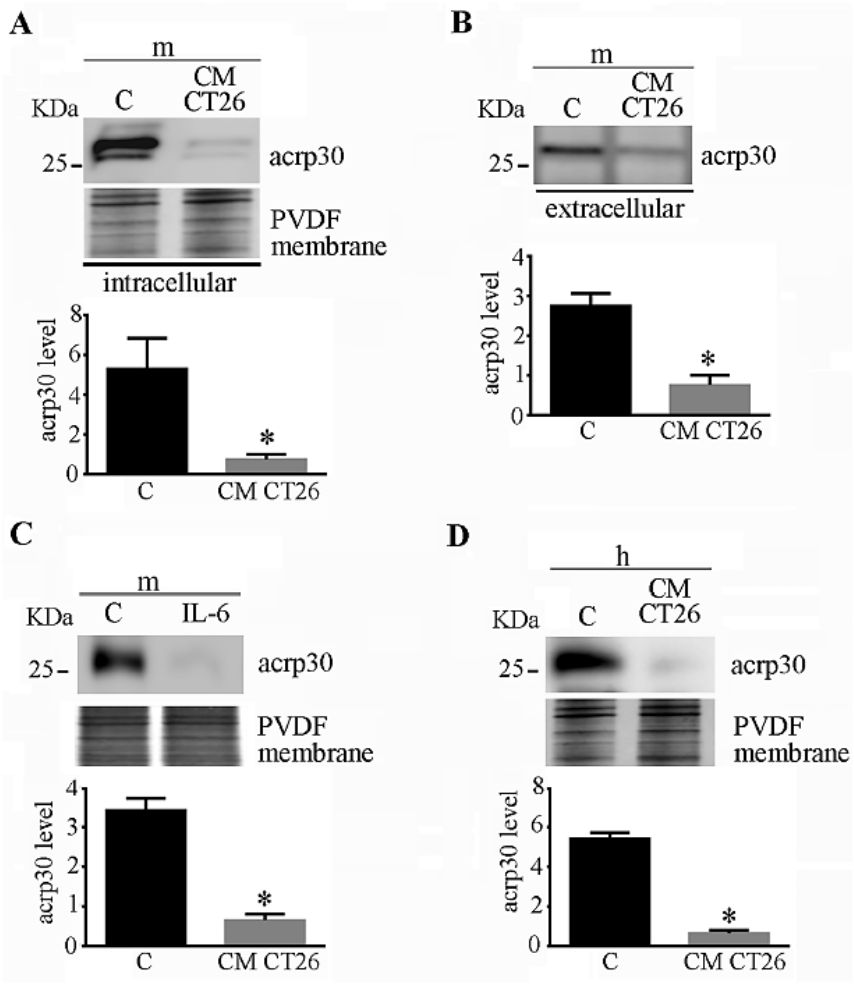


**Figure 31**. Human and murine adipocytes showing decreased levels of adiponectin. Adipocytes were treated with CM CT26 or with IL-6 (240 ng/mL) for 48 h, and adiponectin levels was detected using immunoblots. (**A**) Intracellular adiponectin level and (**B**) secreted adiponectin in murine adipocytes.

(**C**) Intracellular adiponectin in murine adipocytes treated with IL-6. (**D**) Intracellular adiponectin in human adipocytes treated with CM CT26. C, control adipocytes; m, murine adipocytes; h, human adipocytes. CM CT26: conditioned media from colon cancer cell CT26; acrp30: adiponectin; * $p < 0.05$; n = 3.

Figure 32 shows that IL-6 treatment provokes in adipocytes the same consequences induced by CM CT26 regarding myotube phenotype (Figure 32A–C), lactate production (Figure 32D), and oxygen consumption (Figure 32E). The IL-6-treated adipocytes displayed decreased adiponectin production like the cells treated with CM CT26 (Figure 31C). A similar result was obtained for the human adipocytes treated with CM CT26 (Figure 31D).

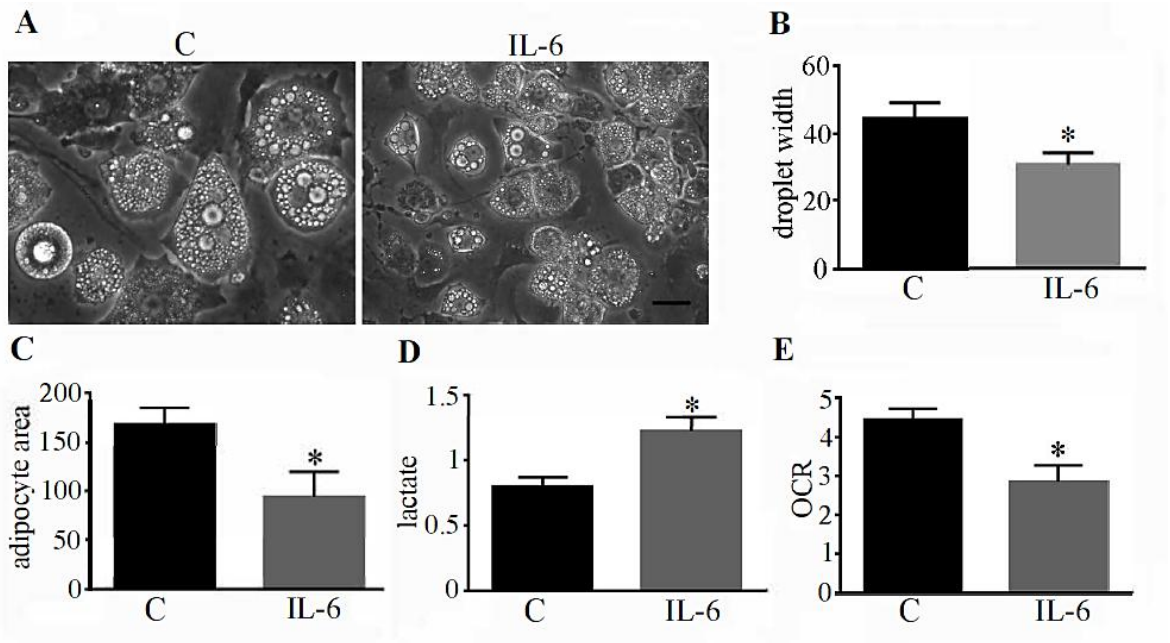


**Figure 32**. IL-6 induces cachectic features in murine adipocytes. Adipocytes were treated with IL-6 (240 ng/ml) for 48 hours. (**A**) Representative images of control (C) and IL-6-treated adipocytes; (**B**) Width of lipid droplets; (**C**) Adipocytes' area. The measures showed in (**B**) and (**C**) are obtained with ImageJ using at least ten randomly chosen fields. (**D**) Lactate amount; (**E**) Oxygen Consumption Rate (OCR). C, control adipocytes; *$p$<0.05; n = 4; scale: 50 μm.

## 4.23. Phenotypic and metabolic alterations involve the STAT3 signalling pathway

The STAT3 signalling pathway plays a prominent role in the induction of cancer cachexia [113,133]. CM CT26 induces the activation of STAT3 in adipocytes after five minutes of stimulation, as shown in Figure 33A. To dissect the role of STAT3 in the acquisition of cachectic features, adipocytes were treated with CM CT26 containing the STAT3 inhibitor WP1066. STAT3 inhibition hinders the acquisition of both phenotypic alterations due to CM CT26, thus impeding the decrease in lipid droplet width (Figure 33B, C) and cellular area (Figure 33D). Regarding metabolism, WP1066 impedes the changes in lactate production and oxygen consumption, which remain similar to those for the control adipocytes (Figure 33E, F).

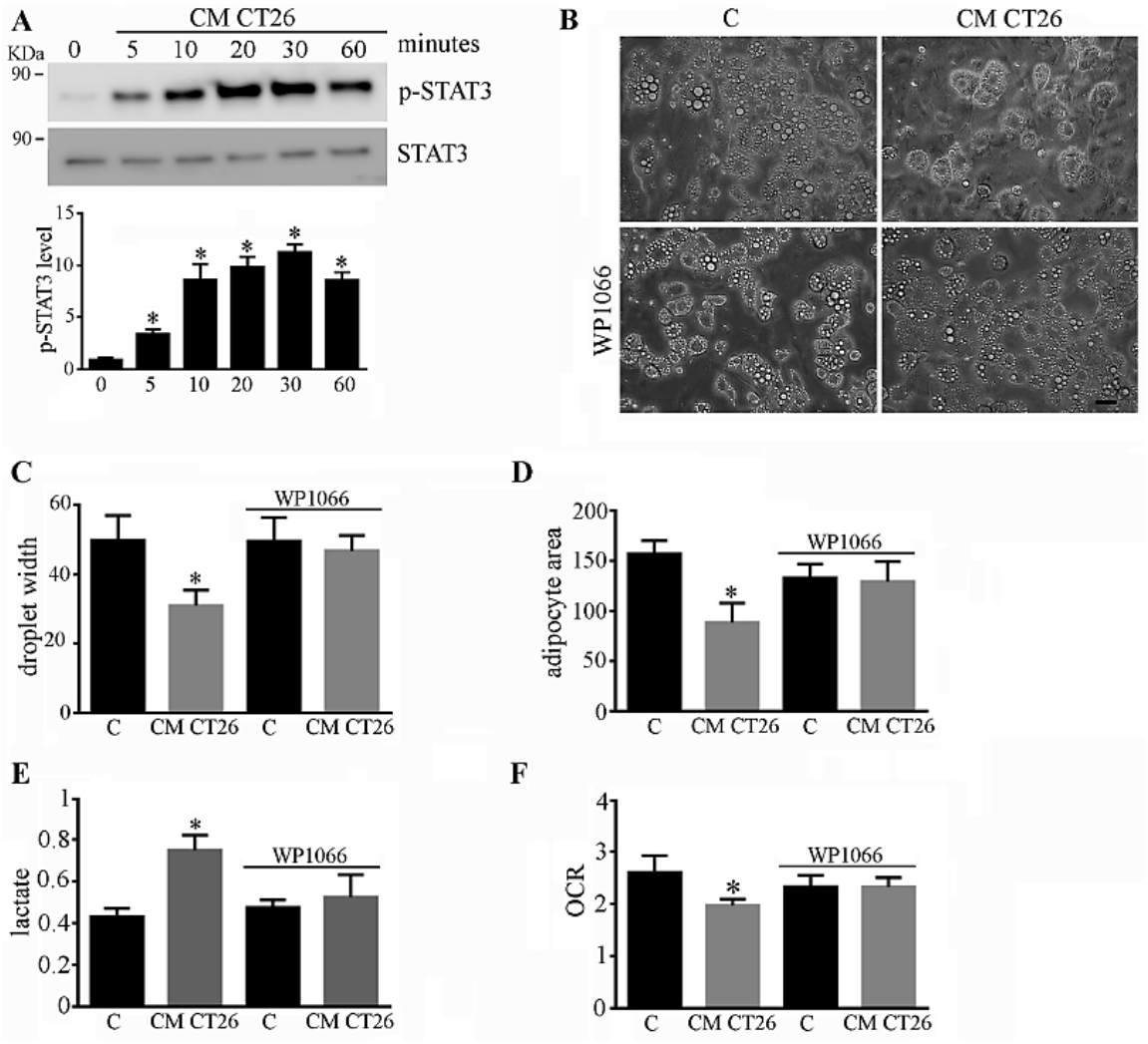


**Figure 33**. STAT3 signalling drives the effects induced by CM CT26. (A) Murine adipocytes were treated with serum-free medium overnight and then stimulated for the indicated time with CM CT26. The levels of total and phosphorylated-Tyr705 of STAT3 were detected using immunoblots. Panels B-F show murine adipocytes that were treated with CM CT26 for 48 h. Where indicated, WP1066

(10 μM) was added to CM CT26 or to the control. (**B**) Representative images of adipocytes. (**C**) Measures of lipid droplet width and (**D**) adipocyte area, both calculated using at least ten fields chosen randomly. (**E**) Lactate assay. (**F**) Analysis of oxygen consumption reported as oxygen consumption rate (OCR). C, control; CM CT26: conditioned media from colon cancer cell CT26; * $p < 0.05$; n = 3; scale: 50 μm.

## 4.24. STAT3 signalling drives LDH and adiponectin levels in CM CT26-treated adipocytes

It was analysed the involvement of STAT3 in the alterations of LDH and adiponectin levels in the CM CT26-treated adipocytes. The treatment of adipocytes with CM CT26 containing the STAT3 inhibitor WP1066 impeded the up-regulation of LDH (Figure 34A) and the downregulation of adiponectin (Figure 34B) provoked by the CT26 secretome, thus showing that the alterations of these two proteins are controlled by STAT3 signalling.

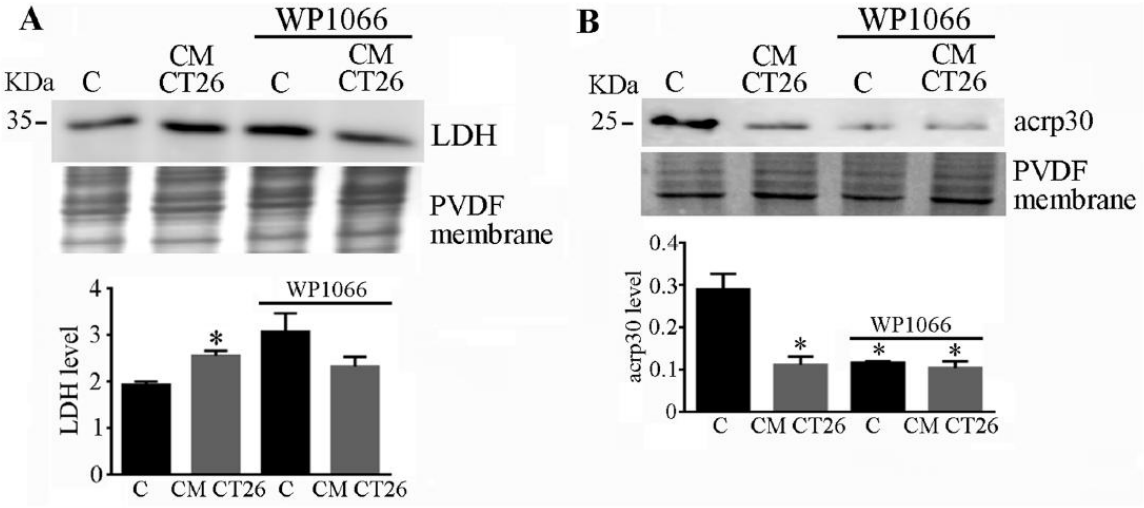


**Figure 34**. STAT3 controls LDH and adiponectin levels. Murine adipocytes were treated with CM CT26 for 48 h. Where indicated, WP1066 (10 μM) was added to CM CT26. (**A**) LDH and (**B**) adiponectin levels assayed using immunoblotting. PVDF membranes were used for normalization, and the mean values are reported in the bar graph. C, control; CM CT26: conditioned media from colon cancer cell CT26; LDH: lactate dehydrogenase; acrp30: adiponectin; * $p < 0.05$; n = 3.

# 5. DISCUSSION

Lactate has traditionally been considered a mere by-product of anaerobic glycolysis, mainly generated during intense muscular activity. However, researchers have refined lactate as a multifunctional molecule with metabolic and signalling functions together with a new, recently discovered role as an epigenetic regulator [160]. During physical exercise, lactate produced by skeletal muscle is transported to the liver, where it acts as a gluconeogenic substrate, forming the basis of the well-known Cori cycle. Lactate is also present in mitochondria, associated with the mLOC. In addition, lactate mediates signalling through the GPR81 receptor, and it can regulate chromatin and gene transcription via histone binding, thereby influencing systemic energy homeostasis. However, lactate accumulation and shuttling may be linked to pathological conditions, since it sustains energy and anabolic support to cancer cells, and it can function as an oncometabolite, leading to an increased aggressiveness of cancer [87,108,134]. In cancer cachexia, which is a severe form of muscle wasting cancer-related with multifactorial metabolic dysfunction, accumulating evidence suggests that lactate can play a pivotal role not only as a metabolic end-product but also as a driver of cellular and molecular pathways leading to muscle degeneration. In this context, recent studies have highlighted a strong association between alterations in lactate metabolism and the onset and progression of cancer-induced muscle wasting [112,113]. These studies demonstrate that metabolic alterations play a central role in the induction of a wasting phenotype in myotubes, and that interventions targeting pyruvate/lactate dynamics can prevent or mitigate the atrophic phenotype. When myotubes are exposed to tumor-derived factors, they undergo a profound metabolic reprogramming, characterized by a shift from oxidative phosphorylation toward aerobic glycolysis (Warburg effect). This metabolic switch promotes glucose fermentation and increases extracellular lactate levels, even in the presence of oxygen. Together with these metabolic changes, myotubes with a wasting phenotype exhibit typical hallmarks of muscle atrophy, including a reduction in myotube diameter, decreased MHC content, and increased ubiquitination of muscle proteins, reflecting the activation of the proteolytic pathway. These morphological and molecular alterations are combined with a marked mitochondrial dysfunction, evidenced by reduced oxygen consumption, impaired mitochondrial membrane potential, decreased pyruvate dehydrogenase (PDH) activity and lower expression levels of the OXPHOS complexes [112]. Significantly, preventing the metabolic shift toward lactate production effectively blocks the wasting phenotype. These findings indicate that lactate production is not merely a metabolic consequence of cancer cachexia, but rather a key factor driving its onset. Restoration of mitochondrial membrane potential under this condition further strengths the

evidence that disruptive oxidative metabolism plays a key role in muscle wasting [112]. Analysing these findings, Mannelli *et al*. explored whether enhancing mitochondrial pyruvate metabolism could protect myotubes from cachectic degeneration. Supplementation of CT26-conditioned media (CM CT26) with sodium pyruvate efficiently prevented the onset of both metabolic and phenotypic hallmarks of muscle degeneration *in vitro*. Pyruvate-treated myotubes maintained normal width and MHC expression levels compared to non-treated myotubes. Treated myotubes also exhibit rates of oxygen consumption, PDH activity and lactate production comparable to control myotubes. The beneficial effects of pyruvate were dependent on its mitochondrial utilization, as pharmacological inhibition of the mitochondrial pyruvate carrier (MPC) using UK5099 reproduced the cachectic phenotype, leading to impaired oxidative metabolism and muscle atrophy [113]. Interestingly, pyruvate treatment significantly reduced STAT3 phosphorylation, a key mediator of muscle atrophy and inflammation in cancer cachexia. This downregulation of STAT3 activity induces the restoration of mitochondrial metabolism, thereby linking cellular energy balance to the regulation of catabolic signalling pathways [113]. Collectively, these studies highlight the central role of lactate metabolism and pyruvate utilization in the pathogenesis of cancer cachexia. A shift toward a fermentative and lactate-producing metabolism leads to mitochondrial dysfunction, energy imbalance and proteolytic pathway activation, ultimately driving muscle wasting. In contrast, restoring mitochondrial pyruvate oxidation preserves energy homeostasis, prevents lactate accumulation, and suppresses catabolic signalling via STAT3. These findings reveal the dual role of lactate as both a metabolic signalling molecule and a pathogenetic mediator in muscle wasting.

Given these premises, the aim of this thesis was to investigate the role of lactate and its involvement in muscle wasting. Specifically, its role was evaluated under two different conditions: (1) in tumor-associated states (cancer cachexia) and (2) during aging (sarcopenia), both *in vitro* and *in vivo*.

Regarding tumor-associated muscle wasting, the results obtained from both monolayer and three-dimensional myotube cultures strongly support the involvement of lactate as both a metabolic substrate and a signalling molecule. In monolayer cultures, treatment with CT26 conditioned medium, lactate and the GPR81 receptor agonist DHBA induced evident phenotypic alterations, particularly a reduction in myotube width, suggesting a catabolic shift consistent with muscle atrophy. These effects were accompanied by metabolic changes, including an increase in extracellular lactate production and a decrease in oxygen consumption, indicative of a shift toward glycolytic metabolism. Similar results were

observed in three-dimensional cultures, namely spheroids, a model that more accurately reproduces the structural organization of skeletal muscle tissue. In this context, both lactate and DHBA treatments led to a reduction in spheroid diameter, likely reflecting a decrease in the number or size of myotubes forming the spheroids. This observation is consistent with a reduction in MHC expression levels, a well-established marker of muscular differentiation. Taken together, these findings highlight a dual role of lactate – as a metabolite and as a signalling molecule – in modulating muscle wasting under tumor-related conditions. Therefore, these results suggest that lactate actively contributes to the onset and progression of muscle wasting in two different types of models.

It is well known that a large number of molecular pathways contribute to the regulation of muscle growth and wasting processes. Among them, the STAT3 pathway plays a pivotal role in muscle wasting mediated by the IL6/JAK/STAT3 signalling cascade. Upon activation, phosphorylated STAT3 (pSTAT3) dimerizes and translocate into the nucleus, where it promotes the transcription of various target genes. STAT3 activation in skeletal muscle has been widely associated with the promotion of muscle atrophy in several pathological context, including diseases and cancer [124]. Based on these observations, it was assessed whether treatment of myotubes with lactate or DHBA could induce activation of the STAT3 signalling pathway. As shown by the results presented in the section 4.3 of the Results, both lactate and DHBA treatments triggered a time-dependent activation of STAT3 signalling cascade. These findings suggest that lactate may exert a signalling function contributing to the activation of molecular pathways involved in muscle wasting and thus being responsible for the phenotypic and metabolic alteration observed in treated myotubes.

Historically, lactate metabolism has been associated with anaerobic energy metabolism, however recent studies revealed a more complex and central role for lactate in cellular metabolism. A key component is the mLOC, which is a protein complex located in the inner mitochondrial membrane that facilitates lactate uptake and oxidation within mitochondria. In this context, lactate has been shown to play a significant role in mitochondrial metabolism, influencing ATP production and mitochondrial function [125]. Considering this evidence, it was investigated whether treatment with CT26 tumor cell conditioned medium could alter mitochondrial lactate content in myotubes. Interestingly, as reported in the section 4.4 of the Results, following a cellular fractionation, the treatment of myotubes with CM CT26 led to a significant up-regulation of LDH-A expression and an increase in mitochondrial lactate levels. These findings suggest that, under tumor-associated conditions, elevated

mitochondrial lactate may play a critical role in promoting myotube degradation, contributing to the molecular mechanisms underlying muscle wasting in cancer.

Lactate is transported across cellular compartments by monocarboxylate transporters via proton-lactate symport [87]. In muscles, MCT4 exports lactate and hydrogen ions in a 1:1 ratio, while MCT1 is responsible for the uptake of lactate and other monocarboxylates into the cell, playing a crucial role in cellular energy metabolism and in the lactate shuttle between tissues [135]. Results obtained with CHC showed that the inhibitor is able to block the wasting phenotype, as evidenced by an increase myotube width, an upregulation of MHC expression, a reduction of atrogin-1 levels, and a decreased lactate production, compared to myotubes treated with CM CT26. Together, these findings indicate that the lactate which enters the cells via MCT1 transporter contributes to the induction of a wasting phenotype in myotubes, highlighting MCT1 as a potential target for the development of novel therapeutic strategies.

The next step was to investigate whether similar alterations could be observed in the skeletal muscles of patients with gastrointestinal tumors undergone surgery. Analysis of these samples revealed elevated lactate levels in muscle tissue, accompanied by increased gene expression of *Ldha* and *Gpr81* in cachectic patients. This suggests that lactate also plays a significant role in promoting muscle wasting in patients, where muscle wasting is induced by cancer pathology. The results obtained from patients' muscle samples are highly promising with respect to potential therapeutic strategies. Nevertheless, the analysis of a larger number of samples would be required to strengthen these findings and obtain a more comprehensive dataset. Importantly, an expanded cohort would also allow stratification of samples into specific subclasses, such as sex and tumor type, thereby providing a more complete and robust framework for data interpretation.

Moreover, in this context the tumor microenvironment plays a critical role in cancer progression, and fibroblasts are key components of this milieu [159]. These mesenchymal-derived cells are essential for tissue homeostasis and contribute to pathological processes such as cancer. Cancer-associated fibroblasts (CAFs), a major component of the tumor stroma, secrete growth factors and proteins that promote tumor growth and immune evasion [126]. For this reason, fibroblasts were isolated from muscular biopsies to evaluate the potential role of lactate. Results presented in sections 4.8, 4.9, 4.10 and 4.11 show that fibroblast derived from muscles of cancer patients exhibited increased extracellular lactate levels, and higher expression of LDH-A and GPR81. Moreover, myotubes treated with conditioned medium derived from fibroblasts, show phenotypic effects typical of muscular

wasting. These observations may form the basis for the hypothesis of a potential lactate-driven crosstalk between muscle cells and fibroblasts (Fig. 35). Lactate produced by muscle fibroblasts could be shuttled to skeletal muscle cells through MCT1-mediated transport or interact with GPR81 receptors on muscle fibers, establishing a potential metabolic crosstalk between fibroblasts and muscle cells. These findings suggest the potential existence of a self-sustaining mechanism that could perpetuate the wasting condition in skeletal muscle through both autocrine and paracrine signalling loops. Also in this case, to further strengthen the robustness of the data, fibroblasts obtained from a larger cohort of patients would be required.

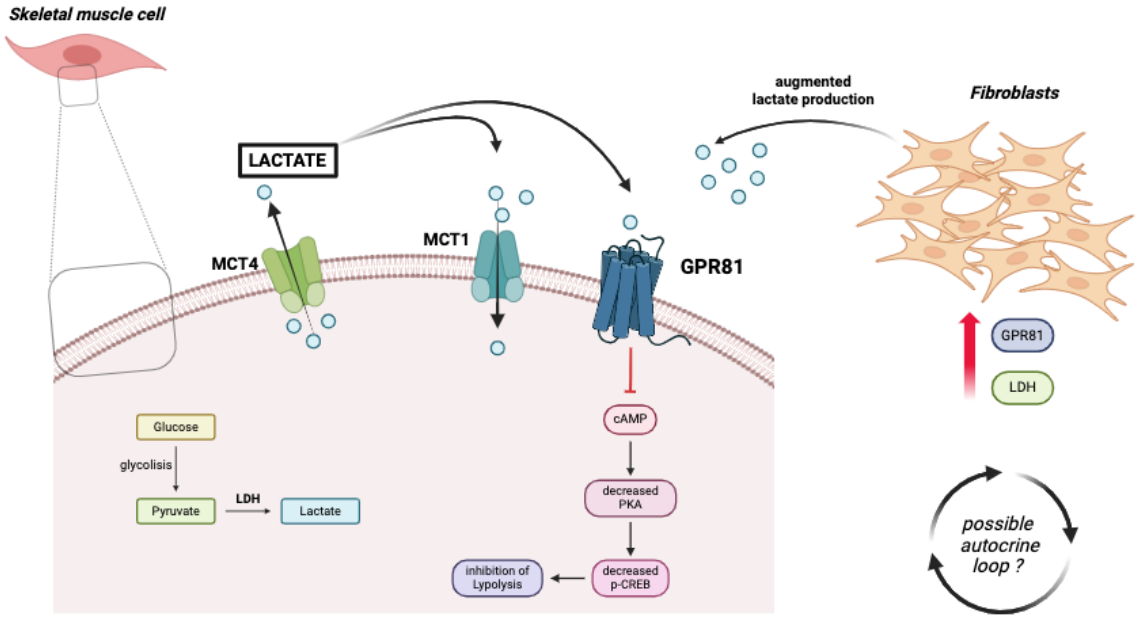


**Figure 35**: Proposed model of crosstalk between skeletal muscle cells and fibroblasts. In skeletal muscle lactate dehydrogenase-A (LDH-A) catalyses the formation of lactate from pyruvate, the end-product of glycolysis. Newly formed lactate can be secreted from the cell via monocarboxylate transporter 4 (MCT4). In the extracellular environment, lactate can re-enter within the cell via monocarboxylate transporter 1 (MCT1). Alternatively, lactate can bind to the GPR81 receptor and trigger a signaling cascade that leads to cAMP inhibition. Moreover, lactate produced by muscle fibroblasts could shuttle to skeletal muscle cells via MCT1 or bind to GPR81, resulting in a crosstalk between the muscle cells and fibroblasts. Image created with biorender.com.

In the context of muscle wasting, it is well-established in literature that oxidative stress plays a pivotal role, associated with elevated production of reactive oxygen species (ROS) and consequent damage to proteins and mitochondrial functions [136]. One of the main antioxidant systems strongly implicated in mitigating oxidative stress is the thioredoxin (Trx) system, in particular thioredoxin reductases (TrxRs), which reduce oxidised

thioredoxin using NADPH and consequently helping to maintain cellular redox homeostasis [137]. Given these premises, the activity of TrxR was investigated in the muscles of cancer patients. Results obtained showed an increase in TrxR activity in muscles of cancer patients, compared to the healthy ones. This finding supports the hypothesis that elevated TrxR activity may play a role in tumor progression, as cachexia typically arises during advanced stages of cancer. In particular, results obtained suggest that this enzyme could represent a critical factor contributing to the development and progression of cancer-associated muscle wasting.

Moreover, it is well established that TrxR is a primary molecular target of Auranofin, a gold-based compound long used in the treatment of rheumatoid arthritis, with a significant anti-inflammatory effect. Auranofin inhibits TrxR by binding to its active site, impairing the thioredoxin system and thereby disrupting redox homeostasis in cells [138]. Because TrxR is critical for antioxidant defences, its inhibition by auranofin has been explored in oncological contexts. In view of this evidence, myotubes were treated with 25 nM Auranofin for 48 hours to evaluate the effects of TrxR inhibition in the model of tumor-associated muscle wasting. The results showed that Auranofin counteracts the deleterious effects induced by CM CT26. Myotube width was increased toward values comparable to control myotubes, indicating a protective effect on muscle structure. This outcome was complemented by an analysis of atrogin-1 expression levels on which the treatment with auranofin normalized its expression to levels similar of control conditions. Together, these findings suggest that the Trx/TrxR antioxidant system plays a significant and potentially causative role in the process of muscle wasting. Although TrxR is considered the primary molecular target of Auranofin, several additional off-target have been reported. These include inhibition of proteasome-associated deubiquitinases, such as USP14 and UCHL5, modulation of mitochondrial function, induction of oxidative and endoplasmic reticulum stress, and interference with redox-sensitive and inflammatory signalling pathways. Collectively, these findings indicate that Auranofin exerts pleiotropic effects beyond TrxR inhibition [137,161].

In addition to investigate the role of lactate in tumor-associated muscle wasting, it was also evaluated its involvement in another wasting condition, namely sarcopenia. Sarcopenia is defined as a progressive and generalized skeletal muscle disorder characterized by a decline in muscle mass and strength or function, often associated with aging and adverse health outcomes [139]. To explore lactate's potential contribution in sarcopenia, experiments were conducted both *in vitro* and *in vivo*. Firstly, myotubes were treated with palmitic acid, a

saturated fatty acid which is known to accumulate during aging and lipid overload, and which has been implicated in impairing myogenesis, promoting lipotoxicity and accelerating muscle cell atrophy [140]. This approach allowed to test whether palmitic acid exposure could recapitulate features of sarcopenic wasting in myotubes, and whether lactate metabolism or its signalling might be involved in this process. Myotubes treated with palmitic acid exhibited a significant reduction in myotube width, together with increased levels of extracellular lactate. To further investigate the involvement of lactate in this process, myotubes were co-treated with sodium oxamate, a competitive inhibitor of LDH, thereby blocking the conversion of pyruvate to lactate. Co-treatment with oxamate at different concentrations resulted in block of myotube wasting, restoring morphology and structure to values comparable to control myotubes. In addition to its well-established role as a competitive inhibitor of LDH, sodium oxamate has been shown to inhibit other metabolic enzymes such as aspartate aminotransferase (AAT), suggesting that its biochemical effects extend beyond LDH inhibition and may influence broader aspects of cellular metabolism [162]. Taken together, these findings indicate that exposure to palmitic acid induces muscle cell atrophy, likely mediated by enhanced lactate production and LDH activation. Simultaneous treatment with sodium oxamate impedes these detrimental effects, preserving myotube integrity and viability. This suggests that LDH inhibition may counteract palmitic acid-induced metabolic imbalance in skeletal muscle cells. This supports the hypothesis that targeting lactate metabolism could represent a potential therapeutic strategy against sarcopenic muscle wasting.

To further investigate the role of lactate in sarcopenia, during my period abroad at the Université Catholique de Louvain (Brussels), I analysed the effects of lactate in murine models of aging. Specifically, in aged mice (23 months old), muscle lactate levels in the triceps were significantly higher compared to those of young mice (3 months old). This observation suggests that lactate accumulation may be involved in the degenerative processes underlying age-related muscle wasting. This hypothesis is further supported by the finding that aged mice exhibited increase expression and activity of LDH compared to the young counterpart, indicating enhanced glycolytic metabolism and lactate production in aged muscle tissue. In addition, the expression levels of the MCT4 were assessed by ELISA assay. MCT4 is a membrane transporter responsible for exporting lactate out of cells, thereby regulating lactate homeostasis. The results showed that MCT4 expression was markedly elevated in aged mice, suggesting that this transporter could play a key role in lactate accumulation and efflux within skeletal muscle during aging. Moreover, GPR81 expression level was analysed by Western blot, revealing an increased expression in muscles of aged

mice. GPR81 activation by lactate is known to modulate intracellular signalling pathways involved in metabolism and inflammation, further supporting its potential contribution to muscle degeneration.

Adiponectin is an adipokine predominantly secreted by adipose tissue that plays a key role in regulating glucose and lipid metabolism, enhancing insulin sensitivity, and exerting anti-inflammatory and cardioprotective effects. It signals primarily via two receptors, AdipoR1 and AdipoR2, which are widely expressed in metabolic tissues such as skeletal muscle and liver [141]. AdipoRon is a synthetic small molecule which is an agonist of the adiponectin receptors AdipoR1 and AdipoR2. When AdipoRon activates these receptors, it mimics many of the biological effects of adiponectin. For instance, it improves metabolic function, enhances mitochondrial biogenesis via AMPK/PGC-1α, and shows protective effects against insulin resistance, inflammation and muscle wasting in experimental models [142]. In addition to agonism at the adiponectin receptors AdipoR1 and AdipoR2, AdipoRon has been reported to engage alternative signalling pathways. These include inhibition of mTOR/p70S6K signalling independent of AMPK activation, modulation of pro-inflammatory pathways such as NF-κB and MAPKs, regulation of mitochondrial dynamics via Drp1, and metabolic reprogramming in cancer cells. Moreover, some cardioprotective effects are retained even when AMPK signalling is compromised, suggesting engagement of additional downstream mechanisms [163, 164]. In light of this evidence, more experiments on mice were carried out to evaluate whether treatment with AdipoRon in aged mice could ameliorate muscle wasting and restore a physiological condition comparable to that observed in younger animals. Indeed, experiments performed on triceps of young mice, aged mice, and aged mice treated with AdipoRon (50 mg/kg/day) demonstrated that AdipoRon is capable of reversing the sarcopenic phenotype in muscles of aged mice. This effect was evidenced by a reduction in lactate production, decreased LDH activity, lower expression levels of LDH and the receptor GPR81, and a decrease in MCT4 expression. In conclusion, these findings suggest that AdipoRon not only improves muscle metabolism in aged mice, but also modulates lactate production and transport, highlighting its potential role as a therapeutic strategy to counteract age-related sarcopenia through the regulation of lactate-associated pathways. Overall, these findings suggest that lactate is strongly implicated in sarcopenia-associated muscle wasting, acting not only as a metabolic by-product, but also as a signalling molecule that may exacerbate degenerative pathways during aging.

Furthermore, additional findings have demonstrated that lactate not only acts as an inducer of skeletal muscle atrophy but also plays a fundamental role in adipose tissue metabolism

and remodelling. Adipose tissue is profoundly affected by metabolic alterations and structural modifications in the context of cancer cachexia, where increased lipolysis, inflammation, and loss of lipid storage capacity contribute to the overall wasting phenotype [143]. In the section of the results dedicated to adipocytes, results obtained showed that the secretome form murine colon carcinoma CT26 induces cachectic-like features and metabolic alterations in adipocytes, characterized by a decrease in oxygen consumption rate and elevated lactate production. Adipocytes exhibit increased LDH-A and decreased adiponectin levels, both hallmarks of metabolic dysregulation. The STAT3 signalling cascade seems to mediate these changes, as its inhibition prevents the formation of the phenotypic, metabolic and molecular alterations observed (Fig. 36). Notably, these findings identify STAT3 as a central regulator of both LDH and adiponectin expression, suggesting that this pathway may contribute to the onset and progression of the cachectic condition. Morphologically, cachectic adipocytes, as reported both in animal models and cachectic patients, typically present a reduction in cell perimeter and area [144]. Concurrently, in the cachectic condition occurs extensive lipid mobilization, leading to a decrease in lipid droplet width and increased levels of circulating free fatty acids, which correlate with disease severity [145]. In line with these observations, these data demonstrate that the CT26 secretome induces morphological alterations typical of cachectic adipocytes, including reduction in lipid droplet size and cell area.

An interesting result is the LDH-A up-regulation induced by the CT26 secretome in adipocytes. Deregulated LDH-A levels have been observed in several types of tumors, suggesting that LDH-A is a tumor-promoting enzyme, since it is often associated with enhanced tumor growth and metabolic reprogramming. Elevated LDH-A levels have been implicated in multiple cancer-related processes, including the epithelial-to-mesenchymal transition [146] and cell invasion and migration [147]. Conversely, LDH-A inhibition decreases tumor growth and metastasis formation [148]. The increase in LDH-A levels leads to elevate extracellular lactate accumulation, which can affect the tumor microenvironment and immune regulation. For instance, lactate accumulation has been shown to inhibit T lymphocyte functions [149], immune surveillance by T and natural killer (NK) cells [150], and innate and adaptive immunity through the recruitment of myeloid-derived suppressor cells [151]. Data obtained show that the CT26 secretome resulted in a marked increase in LDH expression and lactate secretion, suggesting that LDH-A may contribute to the cachectic phenotype in adipocytes. This hypothesis was confirmed using the LDH-A inhibitor oxamate. Co-treatment with oxamate and CM CT26 effectively prevented the effects induced by the CT26 secretome, restoring adipocyte morphology, including droplet

width and cell area, as well as oxygen consumption and lactate production, to levels comparable with untreated cells. Interestingly, oxamate treatment led to an up-regulation of LDH-A levels both in control and CM CT26-treated adipocytes, probably as a compensatory response of adipocytes to LDH-A inhibition by oxamate. Consistently, both control and CM CT26-treated adipocytes exhibited reduced lactate production compared with their untreated counterparts.

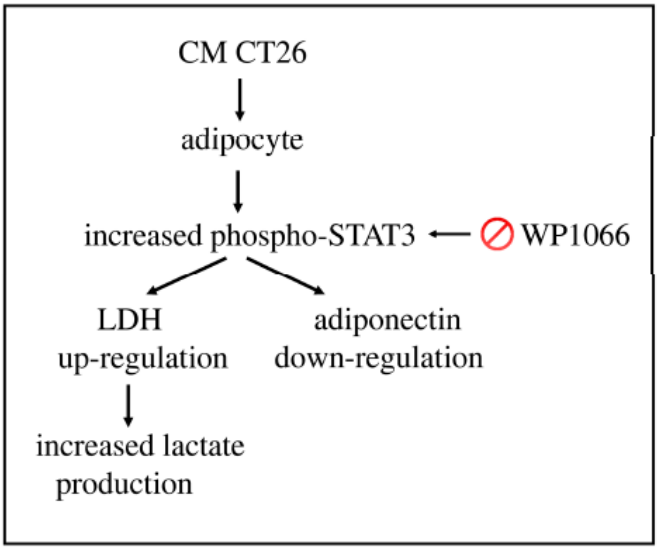


**Figure 36**. Proposed model of CM CT26 effects in adipocytes. Treatment of adipocytes with CM CT26 induces STAT3 phosphorylation on Tyr 205. STAT3 signalling cascade activation led to an increase in lactate production and a decrease in oxygen consumption, associated with enhanced level of LDH and the concomitant decrease in adiponectin. The blocking of STAT3 cascade using the inhibitor WP1066 hinders the down-stream effects due to CM CT26, which becomes ineffective.

Adipose tissue is a major organ that produces and secretes numerous hormones called adipokines, including adiponectin. Concerning metabolism, adiponectin enhances glucose uptake, activates glycolysis and promotes triglyceride breakdown [152], whereas in several tissues including skeletal muscle, it acts as a differentiating hormone [153]. Data from literature indicate that adiponectin levels in cancer cachexia vary depending on tumor type and disease stage [145]. Results obtained show that treatment of adipocytes with CM CT26 led to a marked downregulation of adiponectin expression with a consequent reduction in adiponectin levels in the extracellular environment. This effect was consistently observed in both murine and human adipocytes, suggesting that this effect is not restricted to a specific cell type. Given adiponectin's role in target tissues, it can be hypothesised that the decrease in adiponectin production by cachectic adipocytes affects the functionality of the target organs, which is associated with the worsening of the pathology.

Results obtained demonstrate that the effects induced by the CT26 secretome are mediated by the STAT3 signalling cascade. The involvement of STAT3 signalling has been demonstrated in several human cancers, where it correlates with a poor prognosis [154] and in cancer cachexia [155]. In particular, STAT3 signalling contributes to wasting in both skeletal muscle and adipose tissue [156], driving lipolysis and tissue degradation [157]. Previous work from our group demonstrated that activated STAT3 is involved in the acquisition of cachectic features in myotubes, and that the treatment with pyruvate can counteract this process [113]. In the results obtained, CM CT26 treatment induced STAT3 phosphorylation, while the addition of the STAT3 inhibitor WP1066 prevented these effects, restoring adipocyte morphology and metabolic balance. CT26 secretome contains several cytokines, such as IL-6, known to activate STAT3 signalling [112]. In adipocytes, the CT26 secretome acts by activating the STAT3 signalling cascade, which is responsible for the phenotypic and metabolic alterations observed in CM CT26-treated adipocytes. Interestingly, results obtained demonstrate that STAT3 is responsible for LDH up-regulation and adiponectin down-regulation, as observed in the adipocytes treated with CM CT26 secretome containing WP1066, where both protein levels were like those observed in the control cells. To date, no data report the involvement of STAT3 in the transcriptional control of LDH and adiponectin genes. Specifically, the up regulation of LDH leads to an increased production of lactate that could have a potential role in the onset and exacerbation of the cachectic condition in adipocytes. While the role of extracellular lactate as a signalling molecule in the tumor microenvironment is well established [158], its contribution in cancer cachexia needs to be investigated more accurately.

In conclusion, it is important to highlight that muscle wasting, both in cancer cachexia and sarcopenia, is driven by similar mechanisms across different cell types – including myotubes and adipocytes – as well as in muscle tissues from cachectic patients and in murine models of sarcopenia. Across all these models, both *in vitro* and *in vivo*, an increased lactate production has been shown to promote the onset of the wasting condition. These findings suggest that lactate, acting both as a metabolite and through GPR81-mediated signalling, plays a central role in driving muscle degeneration.

Overall, this evidence points out the lactate-GPR81 axis as a potential therapeutic target for the creation of novel strategies to counteract muscle wasting.

## 6. REFERENCES


1. Yin L, Li N, Jia W, Wang N, Liang M, Yang X, Du G. Skeletal muscle atrophy: From mechanisms to treatments. Pharmacol Res. 2021 Oct;172:105807. doi: 10.1016/j.phrs.2021.105807. Epub 2021 Aug 10. PMID: 34389456.
2. Frontera WR, Ochala J. Skeletal muscle: a brief review of structure and function. Calcif Tissue Int. 2015 Mar;96(3):183-95. doi: 10.1007/s00223-014-9915-y. Epub 2014 Oct 8. PMID: 25294644.
3. Sartori R, Romanello V, Sandri M. Mechanisms of muscle atrophy and hypertrophy: implications in health and disease. Nat Commun. 2021 Jan 12;12(1):330. doi: 10.1038/s41467-020-20123-1. PMID: 33436614; PMCID: PMC7803748.
4. Baskin KK, Winders BR, Olson EN. Muscle as a "mediator" of systemic metabolism. Cell Metab. 2015 Feb 3;21(2):237-248. doi: 10.1016/j.cmet.2014.12.021. PMID: 25651178; PMCID: PMC4398026.Mukund K, Subramaniam S. Skeletal muscle: A review of molecular structure and function, in health and disease. Wiley Interdiscip Rev Syst Biol Med. 2020 Jan;12(1):e1462.
5. Frontera WR, Ochala J. Skeletal muscle: a brief review of structure and function. Calcif Tissue Int. 2015 Mar;96(3):183-95. doi: 10.1007/s00223-014-9915-y. Epub 2014 Oct 8. PMID: 25294644.
6. Ding S, Dai Q, Huang H, Xu Y, Zhong C. An Overview of Muscle Atrophy. Adv Exp Med Biol. 2018;1088:3-19. doi: 10.1007/978-981-13-1435-3_1. PMID: 30390245.
7. Brooks SV, Guzman SD, Ruiz LP. Skeletal muscle structure, physiology, and function. Handb Clin Neurol. 2023;195:3-16. doi: 10.1016/B978-0-323-98818-6.00013-3. PMID: 37562874.
8. Ottenheijm CA, Granzier H. Lifting the nebula: novel insights into skeletal muscle contractility. Physiology (Bethesda). 2010 Oct;25(5):304-10. doi: 10.1152/physiol.00016.2010. PMID: 20940435.
9. Brocca L, Toniolo L, Reggiani C, Bottinelli R, Sandri M, Pellegrino MA. FoxO-dependent atrogenes vary among catabolic conditions and play a key role in muscle atrophy induced by hindlimb suspension. J Physiol. 2017 Feb 15;595(4):1143-1158. doi: 10.1113/JP273097. Epub 2016 Dec 12. PMID: 27767211; PMCID: PMC5309360.
10. Michel JM, Godwin JS, Kerr NR, Childs TE, Booth FW, Mobley CB, Hughes DC, Roberts MD. Skeletal muscle atrophy induced by aging and disuse atrophy are strongly associated with the upregulation of the endoplasmic stress protein CHOP in

rats. Mol Biol Rep. 2025 Mar 18;52(1):322. doi: 10.1007/s11033-025-10415-4. PMID: 40100290; PMCID: PMC11919930.

11. Anker SD, Morley JE, von Haehling S. Welcome to the ICD-10 code for sarcopenia. J Cachexia Sarcopenia Muscle. 2016 Dec;7(5):512-514. doi: 10.1002/jcsm.12147. Epub 2016 Oct 17. PMID: 27891296; PMCID: PMC5114626.
12. Cohen S, Nathan JA, Goldberg AL. Muscle wasting in disease: molecular mechanisms and promising therapies. Nat Rev Drug Discov. 2015 Jan;14(1):58-74. doi: 10.1038/nrd4467. PMID: 25549588.
13. Colpman P, Dasgupta A, Archer SL. The Role of Mitochondrial Dynamics and Mitotic Fission in Regulating the Cell Cycle in Cancer and Pulmonary Arterial Hypertension: Implications for Dynamin-Related Protein 1 and Mitofusin2 in Hyperproliferative Diseases. Cells. 2023 Jul 20;12(14):1897. doi: 10.3390/cells12141897. PMID: 37508561; PMCID: PMC10378656.
14. Domaniku A, Bilgic SN, Kir S. Muscle wasting: emerging pathways and potential drug targets. Trends Pharmacol Sci. 2023 Oct;44(10):705-718. doi: 10.1016/j.tips.2023.07.006. Epub 2023 Aug 17. PMID: 37596181.
15. Ferrer M, Anthony TG, Ayres JS, Biffi G, Brown JC, Caan BJ, Cespedes Feliciano EM, Coll AP, Dunne RF, Goncalves MD, Grethlein J, Heymsfield SB, Hui S, Jamal-Hanjani M, Lam JM, Lewis DY, McCandlish D, Mustian KM, O'Rahilly S, Perrimon N, White EP, Janowitz T. Cachexia: A systemic consequence of progressive, unresolved disease. Cell. 2023 Apr 27;186(9):1824-1845. doi: 10.1016/j.cell.2023.03.028. PMID: 37116469; PMCID: PMC11059056.
16. Cohen BH. Mitochondrial and Metabolic Myopathies. Continuum (Minneap Minn). 2019 Dec;25(6):1732-1766. doi: 10.1212/CON.0000000000000805. PMID: 31794469.
17. Furrer R, Handschin C. Muscle Wasting Diseases: Novel Targets and Treatments. Annu Rev Pharmacol Toxicol. 2019 Jan 6;59:315-339. doi: 10.1146/annurev-pharmtox-010818-021041. Epub 2018 Aug 27. PMID: 30148697; PMCID: PMC6701981.
18. Morley JE, Anker SD, von Haehling S. Prevalence, incidence, and clinical impact of sarcopenia: facts, numbers, and epidemiology-update 2014. J Cachexia Sarcopenia Muscle. 2014 Dec;5(4):253-9. doi: 10.1007/s13539-014-0161-y. Epub 2014 Oct 22. Erratum in: J Cachexia Sarcopenia Muscle. 2015 Jun;6(2):192. doi: 10.1002/jcsm.12038. PMID: 25425503; PMCID: PMC4248415.

19. Mercuri E, Bönnemann CG, Muntoni F. Muscular dystrophies. Lancet. 2019 Nov 30;394(10213):2025-2038. doi: 10.1016/S0140-6736(19)32910-1. PMID: 31789220.
20. Loeffler JP, Picchiarelli G, Dupuis L, Gonzalez De Aguilar JL. The Role of Skeletal Muscle in Amyotrophic Lateral Sclerosis. Brain Pathol. 2016 Mar;26(2):227-36. doi: 10.1111/bpa.12350. PMID: 26780251; PMCID: PMC8029271.
21. Argilés JM, Campos N, Lopez-Pedrosa JM, Rueda R, Rodriguez-Mañas L. Skeletal Muscle Regulates Metabolism via Interorgan Crosstalk: Roles in Health and Disease. J Am Med Dir Assoc. 2016 Sep 1;17(9):789-96. doi: 10.1016/j.jamda.2016.04.019. Epub 2016 Jun 17. PMID: 27324808.
22. Colasuonno F, Price R, Moreno S. Upper and Lower Motor Neurons and the Skeletal Muscle: Implication for Amyotrophic Lateral Sclerosis (ALS). Adv Anat Embryol Cell Biol. 2023;236:111-129. doi: 10.1007/978-3-031-38215-4_5. PMID: 37955773.
23. Ilha J, do Espírito-Santo CC, de Freitas GR. mTOR Signaling Pathway and Protein Synthesis: From Training to Aging and Muscle Autophagy. Adv Exp Med Biol. 2018;1088:139-151. doi: 10.1007/978-981-13-1435-3_7. PMID: 30390251.
24. Liu GY, Sabatini DM. mTOR at the nexus of nutrition, growth, ageing and disease. Nat Rev Mol Cell Biol. 2020 Apr;21(4):183-203. doi: 10.1038/s41580-019-0199-y. Epub 2020 Jan 14. Erratum in: Nat Rev Mol Cell Biol. 2020 Apr;21(4):246. doi: 10.1038/s41580-020-0219-y. PMID: 31937935; PMCID: PMC7102936.
25. Yoshida T, Delafontaine P. Mechanisms of IGF-1-Mediated Regulation of Skeletal Muscle Hypertrophy and Atrophy. Cells. 2020 Aug 26;9(9):1970. doi: 10.3390/cells9091970. PMID: 32858949; PMCID: PMC7564605.
26. Egerman MA, Glass DJ. Signaling pathways controlling skeletal muscle mass. Crit Rev Biochem Mol Biol. 2014 Jan-Feb;49(1):59-68. doi: 10.3109/10409238.2013.857291. Epub 2013 Nov 18. PMID: 24237131; PMCID: PMC3913083.
27. Perrini S, Laviola L, Carreira MC, Cignarelli A, Natalicchio A, Giorgino F. The GH/IGF1 axis and signaling pathways in the muscle and bone: mechanisms underlying age-related skeletal muscle wasting and osteoporosis. J Endocrinol. 2010 Jun;205(3):201-10. doi: 10.1677/JOE-09-0431. Epub 2010 Mar 2. PMID: 20197302.
28. Duan K, Gao X, Zhu D. The clinical relevance and mechanism of skeletal muscle wasting. Clin Nutr. 2021 Jan;40(1):27-37. doi: 10.1016/j.clnu.2020.07.029. Epub 2020 Jul 29. PMID: 32788088.

29. Hoogaars WMH, Jaspers RT. Past, Present, and Future Perspective of Targeting Myostatin and Related Signaling Pathways to Counteract Muscle Atrophy. Adv Exp Med Biol. 2018;1088:153-206. doi: 10.1007/978-981-13-1435-3_8. PMID: 30390252.
30. Sartori R, Milan G, Patron M, Mammucari C, Blaauw B, Abraham R, Sandri M. Smad2 and 3 transcription factors control muscle mass in adulthood. Am J Physiol Cell Physiol. 2009 Jun;296(6):C1248-57. doi: 10.1152/ajpcell.00104.2009. Epub 2009 Apr 8. PMID: 19357234.
31. Winbanks CE, Weeks KL, Thomson RE, Sepulveda PV, Beyer C, Qian H, Chen JL, Allen JM, Lancaster GI, Febbraio MA, Harrison CA, McMullen JR, Chamberlain JS, Gregorevic P. Follistatin-mediated skeletal muscle hypertrophy is regulated by Smad3 and mTOR independently of myostatin. J Cell Biol. 2012 Jun 25;197(7):997-1008. doi: 10.1083/jcb.201109091. Epub 2012 Jun 18. PMID: 22711699; PMCID: PMC3384410.
32. Sartori R, Schirwis E, Blaauw B, Bortolanza S, Zhao J, Enzo E, Stantzou A, Mouisel E, Toniolo L, Ferry A, Stricker S, Goldberg AL, Dupont S, Piccolo S, Amthor H, Sandri M. BMP signaling controls muscle mass. Nat Genet. 2013 Nov;45(11):1309-18. doi: 10.1038/ng.2772. Epub 2013 Sep 29. PMID: 24076600.
33. The clinical relevance and mechanism of skeletal muscle wasting Kaipeng Duan, Xin Gao, Dongming Zhu 2021
34. Scicchitano BM, Faraldi M, Musarò A. The Proteolytic Systems of Muscle Wasting. Recent Adv DNA Gene Seq. 2015;9(1):26-35. doi: 10.2174/2352092209999150911121502. PMID: 26361781.
35. Duan K, Gao X, Zhu D. The clinical relevance and mechanism of skeletal muscle wasting. Clin Nutr. 2021 Jan;40(1):27-37. doi: 10.1016/j.clnu.2020.07.029. Epub 2020 Jul 29. PMID: 32788088.
36. Della Peruta C, Lozanoska-Ochser B, Renzini A, Moresi V, Sanchez Riera C, Bouché M, Coletti D. Sex Differences in Inflammation and Muscle Wasting in Aging and Disease. Int J Mol Sci. 2023 Feb 28;24(5):4651
37. Mukund K, Subramaniam S. Skeletal muscle: A review of molecular structure and function, in health and disease. Wiley Interdiscip Rev Syst Biol Med. 2020 Jan;12(1):e1462. doi: 10.1002/wsbm.1462. Epub 2019 Aug 13. PMID: 31407867; PMCID: PMC6916202.
38. Brown LA, Guzman SD, Brooks SV. Emerging molecular mediators and targets for age-related skeletal muscle atrophy. Transl Res. 2020 Jul;221:44-57. doi:

10.1016/j.trsl.2020.03.001. Epub 2020 Mar 10. PMID: 32243876; PMCID: PMC8026108.

39. Schiaffino S, Dyar KA, Ciciliot S, Blaauw B, Sandri M. Mechanisms regulating skeletal muscle growth and atrophy. FEBS J. 2013 Sep;280(17):4294-314. doi: 10.1111/febs.12253. Epub 2013 Apr 17. PMID: 23517348.
40. Cai D, Frantz JD, Tawa NE Jr, Melendez PA, Oh BC, Lidov HG, Hasselgren PO, Frontera WR, Lee J, Glass DJ, Shoelson SE. IKKbeta/NF-kappaB activation causes severe muscle wasting in mice. Cell. 2004 Oct 15;119(2):285-98. doi: 10.1016/j.cell.2004.09.027. PMID: 15479644.
41. Mittal A, Bhatnagar S, Kumar A, Lach-Trifilieff E, Wauters S, Li H, Makonchuk DY, Glass DJ, Kumar A. The TWEAK-Fn14 system is a critical regulator of denervation-induced skeletal muscle atrophy in mice. J Cell Biol. 2010 Mar 22;188(6):833-49. doi: 10.1083/jcb.200909117. PMID: 20308426; PMCID: PMC2845082.
42. Tajrishi MM, Sato S, Shin J, Zheng TS, Burkly LC, Kumar A. The TWEAK-Fn14 dyad is involved in age-associated pathological changes in skeletal muscle. Biochem Biophys Res Commun. 2014 Apr 18;446(4):1219-1224. doi: 10.1016/j.bbrc.2014.03.084. Epub 2014 Mar 26. PMID: 24680686; PMCID: PMC4049113.
43. Bonetto A, Aydogdu T, Jin X, Zhang Z, Zhan R, Puzis L, Koniaris LG, Zimmers TA. JAK/STAT3 pathway inhibition blocks skeletal muscle wasting downstream of IL-6 and in experimental cancer cachexia. Am J Physiol Endocrinol Metab. 2012 Aug 1;303(3):E410-21. doi: 10.1152/ajpendo.00039.2012. Epub 2012 Jun 5. PMID: 22669242; PMCID: PMC3423125.
44. Chen X, Ji Y, Liu R, Zhu X, Wang K, Yang X, Liu B, Gao Z, Huang Y, Shen Y, Liu H, Sun H. Mitochondrial dysfunction: roles in skeletal muscle atrophy. J Transl Med. 2023 Jul 26;21(1):503. doi: 10.1186/s12967-023-04369-z. PMID: 37495991; PMCID: PMC10373380.
45. Kubat GB, Bouhamida E, Ulger O, Turkel I, Pedriali G, Ramaccini D, Ekinci O, Ozerklig B, Atalay O, Patergnani S, Nur Sahin B, Morciano G, Tuncer M, Tremoli E, Pinton P. Mitochondrial dysfunction and skeletal muscle atrophy: Causes, mechanisms, and treatment strategies. Mitochondrion. 2023 Sep;72:33-58. doi: 10.1016/j.mito.2023.07.003. Epub 2023 Jul 13. PMID: 37451353.
46. Leduc-Gaudet JP, Hussain SNA, Barreiro E, Gouspillou G. Mitochondrial Dynamics and Mitophagy in Skeletal Muscle Health and Aging. Int J Mol Sci. 2021 Jul

30;22(15):8179. doi: 10.3390/ijms22158179. PMID: 34360946; PMCID: PMC8348122.

47. Romanello V, Guadagnin E, Gomes L, Roder I, Sandri C, Petersen Y, Milan G, Masiero E, Del Piccolo P, Foretz M, Scorrano L, Rudolf R, Sandri M. Mitochondrial fission and remodelling contributes to muscle atrophy. EMBO J. 2010 May 19;29(10):1774-85. doi: 10.1038/emboj.2010.60. Epub 2010 Apr 16. PMID: 20400940; PMCID: PMC2876965.
48. Watanabe H, Oshima T. The Latest Treatments for Cancer Cachexia: An Overview. Anticancer Res. 2023 Feb;43(2):511-521. doi: 10.21873/anticanres.16188. PMID: 36697073.
49. You Y, Wang Y, Zhang G, Li Y. The Molecular Mechanisms and Treatment of Cancer-Related Cachexia. J Nutr Sci Vitaminol (Tokyo). 2025;71(1):1-15. doi: 10.3177/jnsv.71.1. PMID: 40024744.
50. Zhong X, Zimmers TA. Sex Differences in Cancer Cachexia. Curr Osteoporos Rep. 2020 Dec;18(6):646-654. doi: 10.1007/s11914-020-00628-w. Epub 2020 Oct 12. PMID: 33044689; PMCID: PMC7732790.
51. Roy A, Kumar A. ER Stress and Unfolded Protein Response in Cancer Cachexia. Cancers (Basel). 2019 Dec 3;11(12):1929. doi: 10.3390/cancers11121929. PMID: 31817027; PMCID: PMC6966641.
52. Baracos VE, Martin L, Korc M, Guttridge DC, Fearon KCH. Cancer-associated cachexia. Nat Rev Dis Primers. 2018 Jan 18;4:17105. doi: 10.1038/nrdp.2017.105. PMID: 29345251.
53. Fearon K, Strasser F, Anker SD, Bosaeus I, Bruera E, Fainsinger RL, Jatoi A, Loprinzi C, MacDonald N, Mantovani G, Davis M, Muscaritoli M, Ottery F, Radbruch L, Ravasco P, Walsh D, Wilcock A, Kaasa S, Baracos VE. Definition and classification of cancer cachexia: an international consensus. Lancet Oncol. 2011 May;12(5):489-95. doi: 10.1016/S1470-2045(10)70218-7. Epub 2011 Feb 4. PMID: 21296615.
54. Berriel Diaz M, Rohm M, Herzig S. Cancer cachexia: multilevel metabolic dysfunction. Nat Metab. 2024 Dec;6(12):2222-2245. doi: 10.1038/s42255-024-01167-9. Epub 2024 Nov 22. PMID: 39578650.
55. Setiawan T, Sari IN, Wijaya YT, Julianto NM, Muhammad JA, Lee H, Chae JH, Kwon HY. Cancer cachexia: molecular mechanisms and treatment strategies. J Hematol Oncol. 2023 May 22;16(1):54. doi: 10.1186/s13045-023-01454-0. PMID: 37217930; PMCID: PMC10204324.

56. Hall KD, Baracos VE. Computational modeling of cancer cachexia. Curr Opin Clin Nutr Metab Care. 2008 May;11(3):214-21. doi: 10.1097/MCO.0b013e3282f9ae4d. PMID: 18403915; PMCID: PMC2693333.
57. Loumaye A, de Barsy M, Nachit M, Lause P, Frateur L, van Maanen A, Trefois P, Gruson D, Thissen JP. Role of Activin A and myostatin in human cancer cachexia. J Clin Endocrinol Metab. 2015 May;100(5):2030-8. doi: 10.1210/jc.2014-4318. Epub 2015 Mar 9. PMID: 25751105.
58. Johns N, Hatakeyama S, Stephens NA, Degen M, Degen S, Frieauff W, Lambert C, Ross JA, Roubenoff R, Glass DJ, Jacobi C, Fearon KC. Clinical classification of cancer cachexia: phenotypic correlates in human skeletal muscle. PLoS One. 2014 Jan 3;9(1):e83618. doi: 10.1371/journal.pone.0083618. Erratum in: PLoS One. 2024 Dec 2;19(12):e0314953. doi: 10.1371/journal.pone.0314953. PMID: 24404136; PMCID: PMC3880262.
59. Geng T, Li P, Yin X, Yan Z. PGC-1α promotes nitric oxide antioxidant defenses and inhibits FOXO signaling against cardiac cachexia in mice. Am J Pathol. 2011 Apr;178(4):1738-48. doi: 10.1016/j.ajpath.2011.01.005. PMID: 21435455; PMCID: PMC3078433.
60. Eskiler GG, Bezdegumeli E, Ozman Z, Ozkan AD, Bilir C, Kucukakca BN, Ince MN, Men AY, Aktas O, Horoz YE, Akpinar D, Genc I, Kaleli S. IL-6 mediated JAK/STAT3 signaling pathway in cancer patients with cachexia. Bratisl Lek Listy. 2019;66(11):819-826. doi: 10.4149/BLL_2019_136. PMID: 31747761.
61. Qiu Z, Wo D, Zhong X, Chen J, Ma E, He J, Peng J, Zhu W, Ren DN. Babao Dan Alleviates Cancer Cachexia in Mice Via Inhibiting IL-6/STAT3 Signaling Pathway. Integr Cancer Ther. 2023 Jan-Dec;22:15347354231168369. doi: 10.1177/15347354231168369. PMID: 37077153; PMCID: PMC10126781.
62. Pettersen K, Andersen S, Degen S, Tadini V, Grosjean J, Hatakeyama S, Tesfahun AN, Moestue S, Kim J, Nonstad U, Romundstad PR, Skorpen F, Sørhaug S, Amundsen T, Grønberg BH, Strasser F, Stephens N, Hoem D, Molven A, Kaasa S, Fearon K, Jacobi C, Bjørkøy G. Cancer cachexia associates with a systemic autophagy-inducing activity mimicked by cancer cell-derived IL-6 trans-signaling. Sci Rep. 2017 May 17;7(1):2046. doi: 10.1038/s41598-017-02088-2. PMID: 28515477; PMCID: PMC5435723.
63. Nishikawa H, Goto M, Fukunishi S, Asai A, Nishiguchi S, Higuchi K. Cancer Cachexia: Its Mechanism and Clinical Significance. Int J Mol Sci. 2021 Aug

6;22(16):8491. doi: 10.3390/ijms22168491. PMID: 34445197; PMCID: PMC8395185.

64. Vander Heiden MG, Cantley LC, Thompson CB. Understanding the Warburg effect: the metabolic requirements of cell proliferation. Science. 2009 May 22;324(5930):1029-33. doi: 10.1126/science.1160809. PMID: 19460998; PMCID: PMC2849637.
65. Baltazar F, Afonso J, Costa M, Granja S. Lactate Beyond a Waste Metabolite: Metabolic Affairs and Signaling in Malignancy. Front Oncol. 2020 Mar 18;10:231. doi: 10.3389/fonc.2020.00231. PMID: 32257942; PMCID: PMC7093491.
66. Certo M, Llibre A, Lee W, Mauro C. Understanding lactate sensing and signalling. Trends Endocrinol Metab. 2022 Oct;33(10):722-735. doi: 10.1016/j.tem.2022.07.004. Epub 2022 Aug 20. PMID: 35999109.
67. Lee TY. Lactate: a multifunctional signaling molecule. Yeungnam Univ J Med. 2021 Jul;38(3):183-193. doi: 10.12701/yujm.2020.00892. Epub 2021 Feb 18. PMID: 33596629; PMCID: PMC8225492.
68. Brooks GA. Lactate as a fulcrum of metabolism. Redox Biol. 2020 Aug;35:101454. doi: 10.1016/j.redox.2020.101454. Epub 2020 Feb 9. PMID: 32113910; PMCID: PMC7284908.
69. Wang ZH, Peng WB, Zhang P, Yang XP, Zhou Q. Lactate in the tumour microenvironment: From immune modulation to therapy. EBioMedicine. 2021 Nov;73:103627. doi: 10.1016/j.ebiom.2021.103627. Epub 2021 Oct 14. PMID: 34656878; PMCID: PMC8524104.
70. Yadav A, Singh A, Phogat J, Dahuja A, Dabur R. Magnoflorine prevent the skeletal muscle atrophy via Akt/mTOR/FoxO signal pathway and increase slow-MyHC production in streptozotocin-induced diabetic rats. J Ethnopharmacol. 2021 Mar 1;267:113510. doi: 10.1016/j.jep.2020.113510. Epub 2020 Oct 24. PMID: 33141056.
71. Plotkin DL, Roberts MD, Haun CT, Schoenfeld BJ. Muscle Fiber Type Transitions with Exercise Training: Shifting Perspectives. Sports (Basel). 2021 Sep 10;9(9):127. doi: 10.3390/sports9090127. PMID: 34564332; PMCID: PMC8473039.
72. Bergman BC, Horning MA, Casazza GA, Wolfel EE, Butterfield GE, Brooks GA. Endurance training increases gluconeogenesis during rest and exercise in men. Am J Physiol Endocrinol Metab. 2000 Feb;278(2):E244-51. doi: 10.1152/ajpendo.2000.278.2.E244. PMID: 10662708.

73. Bergman BC, Tsvetkova T, Lowes B, Wolfel EE. Myocardial glucose and lactate metabolism during rest and atrial pacing in humans. J Physiol. 2009 May 1;587(Pt 9):2087-99. doi: 10.1113/jphysiol.2008.168286. Epub 2009 Mar 16. PMID: 19289551; PMCID: PMC2689346.
74. Glenn TC, Martin NA, Horning MA, McArthur DL, Hovda DA, Vespa P, Brooks GA. Lactate: brain fuel in human traumatic brain injury: a comparison with normal healthy control subjects. J Neurotrauma. 2015 Jun 1;32(11):820-32. doi: 10.1089/neu.2014.3483. Epub 2015 Mar 31. PMID: 25594628; PMCID: PMC4530406.
75. Emhoff CA, Messonnier LA, Horning MA, Fattor JA, Carlson TJ, Brooks GA. Gluconeogenesis and hepatic glycogenolysis during exercise at the lactate threshold. J Appl Physiol (1985). 2013 Feb;114(3):297-306. doi: 10.1152/japplphysiol.01202.2012. Epub 2012 Dec 13. PMID: 23239870; PMCID: PMC8846961.
76. Nalbandian M, Radak Z, Takeda M. Lactate Metabolism and Satellite Cell Fate. Front Physiol. 2020 Dec 11;11:610983. doi: 10.3389/fphys.2020.610983. Erratum in: Front Physiol. 2022 Feb 15;12:817264. doi: 10.3389/fphys.2021.817264. PMID: 33362583; PMCID: PMC7759562.
77. Brooks GA, Arevalo JA, Osmond AD, Leija RG, Curl CC, Tovar AP. Lactate in contemporary biology: a phoenix risen. J Physiol. 2022 Mar;600(5):1229-1251. doi: 10.1113/JP280955. Epub 2021 Feb 25. PMID: 33566386; PMCID: PMC9188361.
78. Warburg O. On respiratory impairment in cancer cells. Science. 1956 Aug 10;124(3215):269-70. PMID: 13351639.
79. Brooks GA. Lactate shuttles in nature. Biochem Soc Trans. 2002 Apr;30(2):258-64. doi: 10.1042/bst0300258. PMID: 12023861.
80. Everse J, Kaplan NO. Lactate dehydrogenases: structure and function. Adv Enzymol Relat Areas Mol Biol. 1973;37:61-133. doi: 10.1002/9780470122822.ch2. PMID: 4144036.
81. Kocianova E, Piatrikova V, Golias T. Revisiting the Warburg Effect with Focus on Lactate. Cancers (Basel). 2022 Dec 7;14(24):6028. doi: 10.3390/cancers14246028. PMID: 36551514; PMCID: PMC9776395.
82. Halestrap AP, Wilson MC. The monocarboxylate transporter family--role and regulation. IUBMB Life. 2012 Feb;64(2):109-19. doi: 10.1002/iub.572. Epub 2011 Dec 9. PMID: 22162139.

83. Brooks GA. Cell-cell and intracellular lactate shuttles. J Physiol. 2009 Dec 1;587(Pt 23):5591-600. doi: 10.1113/jphysiol.2009.178350. Epub 2009 Oct 5. PMID: 19805739; PMCID: PMC2805372.
84. Chen YJ, Mahieu NG, Huang X, Singh M, Crawford PA, Johnson SL, Gross RW, Schaefer J, Patti GJ. Lactate metabolism is associated with mammalian mitochondria. Nat Chem Biol. 2016 Nov;12(11):937-943. doi: 10.1038/nchembio.2172. Epub 2016 Sep 12. PMID: 27618187; PMCID: PMC5069139.
85. Hashimoto T, Hussien R, Brooks GA. Colocalization of MCT1, CD147, and LDH in mitochondrial inner membrane of L6 muscle cells: evidence of a mitochondrial lactate oxidation complex. Am J Physiol Endocrinol Metab. 2006 Jun;290(6):E1237-44. doi: 10.1152/ajpendo.00594.2005. Epub 2006 Jan 24. PMID: 16434551.
86. Bartoloni B, Mannelli M, Gamberi T, Fiaschi T. The Multiple Roles of Lactate in the Skeletal Muscle. Cells. 2024 Jul 10;13(14):1177. doi: 10.3390/cells13141177. PMID: 39056759; PMCID: PMC11274880.
87. Brooks GA. The Science and Translation of Lactate Shuttle Theory. Cell Metab. 2018 Apr 3;27(4):757-785. doi: 10.1016/j.cmet.2018.03.008. PMID: 29617642.
88. Passarella S, de Bari L, Valenti D, Pizzuto R, Paventi G, Atlante A. Mitochondria and L-lactate metabolism. FEBS Lett. 2008 Oct 29;582(25-26):3569-76. doi: 10.1016/j.febslet.2008.09.042. Epub 2008 Oct 1. PMID: 18831974.
89. Liu C, Wu J, Zhu J, Kuei C, Yu J, Shelton J, Sutton SW, Li X, Yun SJ, Mirzadegan T, Mazur C, Kamme F, Lovenberg TW. Lactate inhibits lipolysis in fat cells through activation of an orphan G-protein-coupled receptor, GPR81. J Biol Chem. 2009 Jan 30;284(5):2811-2822. doi: 10.1074/jbc.M806409200. Epub 2008 Dec 1. PMID: 19047060.
90. Brown TP, Ganapathy V. Lactate/GPR81 signaling and proton motive force in cancer: Role in angiogenesis, immune escape, nutrition, and Warburg phenomenon. Pharmacol Ther. 2020 Feb;206:107451. doi: 10.1016/j.pharmthera.2019.107451. Epub 2019 Dec 10. PMID: 31836453.
91. Sun S, Li H, Chen J, Qian Q. Lactic Acid: No Longer an Inert and End-Product of Glycolysis. Physiology (Bethesda). 2017 Nov;32(6):453-463. doi: 10.1152/physiol.00016.2017. PMID: 29021365.
92. Farooq A, Hoque R, Ouyang X, Farooq A, Ghani A, Ahsan K, Guerra M, Mehal WZ. Activation of N-methyl-d-aspartate receptor downregulates inflammasome activity and liver inflammation via a β-arrestin-2 pathway. Am J Physiol Gastrointest Liver

Physiol. 2014 Oct 1;307(7):G732-40. doi: 10.1152/ajpgi.00073.2014. Epub 2014 Aug 7. PMID: 25104498; PMCID: PMC4187065.

93. Hoque R, Farooq A, Ghani A, Gorelick F, Mehal WZ. Lactate reduces liver and pancreatic injury in Toll-like receptor- and inflammasome-mediated inflammation via GPR81-mediated suppression of innate immunity. Gastroenterology. 2014 Jun;146(7):1763-74. doi: 10.1053/j.gastro.2014.03.014. Epub 2014 Mar 20. PMID: 24657625; PMCID: PMC4104305.
94. Hu J, Cai M, Liu Y, Liu B, Xue X, Ji R, Bian X, Lou S. The roles of GRP81 as a metabolic sensor and inflammatory mediator. J Cell Physiol. 2020 Dec;235(12):8938-8950. doi: 10.1002/jcp.29739. Epub 2020 Apr 28. PMID: 32342523.
95. Ahmed K, Tunaru S, Tang C, Müller M, Gille A, Sassmann A, Hanson J, Offermanns S. An autocrine lactate loop mediates insulin-dependent inhibition of lipolysis through GPR81. Cell Metab. 2010 Apr 7;11(4):311-9. doi: 10.1016/j.cmet.2010.02.012. PMID: 20374963.
96. Certo M, Tsai CH, Pucino V, Ho PC, Mauro C. Lactate modulation of immune responses in inflammatory versus tumour microenvironments. Nat Rev Immunol. 2021 Mar;21(3):151-161. doi: 10.1038/s41577-020-0406-2. Epub 2020 Aug 24. PMID: 32839570.
97. Nolt B, Tu F, Wang X, Ha T, Winter R, Williams DL, Li C. Lactate and Immunosuppression in Sepsis. Shock. 2018 Feb;49(2):120-125. doi: 10.1097/SHK.0000000000000958. PMID: 28767543; PMCID: PMC5757670.
98. Pucino V, Bombardieri M, Pitzalis C, Mauro C. Lactate at the crossroads of metabolism, inflammation, and autoimmunity. Eur J Immunol. 2017 Jan;47(1):14-21. doi: 10.1002/eji.201646477. Epub 2016 Dec 21. PMID: 27883186.
99. Errea A, Cayet D, Marchetti P, Tang C, Kluza J, Offermanns S, Sirard JC, Rumbo M. Lactate Inhibits the Pro-Inflammatory Response and Metabolic Reprogramming in Murine Macrophages in a GPR81-Independent Manner. PLoS One. 2016 Nov 15;11(11):e0163694. doi: 10.1371/journal.pone.0163694. PMID: 27846210; PMCID: PMC5112849.
100. Nasi A, Fekete T, Krishnamurthy A, Snowden S, Rajnavölgyi E, Catrina AI, Wheelock CE, Vivar N, Rethi B. Dendritic cell reprogramming by endogenously produced lactic acid. J Immunol. 2013 Sep 15;191(6):3090-9. doi: 10.4049/jimmunol.1300772. Epub 2013 Aug 16. PMID: 23956421.

101. Peter K, Rehli M, Singer K, Renner-Sattler K, Kreutz M. Lactic acid delays the inflammatory response of human monocytes. Biochem Biophys Res Commun. 2015 Feb 13;457(3):412-8. doi: 10.1016/j.bbrc.2015.01.005. Epub 2015 Jan 9. PMID: 25582773.

102. Fischer K, Hoffmann P, Voelkl S, Meidenbauer N, Ammer J, Edinger M, Gottfried E, Schwarz S, Rothe G, Hoves S, Renner K, Timischl B, Mackensen A, Kunz-Schughart L, Andreesen R, Krause SW, Kreutz M. Inhibitory effect of tumor cell-derived lactic acid on human T cells. Blood. 2007 May 1;109(9):3812-9. doi: 10.1182/blood-2006-07-035972. Epub 2007 Jan 25. PMID: 17255361.

103. Husain Z, Huang Y, Seth P, Sukhatme VP. Tumor-derived lactate modifies antitumor immune response: effect on myeloid-derived suppressor cells and NK cells. J Immunol. 2013 Aug 1;191(3):1486-95. doi: 10.4049/jimmunol.1202702. Epub 2013 Jul 1. PMID: 23817426.

104. Hunt TK, Aslam RS, Beckert S, Wagner S, Ghani QP, Hussain MZ, Roy S, Sen CK. Aerobically derived lactate stimulates revascularization and tissue repair via redox mechanisms. Antioxid Redox Signal. 2007 Aug;9(8):1115-24. doi: 10.1089/ars.2007.1674. PMID: 17567242; PMCID: PMC2443402.

105. Porporato PE, Payen VL, De Saedeleer CJ, Préat V, Thissen JP, Feron O, Sonveaux P. Lactate stimulates angiogenesis and accelerates the healing of superficial and ischemic wounds in mice. Angiogenesis. 2012 Dec;15(4):581-92. doi: 10.1007/s10456-012-9282-0. Epub 2012 Jun 3. PMID: 22660894.

106. Ohno Y, Nakatani M, Ito T, Matsui Y, Ando K, Suda Y, Ohashi K, Yokoyama S, Goto K. Activation of Lactate Receptor Positively Regulates Skeletal Muscle Mass in Mice. Physiol Res. 2023 Aug 31;72(4):465-473. doi: 10.33549/physiolres.935004. PMID: 37795889; PMCID: PMC10634564.

107. Nordström F, Liegnell R, Apró W, Blackwood SJ, Katz A, Moberg M. The lactate receptor GPR81 is predominantly expressed in type II human skeletal muscle fibers: potential for lactate autocrine signaling. Am J Physiol Cell Physiol. 2023 Feb 1;324(2):C477-C487. doi: 10.1152/ajpcell.00443.2022. Epub 2023 Jan 9. PMID: 36622074.

108. DeFronzo RA, Tripathy D. Skeletal muscle insulin resistance is the primary defect in type 2 diabetes. Diabetes Care. 2009 Nov;32 Suppl 2(Suppl 2):S157-63. doi: 10.2337/dc09-S302. PMID: 19875544; PMCID: PMC2811436.

109. Choi CS, Kim YB, Lee FN, Zabolotny JM, Kahn BB, Youn JH. Lactate induces insulin resistance in skeletal muscle by suppressing glycolysis and impairing

insulin signaling. Am J Physiol Endocrinol Metab. 2002 Aug;283(2):E233-40. doi: 10.1152/ajpendo.00557.2001. PMID: 12110527.

110. Visavadiya NP, Rossiter HB, Khamoui AV. Distinct glycolytic pathway regulation in liver, tumour and skeletal muscle of mice with cancer cachexia. Cell Biochem Funct. 2021 Aug;39(6):802-812. doi: 10.1002/cbf.3652. Epub 2021 Jun 15. PMID: 34129243; PMCID: PMC8355074.

111. Mannelli M, Gamberi T, Magherini F, Fiaschi T. A Metabolic Change towards Fermentation Drives Cancer Cachexia in Myotubes. Biomedicines. 2021 Jun 20;9(6):698. doi: 10.3390/biomedicines9060698. PMID: 34203023; PMCID: PMC8234377.

112. Mannelli M, Gamberi T, Garella R, Magherini F, Squecco R, Fiaschi T. Pyruvate prevents the onset of the cachectic features and metabolic alterations in myotubes downregulating STAT3 signaling. FASEB J. 2022 Nov;36(11):e22598. doi: 10.1096/fj.202200848R. PMID: 36305891.

113. Wei L, Wang R, Wazir J, Lin K, Song S, Li L, Pu W, Zhao C, Wang Y, Su Z, Wang H. 2-Deoxy-D-glucose Alleviates Cancer Cachexia-Induced Muscle Wasting by Enhancing Ketone Metabolism and Inhibiting the Cori Cycle. Cells. 2022 Sep 25;11(19):2987. doi: 10.3390/cells11192987. PMID: 36230949; PMCID: PMC9562633.

114. Liu X, Li S, Cui Q, Guo B, Ding W, Liu J, Quan L, Li X, Xie P, Jin L, Sheng Y, Chen W, Wang K, Zeng F, Qiu Y, Liu C, Zhang Y, Lv F, Hu X, Xiao RP. Activation of GPR81 by lactate drives tumour-induced cachexia. Nat Metab. 2024 Apr;6(4):708-723. doi: 10.1038/s42255-024-01011-0. Epub 2024 Mar 18. Erratum in: Nat Metab. 2025 Jan;7(1):229. doi: 10.1038/s42255-024-01207-4. PMID: 38499763; PMCID: PMC11052724.

115. Wu Y, Weber JL, Vladutiu GD, Tarnopolsky MA. Six novel mutations in the myophosphorylase gene in patients with McArdle disease and a family with pseudo-dominant inheritance pattern. Mol Genet Metab. 2011 Dec;104(4):587-91. doi: 10.1016/j.ymgme.2011.08.012. Epub 2011 Aug 16. Erratum in: Mol Genet Metab. 2014 Apr;111(4):539. PMID: 21880526.

116. Kitaoka Y, Ogborn DI, Mocellin NJ, Schlattner U, Tarnopolsky MA. Monocarboxylate transporters and mitochondrial creatine kinase protein content in McArdle disease. Mol Genet Metab. 2013 Apr;108(4):259-62. doi: 10.1016/j.ymgme.2013.01.005. Epub 2013 Jan 19. PMID: 23434346.

117. Cuff MA, Shirazi-Beechey SP. The human monocarboxylate transporter, MCT1: genomic organization and promoter analysis. Biochem Biophys Res Commun. 2002 Apr 12;292(4):1048-56. doi: 10.1006/bbrc.2002.6763. PMID: 11944921.

118. Merezhinskaya N, Fishbein WN, Davis JI, Foellmer JW. Mutations in MCT1 cDNA in patients with symptomatic deficiency in lactate transport. Muscle Nerve. 2000 Jan;23(1):90-7. doi: 10.1002/(sici)1097-4598(200001)23:1<90::aid-mus12>3.0.co;2-m. PMID: 10590411.

119. Ulrich CM, Robien K, McLeod HL. Cancer pharmacogenetics: polymorphisms, pathways and beyond. Nat Rev Cancer. 2003 Dec;3(12):912-20. doi: 10.1038/nrc1233. PMID: 14740638.

120. Fei F, Guo X, Chen Y, Liu X, Tu J, Xing J, Chen Z, Ji J, He X. Polymorphisms of monocarboxylate transporter genes are associated with clinical outcomes in patients with colorectal cancer. J Cancer Res Clin Oncol. 2015 Jun;141(6):1095-102. doi: 10.1007/s00432-014-1877-y. Epub 2014 Dec 10. PMID: 25492048; PMCID: PMC11823922.

121. Cantini G, Trabucco M, Di Franco A, Mannucci E, Luconi M. Glucagon modulates proliferation and differentiation of human adipose precursors. J Mol Endocrinol. 2019 Nov;63(4):249-260. doi: 10.1530/JME-19-0095. PMID: 31525727.

122. Selvais CM, Davis-López de Carrizosa MA, Versele R, Dubuisson N, Noel L, Brichard SM, Abou-Samra M. Challenging Sarcopenia: Exploring AdipoRon in Aging Skeletal Muscle as a Healthspan-Extending Shield. Antioxidants (Basel). 2024 Sep 3;13(9):1073. doi: 10.3390/antiox13091073. PMID: 39334732; PMCID: PMC11428238.

123. Guadagnin E, Mázala D, Chen YW. STAT3 in Skeletal Muscle Function and Disorders. Int J Mol Sci. 2018 Aug 2;19(8):2265. doi: 10.3390/ijms19082265. PMID: 30072615; PMCID: PMC6121875.

124. Brooks GA, Curl CC, Leija RG, Osmond AD, Duong JJ, Arevalo JA. Tracing the lactate shuttle to the mitochondrial reticulum. Exp Mol Med. 2022 Sep;54(9):1332-1347. doi: 10.1038/s12276-022-00802-3. Epub 2022 Sep 8. PMID: 36075947; PMCID: PMC9534995.

125. Biffi G, Tuveson DA. Diversity and Biology of Cancer-Associated Fibroblasts. Physiol Rev. 2021 Jan 1;101(1):147-176. doi:

10.1152/physrev.00048.2019. Epub 2020 May 28. PMID: 32466724; PMCID: PMC7864232.

126. Jovanović M, Podolski-Renić A, Krasavin M, Pešić M. The Role of the Thioredoxin Detoxification System in Cancer Progression and Resistance. Front Mol Biosci. 2022 May 19;9:883297. doi: 10.3389/fmolb.2022.883297. PMID: 35664671; PMCID: PMC9161637.

127. Chang L, Ruiz P, Ito T, Sellers WR. Targeting pan-essential genes in cancer: Challenges and opportunities. Cancer Cell. 2021 Apr 12;39(4):466-479. doi: 10.1016/j.ccell.2020.12.008. Epub 2021 Jan 14. PMID: 33450197; PMCID: PMC8157671.

128. Onodera T, Momose I, Kawada M. Potential Anticancer Activity of Auranofin. Chem Pharm Bull (Tokyo). 2019;67(3):186-191. doi: 10.1248/cpb.c18-00767. PMID: 30827998.

129. Matsuba I, Fujita R, Iida K. Palmitic Acid Inhibits Myogenic Activity and Expression of Myosin Heavy Chain MHC IIb in Muscle Cells through Phosphorylation-Dependent MyoD Inactivation. Int J Mol Sci. 2023 Mar 19;24(6):5847. doi: 10.3390/ijms24065847. PMID: 36982919; PMCID: PMC10054354.

130. Abou-Samra M, Selvais CM, Boursereau R, Lecompte S, Noel L, Brichard SM. AdipoRon, a new therapeutic prospect for Duchenne muscular dystrophy. J Cachexia Sarcopenia Muscle. 2020 Apr;11(2):518-533. doi: 10.1002/jcsm.12531. Epub 2020 Jan 21. PMID: 31965757; PMCID: PMC7113498.

131. Massart IS, Kouakou AN, Pelet N, Lause P, Schakman O, Loumaye A, Abou-Samra M, Deldicque L, Bindels LB, Brichard SM, Thissen JP. Administration of adiponectin receptor agonist AdipoRon relieves cancer cachexia by mitigating inflammation in tumour-bearing mice. J Cachexia Sarcopenia Muscle. 2024 Jun;15(3):919-933. doi: 10.1002/jcsm.13454. Epub 2024 Apr 4. PMID: 38572511; PMCID: PMC11154773.

132. Bonetto A, Aydogdu T, Jin X, Zhang Z, Zhan R, Puzis L, Koniaris LG, Zimmers TA. JAK/STAT3 pathway inhibition blocks skeletal muscle wasting downstream of IL-6 and in experimental cancer cachexia. Am J Physiol Endocrinol Metab. 2012 Aug 1;303(3):E410-21. doi: 10.1152/ajpendo.00039.2012. Epub 2012 Jun 5. PMID: 22669242; PMCID: PMC3423125.

133. Van Hall G. Lactate as a fuel for mitochondrial respiration. Acta Physiol Scand. 2000 Apr;168(4):643-56. doi: 10.1046/j.1365-201x.2000.00716.x. PMID: 10759601.

134. Zhang L, Xin C, Wang S, Zhuo S, Zhu J, Li Z, Liu Y, Yang L, Chen Y. Lactate transported by MCT1 plays an active role in promoting mitochondrial biogenesis and enhancing TCA flux in skeletal muscle. Sci Adv. 2024 Jun 28;10(26):eadn4508. doi: 10.1126/sciadv.adn4508. Epub 2024 Jun 26. PMID: 38924407; PMCID: PMC11204292.

135. Ábrigo J, Elorza AA, Riedel CA, Vilos C, Simon F, Cabrera D, Estrada L, Cabello-Verrugio C. Role of Oxidative Stress as Key Regulator of Muscle Wasting during Cachexia. Oxid Med Cell Longev. 2018 Mar 28;2018:2063179. doi: 10.1155/2018/2063179. PMID: 29785242; PMCID: PMC5896211.

136. Rohrbach S, Gruenler S, Teschner M, Holtz J. The thioredoxin system in aging muscle: key role of mitochondrial thioredoxin reductase in the protective effects of caloric restriction? Am J Physiol Regul Integr Comp Physiol. 2006 Oct;291(4):R927-35. doi: 10.1152/ajpregu.00890.2005. Epub 2006 May 4. PMID: 16675629.

137. Zhang X, Selvaraju K, Saei AA, D'Arcy P, Zubarev RA, Arnér ES, Linder S. Repurposing of auranofin: Thioredoxin reductase remains a primary target of the drug. Biochimie. 2019 Jul;162:46-54. doi: 10.1016/j.biochi.2019.03.015. Epub 2019 Apr 1. PMID: 30946948.

138. Santilli V, Bernetti A, Mangone M, Paoloni M. Clinical definition of sarcopenia. Clin Cases Miner Bone Metab. 2014 Sep;11(3):177-80. PMID: 25568649; PMCID: PMC4269139.

139. Carta G, Murru E, Banni S, Manca C. Palmitic Acid: Physiological Role, Metabolism and Nutritional Implications. Front Physiol. 2017 Nov 8;8:902. doi: 10.3389/fphys.2017.00902. PMID: 29167646; PMCID: PMC5682332.

140. Iwabu M, Yamauchi T, Okada-Iwabu M, Sato K, Nakagawa T, Funata M, Yamaguchi M, Namiki S, Nakayama R, Tabata M, Ogata H, Kubota N, Takamoto I, Hayashi YK, Yamauchi N, Waki H, Fukayama M, Nishino I, Tokuyama K, Ueki K, Oike Y, Ishii S, Hirose K, Shimizu T, Touhara K, Kadowaki T. Adiponectin and AdipoR1 regulate PGC-1alpha and mitochondria by Ca(2+) and AMPK/SIRT1. Nature. 2010 Apr 29;464(7293):1313-9. doi: 10.1038/nature08991. Epub 2010 Mar 31. PMID: 20357764.

141. Okada-Iwabu M, Yamauchi T, Iwabu M, Honma T, Hamagami K, Matsuda K, Yamaguchi M, Tanabe H, Kimura-Someya T, Shirouzu M, Ogata H, Tokuyama K, Ueki K, Nagano T, Tanaka A, Yokoyama S, Kadowaki T. A small-molecule AdipoR agonist for type 2 diabetes and short life in obesity. Nature. 2013 Nov 28;503(7477):493-9. doi: 10.1038/nature12656. Epub 2013 Oct 30. PMID: 24172895.

142. Daas SI, Rizeq BR, Nasrallah GK. Adipose tissue dysfunction in cancer cachexia. J Cell Physiol. 2018 Jan;234(1):13-22. doi: 10.1002/jcp.26811. Epub 2018 Aug 4. PMID: 30078199.

143. Batista ML Jr, Henriques FS, Neves RX, Olivan MR, Matos-Neto EM, Alcântara PS, Maximiano LF, Otoch JP, Alves MJ, Seelaender M. Cachexia-associated adipose tissue morphological rearrangement in gastrointestinal cancer patients. J Cachexia Sarcopenia Muscle. 2016 Mar;7(1):37-47. doi: 10.1002/jcsm.12037. Epub 2015 Jun 4. PMID: 27066317; PMCID: PMC4799865.

144. Mannelli M, Gamberi T, Magherini F, Fiaschi T. The Adipokines in Cancer Cachexia. Int J Mol Sci. 2020 Jul 9;21(14):4860. doi: 10.3390/ijms21144860. PMID: 32660156; PMCID: PMC7402301.

145. Hou XM, Yuan SQ, Zhao D, Liu XJ, Wu XA. LDH-A promotes malignant behavior via activation of epithelial-to-mesenchymal transition in lung adenocarcinoma. Biosci Rep. 2019 Jan 15;39(1):BSR20181476. doi: 10.1042/BSR20181476. Erratum in: Biosci Rep. 2020 Jun 26;40(6):BSR-20181476_COR. doi: 10.1042/BSR-20181476_COR. PMID: 30509961; PMCID: PMC6331674.

146. Zhu W, Ma L, Qian J, Xu J, Xu T, Pang L, Zhou H, Shu Y, Zhou J. The molecular mechanism and clinical significance of LDHA in HER2-mediated progression of gastric cancer. Am J Transl Res. 2018 Jul 15;10(7):2055-2067. PMID: 30093943; PMCID: PMC6079134.

147. Xie H, Hanai J, Ren JG, Kats L, Burgess K, Bhargava P, Signoretti S, Billiard J, Duffy KJ, Grant A, Wang X, Lorkiewicz PK, Schatzman S, Bousamra M 2nd, Lane AN, Higashi RM, Fan TW, Pandolfi PP, Sukhatme VP, Seth P. Targeting lactate dehydrogenase--a inhibits tumorigenesis and tumor progression in mouse models of lung cancer and impacts tumor-initiating cells. Cell Metab. 2014 May 6;19(5):795-809. doi: 10.1016/j.cmet.2014.03.003. Epub 2014 Apr 10. PMID: 24726384; PMCID: PMC4096909.

148. Lopez Krol A, Nehring HP, Krause FF, Wempe A, Raifer H, Nist A, Stiewe T, Bertrams W, Schmeck B, Luu M, Leister H, Chung HR, Bauer UM, Adhikary T, Visekruna A. Lactate induces metabolic and epigenetic reprogramming of pro-inflammatory Th17 cells. EMBO Rep. 2022 Dec 6;23(12):e54685. doi: 10.15252/embr.202254685. Epub 2022 Oct 10. PMID: 36215678; PMCID: PMC9724659.

149. Brand A, Singer K, Koehl GE, Kolitzus M, Schoenhammer G, Thiel A, Matos C, Bruss C, Klobuch S, Peter K, Kastenberger M, Bogdan C, Schleicher U, Mackensen A, Ullrich E, Fichtner-Feigl S, Kesselring R, Mack M, Ritter U, Schmid M, Blank C, Dettmer K, Oefner PJ, Hoffmann P, Walenta S, Geissler EK, Pouyssegur J, Villunger A, Steven A, Seliger B, Schreml S, Haferkamp S, Kohl E, Karrer S, Berneburg M, Herr W, Mueller-Klieser W, Renner K, Kreutz M. LDHA-Associated Lactic Acid Production Blunts Tumor Immunosurveillance by T and NK Cells. Cell Metab. 2016 Nov 8;24(5):657-671. doi: 10.1016/j.cmet.2016.08.011. Epub 2016 Sep 15. PMID: 27641098.

150. Morrot A, da Fonseca LM, Salustiano EJ, Gentile LB, Conde L, Filardy AA, Franklim TN, da Costa KM, Freire-de-Lima CG, Freire-de-Lima L. Metabolic Symbiosis and Immunomodulation: How Tumor Cell-Derived Lactate May Disturb Innate and Adaptive Immune Responses. Front Oncol. 2018 Mar 23;8:81. doi: 10.3389/fonc.2018.00081. PMID: 29629338; PMCID: PMC5876249.

151. Yamauchi T, Kamon J, Minokoshi Y, Ito Y, Waki H, Uchida S, Yamashita S, Noda M, Kita S, Ueki K, Eto K, Akanuma Y, Froguel P, Foufelle F, Ferre P, Carling D, Kimura S, Nagai R, Kahn BB, Kadowaki T. Adiponectin stimulates glucose utilization and fatty-acid oxidation by activating AMP-activated protein kinase. Nat Med. 2002 Nov;8(11):1288-95. doi: 10.1038/nm788. Epub 2002 Oct 7. PMID: 12368907.

152. Fiaschi T, Magherini F, Gamberi T, Modesti PA, Modesti A. Adiponectin as a tissue regenerating hormone: more than a metabolic function. Cell Mol Life Sci. 2014 May;71(10):1917-25. doi: 10.1007/s00018-013-1537-4. Epub 2013 Dec 10. PMID: 24322911; PMCID: PMC11113778.

153. Johnson DE, O'Keefe RA, Grandis JR. Targeting the IL-6/JAK/STAT3 signalling axis in cancer. Nat Rev Clin Oncol. 2018 Apr;15(4):234-248. doi: 10.1038/nrclinonc.2018.8. Epub 2018 Feb 6. PMID: 29405201; PMCID: PMC5858971.

154. Zimmers TA, Fishel ML, Bonetto A. STAT3 in the systemic inflammation of cancer cachexia. Semin Cell Dev Biol. 2016 Jun;54:28-41. doi: 10.1016/j.semcdb.2016.02.009. Epub 2016 Feb 6. PMID: 26860754; PMCID: PMC4867234.

155. Fan M, Gu X, Zhang W, Shen Q, Zhang R, Fang Q, Wang Y, Guo X, Zhang X, Liu X. Atractylenolide I ameliorates cancer cachexia through inhibiting biogenesis of IL-6 and tumour-derived extracellular vesicles. J Cachexia Sarcopenia Muscle. 2022 Dec;13(6):2724-2739. doi: 10.1002/jcsm.13079. Epub 2022 Sep 9. PMID: 36085573; PMCID: PMC9745491.

156. Gandhi AY, Yu J, Gupta A, Guo T, Iyengar P, Infante RE. Cytokine-Mediated STAT3 Transcription Supports ATGL/CGI-58-Dependent Adipocyte Lipolysis in Cancer Cachexia. Front Oncol. 2022 Jun 15;12:841758. doi: 10.3389/fonc.2022.841758. PMID: 35785158; PMCID: PMC9240385.

157. Pérez-Tomás R, Pérez-Guillén I. Lactate in the Tumor Microenvironment: An Essential Molecule in Cancer Progression and Treatment. Cancers (Basel). 2020 Nov 3;12(11):3244. doi: 10.3390/cancers12113244. PMID: 33153193; PMCID: PMC7693872.

158. Bordignon C, Dos Santos BS, Rosa DD. Impact of Cancer Cachexia on Cardiac and Skeletal Muscle: Role of Exercise Training. Cancers (Basel). 2022 Jan 11;14(2):342. doi: 10.3390/cancers14020342. PMID: 35053505; PMCID: PMC8773522.

159. Zhang F, Ma Y, Li D, Wei J, Chen K, Zhang E, Liu G, Chu X, Liu X, Liu W, Tian X, Yang Y. Cancer associated fibroblasts and metabolic reprogramming: unraveling the intricate crosstalk in tumor evolution. J Hematol Oncol. 2024 Sep 2;17(1):80. doi: 10.1186/s13045-024-01600-2. PMID: 39223656; PMCID: PMC11367794.

160. Li Y, Feng L, Shen Q, Jiang X, Liu F, Zhang C, Qi R, Pang B. From metabolic reprogramming to epigenetic modification: association network and targeted treatment strategy between histone lactylation and tumor progression. Front Immunol. 2025 Sep 17;16:1542664. doi: 10.3389/fimmu.2025.1542664. PMID: 41041328; PMCID: PMC12484167.

161. Zou P, Chen M, Ji J, Chen W, Chen X, Ying S, Zhang J, Zhang Z, Liu Z, Yang S, Liang G. Auranofin induces apoptosis by ROS-mediated ER stress and mitochondrial dysfunction and displayed synergistic lethality with piperlongumine

in gastric cancer. Oncotarget. 2015 Nov 3;6(34):36505-21. doi: 10.18632/oncotarget.5364. PMID: 26431378; PMCID: PMC4742192.

162. Rej R. Measurement of aspartate aminotransferase activity: effects of oxamate. Clin Chem. 1979 Apr;25(4):555-9. PMID: 466765.

163. Fairaq A, Shawky NM, Osman I, Pichavaram P, Segar L. AdipoRon, an adiponectin receptor agonist, attenuates PDGF-induced VSMC proliferation through inhibition of mTOR signaling independent of AMPK: Implications toward suppression of neointimal hyperplasia. Pharmacol Res. 2017 May;119:289-302. doi: 10.1016/j.phrs.2017.02.016. Epub 2017 Feb 22. PMID: 28237515; PMCID: PMC5392421.

164. Lindfors S, Polianskyte-Prause Z, Bouslama R, Lehtonen E, Mannerla M, Nisen H, Tienari J, Salmenkari H, Forsgård R, Mirtti T, Lehto M, Groop PH, Lehtonen S. Adiponectin receptor agonist AdipoRon ameliorates renal inflammation in diet-induced obese mice and endotoxin-treated human glomeruli ex vivo. Diabetologia. 2021 Aug;64(8):1866-1879. doi: 10.1007/s00125-021-05473-9. Epub 2021 May 14. PMID: 33987714; PMCID: PMC8245393.